University of Alberta

Adhesion Between Thin Spray-on Liners and Rock or Concrete

by

Hasan Ozturk

A thesis submitted to the Faculty of Graduate Studies and Research in partial fulfillment of the
requirements for the degree of Doctor of Philosophy

in

Mining Engineering

Department of Civil & Environmental Engineering

Edmonton, Alberta

Fall 2005

Library and Archives Canada

Published Heritage Branch

395 Wellington Street
Ottawa ON K1A 0N4
Canada

Bibliothèque et Archives Canada

Direction du Patrimoine de l'édition

395, rue Wellington
Ottawa ON K1A 0N4
Canada

0-494-08709-9

Your file *Votre référence*
ISBN:
Our file *Notre reference*
ISBN:

NOTICE:
The author has granted a non-exclusive license allowing Library and Archives Canada to reproduce, publish, archive, preserve, conserve, communicate to the public by telecommunication or on the Internet, loan, distribute and sell theses worldwide, for commercial or non-commercial purposes, in microform, paper, electronic and/or any other formats.

The author retains copyright ownership and moral rights in this thesis. Neither the thesis nor substantial extracts from it may be printed or otherwise reproduced without the author's permission.

AVIS:
L'auteur a accordé une licence non exclusive permettant à la Bibliothèque et Archives Canada de reproduire, publier, archiver, sauvegarder, conserver, transmettre au public par télécommunication ou par l'Internet, prêter, distribuer et vendre des thèses partout dans le monde, à des fins commerciales ou autres, sur support microforme, papier, électronique et/ou autres formats.

L'auteur conserve la propriété du droit d'auteur et des droits moraux qui protège cette thèse. Ni la thèse ni des extraits substantiels de celle-ci ne doivent être imprimés ou autrement reproduits sans son autorisation.

In compliance with the Canadian Privacy Act some supporting forms may have been removed from this thesis.

While these forms may be included in the document page count, their removal does not represent any loss of content from the thesis.

Conformément à la loi canadienne sur la protection de la vie privée, quelques formulaires secondaires ont été enlevés de cette thèse.

Bien que ces formulaires aient inclus dans la pagination, il n'y aura aucun contenu manquant.

Canada

ABSTRACT

A test method was developed to measure the adhesion of spray-on liners to rock and concrete substrates. The test can be performed in the laboratory or the field, and is easy, practical, and inexpensive.

The impact of substrate type and roughness, the effect of contamination parameters (oil, dust, and water), and the effect of curing time on the adhesion were studied. Substrates tested included cinder block, paving stone, limestone, granite and sandstone. Thin spray-on liner products tested were Tekflex, Tekflex PM, Castonite, MBT CS 1251 2K, Tunnelguard, and Rock Web.

Under room temperature and humidity conditions, the adhesive strength between the Tekflex liner and concrete paving stones is about 1.9 MPa. Adhesion tests on five other liner products showed an order of magnitude range in adhesion, between 0.2 and over 2.4 MPa. An innovative test set up was developed for Tekflex creep testing; the results showed that adhesion could drop at least 50% when the liner carries load for about a month.

A new methodology using pull out load-displacement data was developed to calculate the work of adhesion between a liner and a substrate. Closed-form solutions were derived which predict that adhesion has an inverse square-root relationship with liner thickness. This relationship was confirmed with the laboratory tests.

Prior to this research, it was not recognized that adhesive strength not only depends on the substrate type and condition but also the liner thickness. The interface property known as work of adhesion incorporates both adhesion and effective bond width and in doing so becomes independent of the liner thickness. Therefore, the work of adhesion is a more important physical property and liner manufacturers should measure and document work of adhesion for their products. Most liner products when sprayed on clean strong substrates will likely have work of adhesion values greater than 2000 N/m.

ACKNOWLEDGEMENT

I wish to express my most profound thanks and appreciation to Dr. Dwayne D. Tannant for his kind supervision, invaluable suggestions, discussion, friendship and help towards the completion of my thesis.

I would like to express my sincere appreciation to committee members for their suggestions, comments and valuable contributions to the research and for serving on the Ph.D. thesis committee.

Particular thanks are extended to Sean Watt for his suggestions and invaluable help throughout the experimental side of the study.

TABLE OF CONTENTS

CHAPTER 1 INTRODUCTION **1**

1.1 Thin Spray-on Liners for Rock Support 1

1.2 Liner Adhesion 3

1.3 Adhesion and Liner Performance Observed by Others 4

1.4 Problem Statement 4

1.5 Objectives 5

1.6 Organization and Scope of Thesis 5

CHAPTER 2 REVIEW OF ADHESION TEST METHODS **7**

2.1 Test Method for Thin Coating (<0.1 mm) 7

2.1.1 Direct pull-off 7

2.1.2 Peel test 10

2.1.3 Scratch test 11

2.1.4 Non-destructive methods 11

2.2 Test Methods for Concrete and Concrete Coatings 12

2.2.1 Concrete patch test 12

2.2.2 Blister test 14

2.2.3 Peel test (double cantilever beam test) 15

2.3 Test Methods for Spray-on Liners 16

2.3.1 Embedded dolly 16

2.3.2 Glued dolly 18

2.3.3 Importance of non eccentric loading or uniform stress 18

2.4 Comparison of Test Procedures 20

CHAPTER 3 PULL-OFF TEST PROCEDURE FOR MEASURING ADHESION **23**

3.1 Scope and Overview of Test Method 23

3.2 Test Specimen Preparation and Procedure 23

3.2.1 Substrate preparation 24

3.2.2 Thin spray-on liner preparation and application 24

3.2.3 Coring of test samples before adhesion test 25

3.2.4 Epoxy 26

3.2.5 Application of dollies on the cored samples 27

3.3 Test Apparatus 27

3.3.1 Tensile testing machine and instrumentation 27

3.3.2 Loading fixture (elevator bolt) 28

3.3.3 Devices to connect test fixture to a load cell 29

3.3.4 Test specimen restraint 29

3.4 Test Procedure and Interpretation of Results 30

CHAPTER 4 IMPACT OF SUBSTRATE AND LINER TYPE ON ADHESION **32**

4.1 Substrates 32

4.2 Tekflex 33

4.3 Tekflex PM 38

4.4 Castonite 40

4.5 Tunnelguard 42

4.6 MBT CS1251 2k 43

4.7 Rock Web 44
4.8 Summary 44

CHAPTER 5 IMPACT OF SURFACE CONTAMINANTS ON ADHESION 46
5.1 Dust 46
5.1.1 Tekflex 46
5.1.2 Rock Web 48
5.1.3 Other products 49
5.1.4 Summary 49
5.2 Oil 49
5.2.1 Tekflex 49
5.2.2 Other products 50
5.3 Moisture 50

CHAPTER 6 IMPACT OF CURING TIME, LOADING RATE, CREEP AND LINER THICKNESS ON ADHESION 52
6.1 Curing Time 52
6.2 Loading Rate 52
6.2.1 Creep 52
6.3 Liner Thickness 54

CHAPTER 7 ADHESION THEORY 57
7.1 Introduction 57
7.2 Elastic Material Loaded by a Circular Punch 57
7.2.1 Half space model 57
7.2.2 Thin layer model 58
7.3 Work of Adhesion 59
7.3.1 Force-displacement relationship of thin film 61
7.4 Debonding Approach 64
7.5 'Elastic' Properties of Liner Materials 69
7.6 Comparison of Theoretical Studies with Tekflex Adhesion Test Results 71
7.7 Methodology for Work of Adhesion Calculation 73
7.8 Adhesion Normalization 76
7.8.1 Effective bond width 77

CHAPTER 8 IMPLICATIONS FOR BETTER TSL DESIGN 80
8.1 Potential Liner Failure Modes 80
8.1.1 Tensile failure 80
8.1.2 Adhesive failure 81
8.2 Parameters Affecting Liner Failure 83
8.3 Thickness Based Liner Support Design 84

CHAPTER 9 CONCLUSIONS 86
9.1 Test Method 86
9.2 Adhesion Test Results 87
9.3 Work of Adhesion and Implications for Better Liner Design 87

REFERENCES 89

APPENDIX A: FEM MODELS **93**

APPENDIX B: PHYSICAL AND SURFACE PROPERTY DETERMINATION **98**

APPENDIX C: LINER PRODUCTS **101**

APPENDIX D: DETAILED TEST RESULTS **107**

APPENDIX E: TEST OF SIGNIFICANCE **128**

LIST OF TABLES

Table 1 Various thin spray-on liner products (after Potvin 2002). 2
Table 2 Comparisons of adhesion test methods 21
Table 3 Substrate tensile strength, porosity, density, surface roughness and average grain/crystal size. 32
Table 4 Test parameters used in the tests. 33
Table 5 Comparison of Tekflex adhesive tests on different substrates. 35
Table 6 Comparison of Tekflex PM adhesive tests on different substrates 40
Table 7 Comparison of Castonite adhesive tests on different substrates. 41
Table 8 Comparison of Tunnelguard adhesive tests on different substrates. 43
Table 9 Comparison of CS 1251 2k adhesive tests on different substrates. 44
Table 10 Adhesion test results compared to reported values. 45
Table 11 Dust quantities. 46
Table 12 Comparison of Tekflex adhesive tests on dusty paving stone substrates. 48
Table 13 Comparison of significance of test results for Tekflex on dusty paving stone substrate. 48
Table 14 Summary of dust-controlled tests. 49
Table 15 Oil classification table. 50
Table 16 Summary of tests to evaluate the effect of moist substrate surfaces on adhesion 51
Table 17 Measured adhesion (mean & standard deviation in MPa) after 1 week and 1 month of curing time. 52
Table 18 Creep test parameters. 54
Table 19 Thickness test variables and substrates. 55
Table 20 Overall results for Tekflex work of adhesion. 75
Table 21 Overall results for Castonite work of adhesion. 76
Table 22 Effective bond width values for Tekflex. 77

LIST OF FIGURES

Figure 1 Current area support methods (a) bolts-and-screen, (b) shotcrete, and (c) spray-on liners (after Archibald 2001)..... 1
Figure 2 Interaction between liner adhesion and tensile strength to support the weight of a displaced block (only half of the model is shown) (after Tannant 2001). 3
Figure 3 Schematic diagram of pull-test apparatus (after Erck 1994)..... 7
Figure 4 Schematic diagram of the direct pull-off test (after Chalker et al. 1991)..... 8
Figure 5 ASTM Testers a) 50 mm b) 20 mm c) 12.5 mm aluminium dolly diameter d) 19.5 mm outside 3 mm inside dolly diameter (ASTM 4541-02)..... 8
Figure 6 Stud pull test (www.quadgroupinc.com). 9
Figure 7 Rectangular and circular punch adhered to a thin film (after Wan and Duan 2002)..... 9
Figure 8 Poker chip test..... 9
Figure 9 Schematics of adhesion tests on thin compliant layers. (a) Tack test (b) JKR test (after Lin et al. 2000). 10
Figure 10 Peel test geometry. 10
Figure 11 Schematic drawing of scratch test..... 11
Figure 12 Experimental device composed by the laser source (Nd:YAG laser) sample and the interferometer in epicentre configuration (after Rosa et al. 2002)..... 12
Figure 13 Laser-ultrasonic technique (after Rosa et al. 2002)..... 12
Figure 14 Pull-off test method for concrete patch repairs (after Cleland and Long 1997)..... 13
Figure 15 "Limpet" pull-off equipment (after Bungey and Madandoust 1992). 13
Figure 16 "Hydrajaws" pull-off equipment (after Bungey and Madandoust 1992). 14
Figure 17 Blister test set up (after Gunter 1999). 14
Figure 18 Generation of local defect for the blister test (after Gunter 1999). 15
Figure 19 Experimental setup for determining the fracture toughness of the bond between the composite overlay and the concrete substrate (after Giurgiutiu et al. 2001)..... 16
Figure 20 Adhesion pull test assembly schematic and test equipment (after Archibald 2001). 17
Figure 21 (a) Generic view of a test dolly and (b) Typical test setup in the laboratory (after Tannant et al. 1999)..... 17
Figure 22 Underground adhesion testing & in situ result (after Espley et al. 2001). 17
Figure 23 A specimen being cored and faced (after Lewis 2001). 18

Figure 24 A specimen adaptor being employed to attach the glued on "dolly" to the puller (after Lewis 2001)..... 18
Figure 25 Eccentric loading..... 18
Figure 26 Free body diagram of the loading. 19
Figure 27 Effect of load eccentricity on failure load..... 20
Figure 28 A typical sample after splitting. 24
Figure 29 Preparation of spray-on liner in the laboratory. 25
Figure 30 Core barrel used for coring. 25
Figure 31 Drill press coring machine. 25
Figure 32 Back to back elevator bolt tension test..... 26
Figure 33 Epoxy adhesion test results (ace: acetone cleaned, no: no acetone cleaned). 26
Figure 34 Sample after application of dollies..... 27
Figure 35 Screw drive tensile strength machine..... 28
Figure 36 (a) 500 lbf load cell with with <±0.03% non linearity and with <±1% zero balance (b) 0-6.25 mm LVDT with 0.25% linearity and 0.125% stability to measure displacement..... 28
Figure 37 Elevator bolts used as load transfer fixture..... 29
Figure 38 Ball joint end bearing..... 29
Figure 39 Typical test set-up showing a moveable vise mounted on test machine platen, connecting devices, shackle and load cell..... 30
Figure 40 Substrate and liner after a pull-off test..... 31
Figure 41 Various Tekflex application examples (mine portal, longwall face support, escape raise support, and ore bin maintenance support) (www.minova.com)..... 34
Figure 42 Typical flat cinder block substrate..... 34
Figure 43 Tekflex cast paving stone substrate..... 35
Figure 44 Normalized average adhesion versus substrate properties using Tekflex..... 36
Figure 45 Normalized adhesion versus rough substrate properties..... 37
Figure 46 Normalized adhesion versus flat substrate properties..... 37
Figure 47 Tekflex PM mixture prepared in the lab. 38
Figure 48 Tekflex PM cast paving stone sample..... 38
Figure 49 Adhesive failure after the test. 39
Figure 50 Typical adhesive failure for Tekflex PM cast split granite substrate..... 39
Figure 51 Typical Castonite product. 40
Figure 52 Sandstone test picture..... 41

Figure 53 Tensile failure within sandstone substrate after the test. 41
Figure 54 Typical Tunnelguard sample cured on the substrate. 42
Figure 55 Adhesive failure of Tunnelguard on split sandstone. 42
Figure 56 MBT CS 1251 2K sprayed substrate samples. 43
Figure 57 Saw-cut paving stones with varying amounts of dust (a) highly dusty, (b) moderately dusty and (c) lightly dusty. 47
Figure 58 Lightly oily paving stone surface. 50
Figure 59 Loading rate versus adhesion. 52
Figure 60 Typical creep test sample. 53
Figure 61 Creep test set up 53
Figure 62 Adhesion versus time to failure after application of the load. 54
Figure 63 Effect of changing liner thickness on clean paving stone substrate. 55
Figure 64 Effect of changing liner thickness on clean saw cut granite substrate. 55
Figure 65 Relationship between the adhesion and thickness of liner. 56
Figure 66 Contact between a rigid disc and an infinite elastic medium. 57
Figure 67 Contact between a rigid disc and elastic thin film. 58
Figure 68 Vertical stress under a 33 mm diameter punch on a 4 mm thick liner (ν =0.25) 59
Figure 69 Elastic glue film sandwiched between rigid plane surfaces. 61
Figure 70 Thin disc film under loading. 61
Figure 71 Thin disc cut out from the liner. 62
Figure 72 Enlarged film back in the hole. 62
Figure 73 Enlarged hole. 63
Figure 74 The basic failure mechanisms observed in thin layers under normal loads: (a) Edge crack propagation; (b) internal crack propagation; (c) cavitation; (d) bulk fingering (Crosby et al. 2000). 65
Figure 75 Deformation map for ν=0.5 and a_c/a=2x10^{-4} (Crosby et al. 2000). 67
Figure 76 Deformation map for different Poisson's ratios and a_c/a=0.016. 68
Figure 77 Cylindrical liner specimen under uniaxial loading. 69
Figure 78 Stress strain curve for cylindrical Tekflex specimen. 70
Figure 79 Shape and dimensions of an ASTM D638 Type 1 test specimen. 70
Figure 80 Dog-bone test results. 71
Figure 81 Load displacement curve for Tekflex adhesion tests. 71
Figure 82 Comparison of analytical results with Tekflex results for E = 13 MPa. 72
Figure 83 Comparison of analytical results with Tekflex results for E= 2 MPa. 72

Figure 84 Back to back pull test with Tekflex liner and epoxy. 73
Figure 85 Schematic view of typical tests. 74
Figure 86 Dogbone, back-to-back and pull out tests for Tekflex for the same strain-loading rate. 75
Figure 87 Work of adhesion versus liner thickness for Tekflex 76
Figure 88 Effective bond width versus Tekflex thickness on paving stone and saw cut granite. 77
Figure 89 Liner thickness versus adhesive strength. 78
Figure 90 Model for rock support by a liner assuming a square block moving vertically downward (after Tannant 2004). 80
Figure 91 Liner failure modes at small block displacements caused either by shear rupture or diagonal tensile rupture (after Tannant 2004). 80
Figure 92 Interaction between liner adhesion and tensile strength to support the weight of a displaced block (only half of the model is shown) (Tannant 2004). 81
Figure 93 Top view of the debonded liner and loose square block. 82
Figure 94 Block area versus block height for given work of adhesion. 84
Figure 95 Supportable block height for a 1 m square block (density = 2600 kg/m^3) versus liner thickness based on work of adhesive and tensile failure modes 85

CHAPTER 1 INTRODUCTION

1.1 Thin Spray-on Liners for Rock Support

A number of passive area support techniques (Figure 1) have been used by the mining industry to restrict the movement of loose and broken rock fragments, which form as the result of convergence and failure of excavations made in ground. Typical area support techniques currently used by the industry are bolts-and-screen, shotcrete and thin spray-on liners (Archibald 2001).

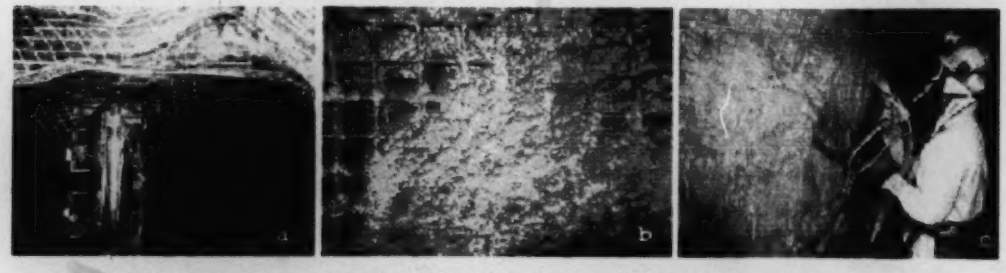

Figure 1 Current area support methods (a) bolts-and-screen, (b) shotcrete, and (c) spray-on liners (after Archibald 2001).

Bolt-and-screen materials are able to offer support resistance, which is controlled by the friction between bolts and rocks. In shotcrete applications, support resistance is mobilized largely by the compressive and shear strength properties of the shotcrete material (Archibald et al. 1998). These techniques have been in use for many years.

Thin spray-on liner (TSL) use is a relatively new area support technique consisting of rapid setting, thin, spray-on multi component polymeric liner materials. A listing of the thin spray-on liners either available commercially or known to be under development is presented in Table 1.

Various in-situ and laboratory studies have been done on thin spray-on liners. According to Archibald (2001),

> Ontario mining industry research trials have shown that spray-on polymer rock support agents have a specialized support function, quite unique from traditional concrete, steel and shotcrete arches ...(which) allows the rock mass to support itself.. These in-situ trials have indicated that considerable potential exists for spray-on polymer and other material use as a short term, stand-alone support in high-speed mine development applications, as a replacement technique for two pass bolting and screening in sill headings, and as screen replacement in drift sidewalls. Various mines in Ontario started evaluating a range of spray-on materials as replacement media for both bolts-and-screen and shotcrete. These materials include polyurethane liners (Mineguard), polyurea liners (Rock Web), polyurethane-polyurea hybrid liners (Rockguard), and two forms of latex/acrylic liner derivatives (Fosroc's Tekflex and Master Builders' Masterseal).
>
> Espley et al. (1996) have determined that one polymer form (Mineguard), tested by INCO Limited, is "a highly feasible product for use in the mining industry. Both shotcrete and Mineguard provide a means of replacing conventional support in appropriate applications". This similar conclusion has been reached by other Ontario mining operators, such as Falconbridge Limited, which has promoted

investigation into the safety and support benefits of other flexible liner materials. Swan et al. (1997) identified a simple worker exposure index consisting of four hazard levels that are defined by the average time spent by workers performing a given operation within a specified distance from an underground work face. By switching from a manual to an automated bolt and screening support system, for example, a worker's exposure time can be reduced by 26% while installing rock support less than 3 metres from the face. By switching from a manual system to a pre-support system, where shotcrete is initially applied and then rockbolts and screen are later installed as secondary support, a worker's hazard index was judged to be reduced by 78%. Archibald et al. (1993) states that with even faster installation capability and more rapid development of full strength cure rates being offered by polymer linings relative to shotcrete, it would be expected that the installation of such liners could provide an equivalent or safer form of rapid support when followed by subsequent bolting to provide secondary support. Additional benefits which may be attributed to use of spray-on liners, other than for support improvement and worker hazard reduction from ground falls, include their potential for lighting enhancement in dark and highly restricted underground sites, ability to restrict gas diffusion from rock media (including radon) and the capability to enhance ventilation flow capacity in mines by reducing wall friction resistance (Archibald et al. 1993).

Table 1 Various thin spray-on liner products (after Potvin 2002).

Product	Manufacturer	Mix Base	Material Type	Fast/Slow
Tekflex	Fosroc Inc.	Cement Latex	Liquid/Powder	Slow
Tekflex PM	Fosroc Inc.	Cement Latex	Water/Powder	Slow
Castonite	Rohm & Haas Co.	Acrylic polymer	Liquid/liquid	Fast
CS1251 2K	MBT	Polymer	Liquid/liquid	Fast
Mineguard	Mineguard Canada	Polyurethane	Liquid/liquid	Fast
Rockguard	Engineered Coatings	Polyurea/ polyurethane	Liquid/liquid	Fast
Rock Web	Spray On Plastics	Polyurea	Liquid/liquid	Fast
Rock Hold	Mondi Mining Supplies	Methacrylate	Liquid/powder	Slow
Masterseal	Master Builder Technologies	Methacrylate	Liquid/liquid	Fast
?	3M	Polyurethane	?	Fast
Tunnelguard	Reynolds Soil Technologies	Cement latex	?	Slow
Everbond	CSIR MiningTek	Cement/Acrylic	Liquid/powder	Slow
Evermine	CSIR MiningTek	Cement/Acrylic	Liquid/powder	Slow
CS 1266	Master Builder Technologies	?	?	?
Ardumin TMO 20	Ardex	Cement+adm+graded fillers	?	Fast

1.2 Liner Adhesion

When liners are used for area support, there is an intimate contact between the liner and rock surfaces, which is true for shotcrete as well, and which makes the adhesion between liner and rock one of the important issues in terms of support resisting capacity.

According to Archibald (2001), "where adequate adhesion bonds exist, liners have the potential to transfer or carry load, created by gravity falls of loose rock in contact with liners, onto stable or unfractured rock surfaces that also maintain liner contact. In the absence of strong adhesion bonds, any restraint of rock movement must be mobilized solely by the tensile strength of the liner materials themselves. The ability of liners to effect strong adhesion bonds will also serve to prevent any unravelling or loosening of discrete rock blocks which may be otherwise free to deform away from excavation surfaces if no adhesion restraint exists."

From previously published research, consensus exists that tensile and adhesion strengths, as well elongation capacity, are key assessment factors for demonstrating the viability of liner support performance (Archibald 2001, Tannant 2001).

Tannant (2004) defines that the resistance of liners for small deformations (<1 mm) is achieved by using a combination of shear, adhesive and tensile strength and postulates failure modes and limiting strength conditions for liners. Adhesion loss followed by tensile rupture is an important process from a design point of view. When the adhesion is less than the tensile strength, the liner adhesive bond may progressively fail around the displacing block as seen in Figure 2. The weight of the block carried by the liner can be calculated by the following equation (assuming no friction between blocks). This equation was also used by Hadjigeorgiou and Grenon (2002), Kuijpers and Toper (2002).

$$A = 4\sigma_a (s + 2x) w_b = W \tag{1}$$

The weight of the block is W, A is the adhesive force, σ_a is the average adhesion of the membrane acting over the effective bond width w_b, x is the debonded length, and s is the width of the block. As can be seen from Equation (1), adhesion and effective bond parameters are important input parameters.

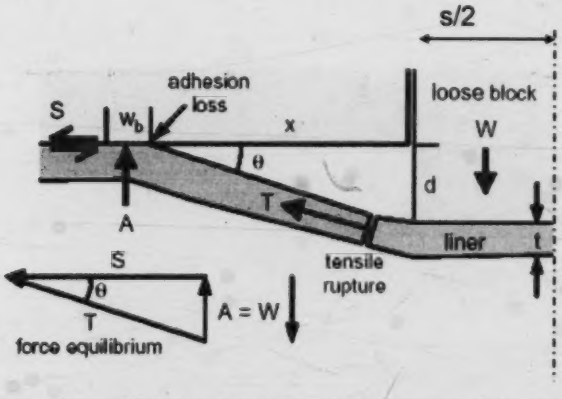

Figure 2 Interaction between liner adhesion and tensile strength to support the weight of a displaced block (only half of the model is shown) (after Tannant 2001).

While adhesion between a liner and substrate has an important influence on TSL performance, very little test data exists to quantify adhesion values. Furthermore, there is almost no knowledge of the on the effect of environmental and curing conditions on TSL adhesion. In the following section, case studies on effect of environmental conditions on adhesive bond are explained.

1.3 Adhesion and Liner Performance Observed by Others

Adhesion tests have been carried out under different environmental conditions. Borejszo and Bartlett (2002) reported different adhesion values for Tunnelguard spray-on liner for different rock types and reported good results with weak sedimentary and igneous rocks, serpentine and burnt coal. Laurence (2001) tested some rocks with Evermine and found that quartzite gave an adhesion of 2 MPa while lava, norite, serpentine, coal, and shale yielded 1 MPa adhesion. Similar results were found with Bondi Rock Hold. Espley et al. (2001) measured poor adhesion on chloritic rock and joint surfaces.

Field trials in Australia, Canada, and the USA showed that oil, dust, dirt, and loose materials on rock surface have a big negative effect on adhesion (Hepworth and Lobato 2002, Espley et al. 2001). Bonding problems were seen with Tekflex and Evermine on grimy surfaces and dusty substrates (Nagel and Joughin 2002).

The effects of temperature and humidity of the environment have also been reported by some in-situ observations (Spearing and Gelson 2002, Lacerda and Rispin 2002, Nagel and Joughin 2002). A copper mine in Chile was satisfied with the support and long term durability of MBT with laminated shale under 24°C and 88% humidity (Spearing and Gelson 2002). It has been observed that some liner materials have an inability to adhere to wet surfaces. Espley (2001) states that 60% moisture content is detrimental for Mineguard. One exception is Tekflex, a cement-based product that adhered well to black shale that was moist and soft (Hepworth and Lobato 2002). A colliery in Australia using MBT for the control of spalling (fretting) on a coal ribside under the ambient temperature of 23°C was satisfied with the application and is monitoring long-term durability (Spearing and Gelson 2002). According to Lacerda and Rispin (2002), in high humidity environments, over 80% relative humidity, CS 1251 liner product may fail during application and over-spraying (4 mm or more) is easily detectable because the product, CS 1251, runs down the rock. Nagel and Joughin (2002) stated that during the early stages of application of Evermine, problems were encountered with the product setting quickly under high ambient temperatures (31° wet bulb), though under moderately cooler conditions this was not observed. A different product, Ardex TMO 20, used in a humid environment appeared to harden on the sidewall where it has been compacted, but not on rock samples taken from the floor. The product did not exhibit good bonding and the next day the sample was easily peeled by hand. After one week, it appeared to have bonded well to the sidewall in the areas checked (Nagel and Joughin 2002).

1.4 Problem Statement

So far, there is no existing testing standard to measure adhesion of liners on rocks. Previous researchers (Mercer 1992, Tannant et al. 1999, Archibald 2001, Espley et al. 2001, Lewis 2001) have tried various test geometries and methods. Each test method has some disadvantages in terms of testing geometry, test setup, interpretation and practicality. In addition, there has been little research done on the adhesion of different TSL material types.

One concern with polymer liners is their creep behaviour. Simple tests have demonstrated that most liner materials will creep and rupture at stresses much less than the values quoted for their

tensile strengths. The impact of creep on the load capacity of a liner in conditions where a liner is supporting the gravitation load from loose broken rock is unknown (Tannant 2004).

Development of new TSL materials or the design of TSL support requires knowledge of the work of adhesion of a TSL, which is the work required to separate a unit area of TSL from its substrate. This knowledge and even the terminology do not currently exist within the rock support community and the proposed research will focus on determination of this parameter for different TSL types on different substrates. The effects of substrate surface conditions (dust, oil, and moisture) will be measured.

In summary, problems can be listed as follows:

- No standardized adhesion test methods exist.
- Existing adhesion test methods for TSL materials have the following problems: testing geometry (bending of loading fixtures during pull-out tests), test setup (eccentric loading or no load displacement data record), interpretation (cohesive, tensile or interfacial failure determination in pull-out tests) and impracticality.
- Little test data for TSL materials under controlled laboratory testing conditions exist.
- There has been no attempt to examine the theoretical or physical basis for adhesion (when dealing with TSL).
- Creep behaviour of TSL has not been studied.

1.5 Objectives

The objectives of this study were to:

- Develop a test method and equipment to measure the adhesion of spray-on liners to rock and concrete substrates that is, practical, quick, and inexpensive.
- Study the effects of different TSL material types (cement and polyurea/polyurethane based) on the TSL adhesion.
- Study the effects of different substrates (roughness, grain size, and tensile strength) on TSL adhesion.
- Study the effects of surface contamination (dust, oil and moisture) on TSL adhesion.
- Study the effects of curing time and creep on the adhesion of liners.
- Use analytical studies to interpret the test results to determine the work of adhesion of different liners, which is a unique material interface property.
- Link experimental results and analytical studies to a more rational design approach for thin spray-on liners.

1.6 Organization and Scope of Thesis

A review of adhesion test methods used elsewhere is presented in Chapter 2 and the adhesion test method developed for TSL study is explained in Chapter 3.

The impact of substrate and liner type on adhesion is presented in Chapter 4. There was no intention to evaluate all TSL materials nor was the testing designed to evaluate a comprehensive range of substrate types and surface conditions. The substrates tested included cinder block,

paving stone, limestone, granite, sandstone, and norite. Liner products used for testing were Tekflex, Tekflex PM, Castonite, MBT CS 1251 2K, Tunnelguard, and Rock Web.

The effect of substrate contamination parameters (oil, dust, and moisture) on the adhesion of different liner products is presented in Chapter 5. The effect of curing time, liner thickness, loading rate and creep behaviour on Tekflex adhesion are studied in Chapter 6. A different testing set up was developed for the creep tests. In Chapter 7, a new methodology was developed for calculating the work of adhesion using data from the adhesion tests. Chapter 8 discusses the effects of liner thickness on support design.

CHAPTER 2 REVIEW OF ADHESION TEST METHODS*

The following section presents a review of test methods used on coatings, thin films, composites, adhesives, concretes, and liner materials. Each test has its own limitations and advantages, which are discussed.

2.1 Test Method for Thin Coating (<0.1 mm)

2.1.1 Direct pull-off

In the coatings industry, a common adhesion test is performed with a Sebastian V type pull test machine as illustrated in Figure 3. Tapered Al pins (2.69 mm head diameter) are bonded to the coating with an epoxy adhesive that is cured for 30 minutes at 150°C. The adhesion is determined from the force required to pull a pin from the specimen divided by the area of the pin's head. A typical loading rate is 2 MPa/s (Erck 1994).

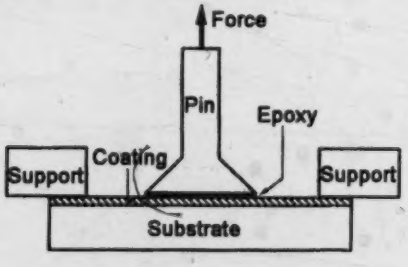

Figure 3 Schematic diagram of pull-test apparatus (after Erck 1994).

Alternatively, rods can be bonded to the coating and substrate using commercially available adhesives, usually an epoxy resin, and then a force applied normal to the coating-substrate interface to determine the force for detachment as shown in Figure 4. This method suffers from the following deficiencies i) the test usually involves a mixture of tensile and shear forces which make interpretation difficult ii) alignment must be perfect to ensure uniform loading across the interface, and iii) there is a possibility that the adhesive or solvent may penetrate the coating and affect the film-substrate interface (Chalker et al. 1991).

One important disadvantage in terms of spray-on liner testing is that the testing area is not isolated. Due to the relatively small thickness of coating used in this type of test, failure occurs at the tip of the pin, but for the spray-on liner, which is relatively thick and stiff, the testing area should be isolated.

---

* *A version of this chapter has been published. D.D. Tannant, H. Ozturk., 2004. Evaluation of Test Methods for Measuring Adhesions between a Liner and Rock. Chapter 10 (Section 6.2 - Testing of Thin Spray-on Liner Properties and Behaviour) in Surface Support in Mining. Potvin, Y., Stacey, T.R. and Hadjigeorgiou, J. Editors, Australian Centre for Geomechanics. 125-134.*

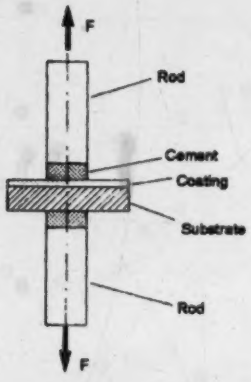

Figure 4 Schematic diagram of the direct pull-off test (after Chalker et al. 1991).

Katz (1976), performed pull-off adhesion tests of copper films to aluminum oxide with a pulling velocity of 0.0254 mm/min and 3.175 mm diameter dolly. Since getting the exact area under pull-off is difficult, he assumed the real contact area as 10% less than the theoretical one, to calculate the adhesion strength.

ASTM D4541-02 (Standard test method for pull-off strength of coatings using portable adhesion testers) specifies the test method for a pull-off test. The test is based on pulling fixture (dolly, stud) normal to the surface of the coating. An adhesive is used to attach the fixture to the coating being tested. The area around the fixture is scored before load is applied. A typical loading rate is 1 MPa/s.

Types of testers that can be used are shown in Figure 5, which shows three fixed alignment testers with 50 mm, 20 mm, and 12.5 mm diameter aluminium loading fixtures. Figure 5d shows a hydraulic tester with a 19 mm outside and 3 mm inside diameter dolly.

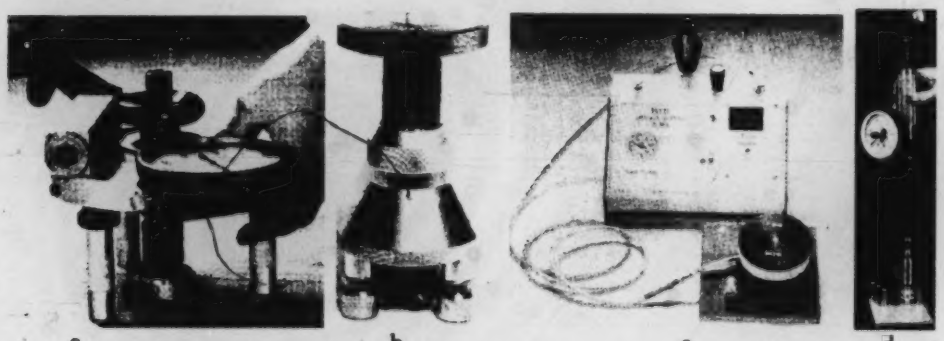

Figure 5 ASTM Testers a) 50 mm b) 20 mm c) 12.5 mm aluminium dolly diameter d) 19.5 mm outside 3 mm inside dolly diameter (ASTM 4541-02).

Another destructive test used in the microelectronics coating industry is the stud pull test (Figure 6). This test is used for many types of coatings, hybrids, decorative coatings, or other "thin film" testing on rigid substrates (adhesion range of 0 to 100 MPa).

Figure 6 Stud pull test (www.quadgroupinc.com).

A nail-shaped stud with the smallest practical diameter (2.65 mm) is coated with a 25 μm thick bonding agent capable of supporting a maximum stress of 70-100 MPa. The uncured stud is installed in a spring-supported mounting clip that assures flat contact to the coating surface, and is cured at 150 C for one hour. Testing can be done immediately after cooling, but delays up to 10 days do not have any serious effect on test values. By microscopic examination, determination is made whether the failure is adherence of the coating/substrate interface, cohesive failure of the substrate, or detachment of the stud from the surface of the bonding agent.

Nano-scale adhesion testing in the polymer industry also uses film detachment by normal forces. Spherical and rectangular punches are used. Either a rectangular or spherical flat punch is pulled away from the membrane by an external load (Figure 7) and contact area and force relationships are derived (Wan and Duan 2002). For the rectangular punch case, a rectangular opening (50 mm x 65 mm) is machined into an aluminium plate (100 mm x 150 mm and 6 mm thick). A sticky tape 5 mm wide and 50 μm thick is adhered to the back of the substrate. A polished flat aluminium punch (49.2 mm x 52 mm) is brought into contact with the film via the rectangular opening and it is pulled away with loading rates of 1, 2, and 5 mm/min.

Figure 7 Rectangular and circular punch adhered to a thin film (after Wan and Duan 2002).

Another test is the poker chip test, as illustrated in Figure 8. The substrate is a rigid cylinder having the same diameter as the compliant layer. The diametrical contraction of the sample makes the interpretation of the test results complex.

Figure 8 Poker chip test.

The test illustrated in Figure 9a also is referred to as a "tack" test. In a typical tack test, the compliant layer (the adhesive), of thickness h, is brought into contact with a rigid flat cylindrical punch of radius a at a certain rate. This usually is followed by a holding period during which the displacement of the rigid punch is held constant for a period of time. The layer then is separated from the punch, and the energy required for this pull-out process is calculated by the area under the load displacement curve. In the second test, illustrated in Figure 9b, the compliant layer is brought into contact with a rigid cylindrical punch having a hemispheric surface. This test therefore is an extension of the Johnson–Kendall–Roberts (JKR) adhesion test (Lin et al. 2000) where the thickness of the compliant layer is much greater than the radius (R) of the hemisphere.

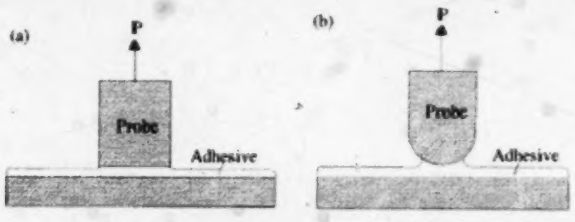

Figure 9 Schematics of adhesion tests on thin compliant layers. (a) Tack test (b) JKR test (after Lin et al. 2000).

The entire test used in nano-scale testing is based on the detachment of the material whether cylindrical or spherical head, not on the substrate, whose adhesion with the adhesive is a concern. Therefore, all the analyses are done assuming complete bonding of adhesive to the substrate. Other difference of this kind of test is that adhesives or coatings tested are tacky and pressure sensitive (Young's Modulus <1 MPa) and force displacement relations (compliance) are testing geometry dependent which is very different than spray-on liners' properties. Therefore, this kind of test cannot be appropriate for liner testing.

2.1.2 Peel test

This is a useful test to measure surface-coating adhesion. The films can be peeled from the substrate in two ways: (a) by directly holding the film and (b) by applying some sort of backing material to the film and then holding the backing. The tensile force that causes peeling may be applied with an initial angle of 90° or 180° with respect to the substrate Figure 10.

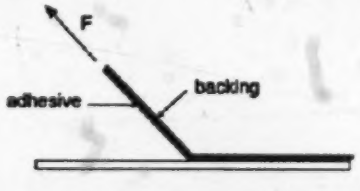

Figure 10 Peel test geometry.

The durability of the bond between the composite and the substrate is also a critical issue. Therefore, a peel test method is again used in this industry, as well.

Detailed information can be found in ASTM D3330/D3330M-02 (Standard Test Method for Peel Adhesion of Pressure-Sensitive Tape) and ASTM D903-98 (Standard Test Method for Peel or Stripping Strength of Adhesive Bonds).

2.1.3 Scratch test

The methods most widely used by paint technologists belonging to this category are bend, cupping or impact tests, or by attacking the paint film by plough or knife tests or in some instances both together, as in most scratch test variants. Many of these tests lead to cohesive cracking of the film, but careful inspection often reveals that the coarseness of the crack pattern is directly related to inadequacy of adhesion.

The scratch test (Figure 11) involves drawing under a vertical load a rounded chrome steel, tungsten carbide or diamond tip (0.03-0.05 mm radius) across the film surface. The vertical load applied to the point is gradually increased until the film is completely removed, resulting in a clear channel. The critical load at which the clear track is formed is taken as a measure of adhesion. Often the scratch does not have straight edges; instead, the paint is torn from areas not actually traversed by the needle. A detailed analysis showed that the action of the point always involves plastic deformation of the surface and this deformation produces a shearing force at the film-substrate interface around the rim of indentation produced by the point (Paul 1985).

Detailed information can be found in ASTM F548-01 (Standard Test Method for Intensity of Scratches on Aerospace Transparent Plastics).

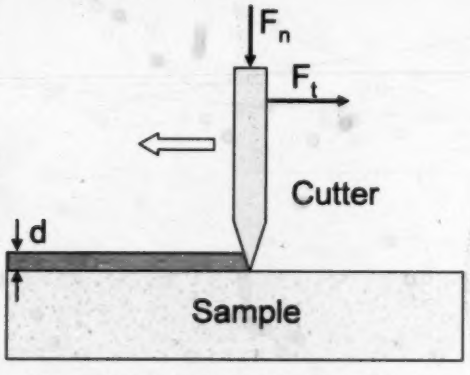

Figure 11 Schematic drawing of scratch test.

2.1.4 Non-destructive methods

A non-destructive technique is the ultrasonic impedometer. The experimental setup consists of a *Q*-switched Nd:YAG laser and an interferometer probe enabling one to measure the normal component of the displacement (Figure 12). The laser beam is focused on the specimen surface using an optical fibre 1.5 mm diameter and 2 m long. At the fibre output the spatial distribution of the energy is smoothed but remains Gaussian. Experiments are carried out applying different energies. The acoustic signal is recorded *in situ* on the free surface of the substrate (in epicentre configuration) using a laser heterodyne interferometer combined with a digital oscilloscope. This setup allows detecting the normal displacements at the epicentre.

This measurement at the epicentre gives the reference. The model of propagation contains many parameters (especially concerning the elastic constants of the material) that are determined by fitting the computation with the measurement of the displacement at the epicentre (Figure 13). When parameters are determined for one kind of coating and substrate, they are introduced into

the modeling of the mechanical displacement and of the mechanical stress tensor at the interface, which gives critical stress intensity factor and adhesion (Rosa et al. 2002).

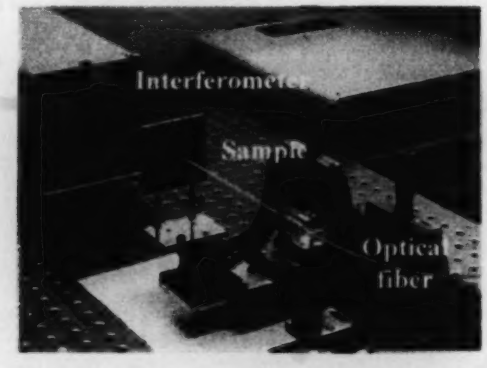

Figure 12 Experimental device composed by the laser source (Nd:YAG laser) sample and the interferometer in epicentre configuration (after Rosa et al. 2002).

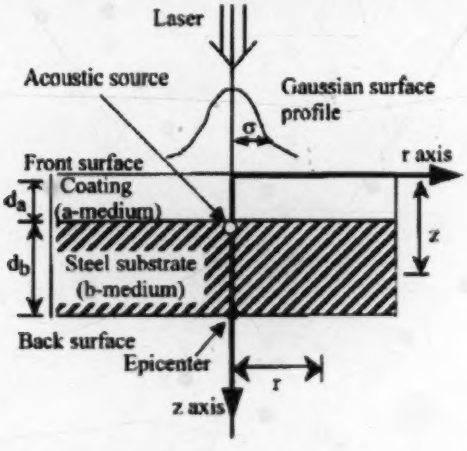

Figure 13 Laser-ultrasonic technique (after Rosa et al. 2002).

2.2 Test Methods for Concrete and Concrete Coatings

2.2.1 Concrete patch test

Direct pull-out tests are also used in the concrete industry. One of the concrete patch repair tests is the pull-off test in which a partial core, usually 50 mm in diameter, is drilled perpendicular to the surface of the repair and extending beyond the interface into the substrate. A circular metal disc is attached to the surface of the concrete core with a suitable epoxy resin. When the resin has achieved sufficient strength, a force is applied to the disc by means of a device, which in turn reacts against the surrounding area of repair or concrete (Figure 14). The load is applied at a steady rate until failure occurs. Dividing the failure load by the cross-sectional area of the core gives the nominal tensile strength or if failure occurs at the interface between the substrate and the repair material, yields the adhesion.

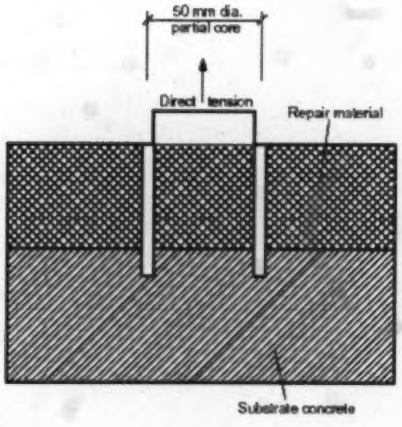

Figure 14 Pull-off test method for concrete patch repairs (after Cleland and Long 1997).

The equipment used for this test, called "Limpet" (Figure 15), is well established in the UK and has a 10 kN pull-off capacity. The load is applied axially to a 50 mm diameter disc through a metal rod, with the reaction transferred to the surface through a bearing ring of 85 mm inside diameter. The equipment is operated manually by a steady turning of the handle, and the load is presented digitally. When operated in accordance with manufacturer's instructions, a load rate of 2.4 kN/min is achieved. Some other available loading devices incorporate tripod reaction systems, as shown in Figure 16, in conjunction with hydraulic or mechanical load application, and provide a wide range of loading rates and capacities (Bungey and Madandoust 1992).

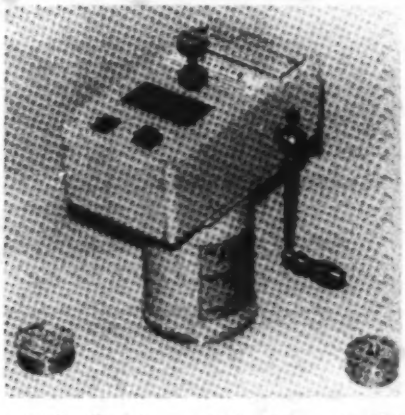

Figure 15 "Limpet" pull-off equipment (after Bungey and Madandoust 1992).

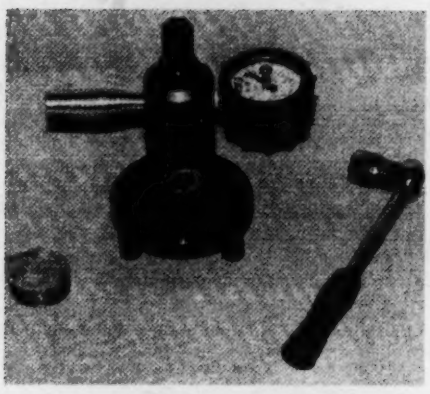

Figure 16 "Hydrajaws" pull-off equipment (after Bungey and Madandoust 1992).

With this pull-off equipment, the following loading rates are used: 0.02-0.1 MPa/s (Bungey and Madandoust 1992), 0.05±0.01 MPa/s British (1984) and Dutch Standards (1990), 0.02 MPa/s (Austin et al. 1995).

2.2.2 Blister test

Another test for a polymer coating-concrete interface is the blister test. A liquid or gas pressure is generated in an artificial local defect, which is created at a coating-substrate interface. The pressure is increased until adhesion failure of the coating occurs i.e. the local defect grows and a blister appears near the initial defect. During the test the diameter of the defect as well as the corresponding pressure and in some instances also shape, volume and height of the blister are recorded. The test set-up for the testing of polymer coating-concrete substrate interfaces is shown in Figure 17 (Gunter 1999).

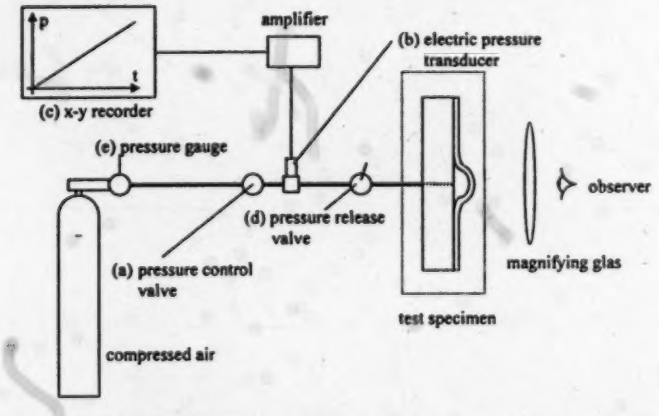

Figure 17 Blister test set up (after Gunter 1999).

To generate an initial defect (5 to 10 mm radius) in the coating-substrate interface before coating, small circular layers of wax (Figure 18) are placed on the surface of the slab around the axis of the steel pressure injection tube.

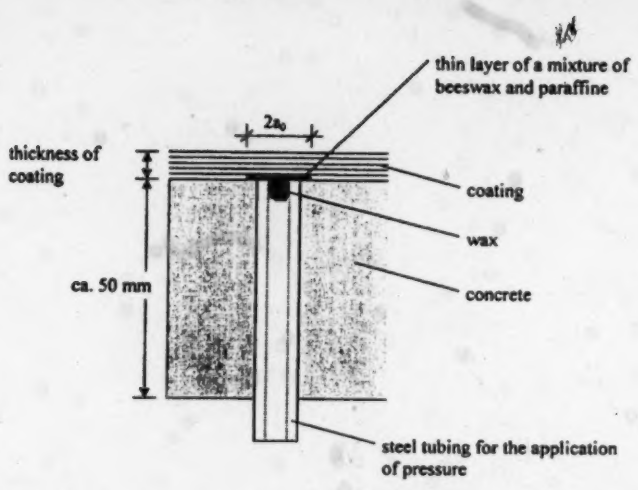

Figure 18 Generation of local defect for the blister test (after Gunter 1999).

In a composite consisting of a polymer coating and a concrete substrate, differences in the physical and the chemical properties of polymers and concrete lead to internal stresses. The pores in the concrete as well as moisture transported therein are of particular significance for the magnitude of such stresses. In particular, a coating may be exposed to liquid, air or vapour pressures acting inside the bond system. Near inevitable local defects, (e.g., caused by foreign particles and substances at the concrete surface or in the coating material) these pressures lead to stress concentrations that are significantly higher than the average stresses (Gunter 1999). Therefore, the stress generated in the blister test resembles the stress state in an actual system. But complexity of the apparatus and testing method makes it impractical.

2.2.3 Peel test (double cantilever beam test)

Test specimens consisted of a concrete substrate and a composite overlay applied on its upper surface. The concrete substrate consisted of a 51 mm x 51 mm x 178 mm concrete block. During the block casting process, two anchorage bolts (12.5 mm diameter) are inserted and set in place. These bolts attach the specimen to the test fixture and take up the reaction forces.

A piano hinge is embedded in the composite layer (3-6 mm fibre reinforced polymer).

The load is introduced into the specimen through a piano hinge attached at the tip of the composite layer with a rate of 0.13 mm/s (Giurgiutiu et al. 2001). The experimental set up can be seen in Figure 19.

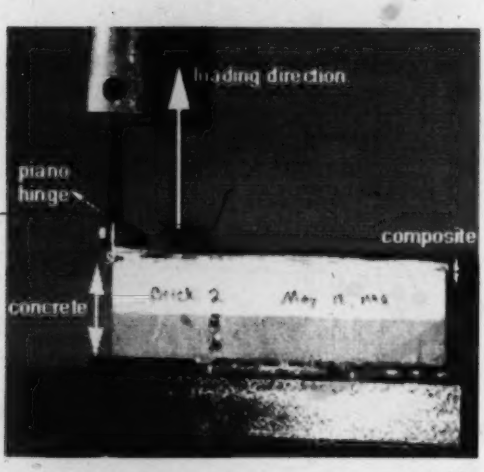

Figure 19 Experimental setup for determining the fracture toughness of the bond between the composite overlay and the concrete substrate (after Giurgiutiu et al. 2001).

The test is based on the strain energy release rate of a crack. First, a crack is introduced between the composite and concrete interface and the sample is loaded. When the crack propagation is observed, loading is stopped and the crack is allowed to propagate and its final length is measured, whereupon and loaded again, and this cycle continuing until full delamination is observed.

In this method, a hinge is embedded in the composite layer and therefore it is a disturbance to the composite, and its hygiene and adherence to the composite is an important issue. Initiation of the first crack, catching successive cracks and recording them are not practical in terms of field application, but its interpretation is easy.

2.3 Test Methods for Spray-on Liners

2.3.1 Embedded dolly

Tannant et al. (1999) and Archibald (2001) used direct pull tests on perforated steel plates to measure adhesion between thin spray-on liners and various substrate materials. The perforated steel plates or test dollies were embedded within a liner membrane, which was sprayed directly onto a rock or like test surface. Various dolly diameters (59, 125 and 250 mm) and thicknesses (3.5 and 6.0 mm) were used. In early tests (Mercer 1992), large diameter (250 mm) plate trials were conducted to assess adhesion bond strengths on rough and irregular rock wall surfaces in underground sites and on thick concrete slabs in a laboratory. In more recent studies (Tannant et al. 1999), small diameter (59 mm) thin plates were applied to rock slabs and tested within laboratory settings.

Both Tannant el al. (1999) and Archibald (2001) used 'Penny Saver' concrete blocks (Figure 20) with the dimensions of 305 mm diameter by 38 mm thick circular concrete as a test surface for adhesion tests to avoid problems associated with variable surface conditions when using rock slabs. The embedded dolly was overcored with a hole saw to isolate the testing area. A displacement rate of 1 mm/minute was used for the testing.

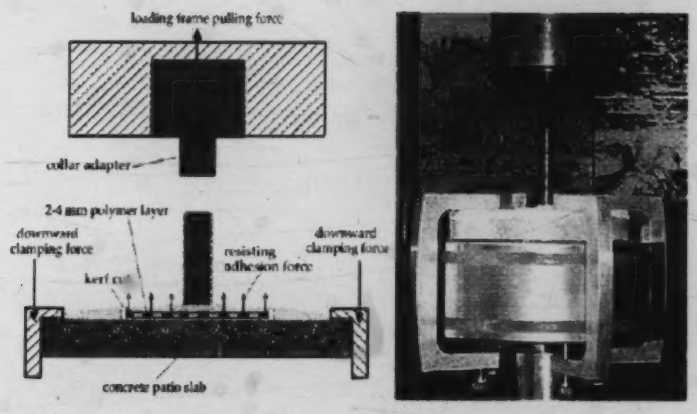

Figure 20 Adhesion pull test assembly schematic and test equipment (after Archibald 2001).

The dolly used by Tannant et al. (1999) consisted of a dolly welded to a circular disk of perforated steel as illustrated in Figure 21. A 'female' eyebolt was threaded onto the elevator bolt. A shackle and eyebolt were used to complete the connection to a load cell.

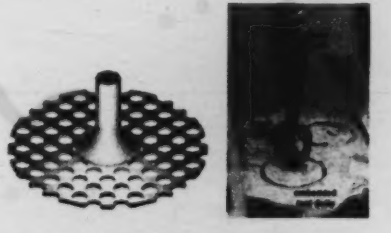

Figure 21 (a) Generic view of a test dolly and (b) Typical test setup in the laboratory (after Tannant et al. 1999).

Espley et al. (2001) carried out some underground trials on rock and shotcrete with a range of cure times and moisture levels. Again, like other researchers they embedded the dolly in the liner (Figure 22)

Figure 22 Underground adhesion testing & in situ result (after Espley et al. 2001).

2.3.2 Glued dolly

Lewis (2001) did adhesion tests on granite slices, by gluing steel dollies on the substrate and pulling them off after overcoring the test area (Figure 23, Figure 24).

Figure 23 A specimen being cored and faced (after Lewis 2001).

Figure 24 A specimen adaptor being employed to attach the glued on "dolly" to the puller (after Lewis 2001).

2.3.3 Importance of non eccentric loading or uniform stress

An important requirement for pull-off testing equipment is that it applies an almost pure axial load with no bending. Eccentricity may arise due to poor setting up of the test equipment (inclined loading or non-concentric loading) or inaccurate coring. Eccentric loading will cause stress concentrations at the edge of the loading fixture, which can result in progressive debonding and failure at a pull-off load that is smaller than could be achieved with a uniform stress distribution. The impact of eccentric loading can be estimated with the simple 2D analytical model shown in Figure 25.

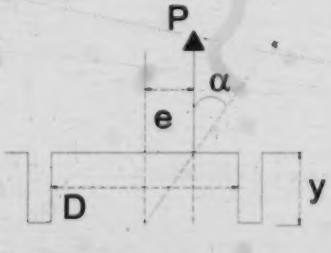

Figure 25 Eccentric loading.

Assuming a unit width for the loading area, and axial and bending forces are equal at given eccentricity, the ratio of the failure load for any value of α to the failure load at zero misalignment is given by:

$$\frac{1}{1+(6\tan\alpha/D)y} \tag{2}$$

where y is coring depth, D is width of the loading area, and α is the angle of eccentricity. If the loading area is assumed as circular, Equation (2) is replaced with the following equation (Cleland and Long 1997).

$$\frac{1}{1+(8\tan\alpha/D)y} \tag{3}$$

A derivation of Equation (2) is given below. As can be seen from Figure 25, eccentric loading causes an offset of e, which is

$$e = y\tan\alpha \tag{4}$$

The free body diagram of load distribution can be seen in Figure 26.

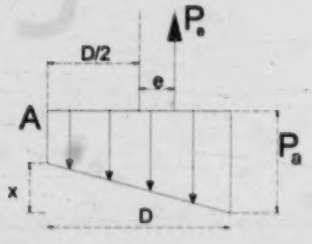

Figure 26 Free body diagram of the loading.

When the equilibrium equation is written for the vertical forces, the following equation is found

$$x = 2P_a - P_e\frac{2}{D} \tag{5}$$

The sum of moments about the point A, yields:

$$\frac{D^2(P_a - x)}{2} + \frac{D^2 x}{3} = P_e\left(\frac{D}{2} + e\right) \tag{6}$$

Substitution of Equation (5) into Equation (6) gives:

$$P_e = \frac{D^2 P_a}{D+6e} \tag{7}$$

The load for zero misalignment, when e =0, is

$$P = P_a D \tag{8}$$

Therefore, the ratio of the misaligned failure load to the failure load of zero misalignment is found as

$$\frac{P_e}{P} = \frac{D}{D+6e} = \frac{1}{1+(6\tan\alpha/D)y} \tag{9}$$

The influence of eccentric loading on the failure load is presented in Figure 27 for a 33 mm diameter test with 4 mm liner thickness. A 6° eccentricity causes about 10% error in the measured adhesion. More importantly, eccentric loading promotes progressive failure at the interface, which will cause further underestimation of adhesion strength.

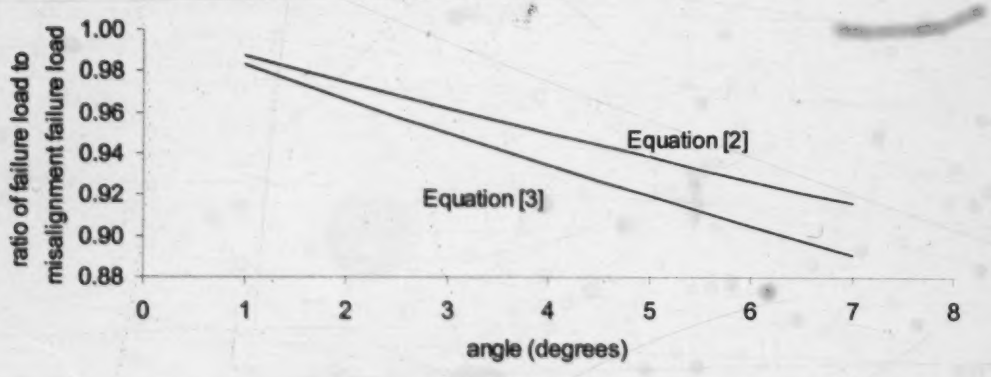

Figure 27 Effect of load eccentricity on failure load.

2.4 Comparison of Test Procedures

Comparison of all adhesion tests can be seen in Table 2. After comparison of all parameters listed in Table 2, it was decided to adopt a testing method that has no eccentric loading and bending problems, is practical, cheap and gives the force displacement recording. It was concluded that a direct pull-off method with the suitable loading fixture could work for testing.

The size of the loading fixture is an important consideration. Table 2 lists ratios of fixture radius to coating thickness for various test methods. Larger size loading fixtures are used to measure adhesion for thicker coatings. A typical radius to thickness ratio used in the past for thin spray-on liners is 10. Smaller ratios have been used on the more standardized, very thick coatings tests. Assuming a reasonable upper limit is 10 and taking the design thickness for thin spray-on liners in the range of 2 to 6 mm, this would imply the need for loading fixtures not larger than 40 to 120 mm in diameter.

If the loading fixture diameter is too large, there is a greater chance that the liner failure during a test will be progressive in nature. This means that the calculated adhesion will be less than the actual adhesion because the peak force is divided by an area that is larger than the true area carrying the load. If the loading fixture is too small, inherent variations in surface texture and roughness of the substrate may not be adequately reflected in the test results unless a large number of tests are completed at various locations.

Table 2 Comparisons of adhesion test methods

Method	Coating thickness	Loading fixture dia. (mm)	Radius / thickness ratio	Disp. or load rate	Cored	L vs d record
Direct pull-out						
Erck 1994	0.5μm	2.7	3000	2MPa/s		yes
Jankowski 1987	30μm	25.4	500	8.5μm/s		yes
Ganghoffer & Gent 1995	3-35mm	2.5-10	0.1-0.5	10mm/min		yes
Tuck						
Kendall 1971 (Lin et al. 2000)	<4.8mm	<44	<100			yes
Creton & Lakrout 2000	10-100μm	2-10				yes
JKR						
Crosby& Shull 1999	70-300μm	12	2.5-20	2.5μm/s		yes
Lin et al. 2000			<5			yes
Patch - Cleland & Long 1997	na	50	na	2.4kN/min	yes	yes
Coating pullout - ASTM D4541	na	12.5, 20, 50	na	1MPa/s	yes	
Blister - Gunter 1999	2-4mm	20	2.5-5	4kPa/min		yes
Composite - Giurgiutiu et al. 2001	3-6mm			0.13mm/s		yes
Peel - Kendall 1971	<300μm			<1μm/s		yes
Scratch - Chalker et al. 1991	<1μm			<2mm/s		
Embedded dolly						
Tannant et al. 1999	2-4mm	59	7.5-15	1mm/min	yes	yes
Mercer 1992	2-4mm	250	31-62.5	1mm/min	yes	yes
Archibald 2001	2-4mm	100	12.5-25	1mm/min	yes	yes
Espley et al. 2001	na	na	na	na	yes	

Similar to the rule of thumb for compressive strength tests on rock cylinders, it seems appropriate that the loading fixture for the adhesion test should have a diameter that is at least 10 times the grain size of the rock in order to yield a reasonable adhesion measurement from a single test.

When using loading fixtures of a shape similar to an elevator bolt it is important to consider bending of the flat contact surface. If the steel contact does not stay planar during a test, the bending will result in non-uniform stresses beneath the fixture. Non-uniform stresses will result in progressive failure and measured adhesions less than true values. Finite element analysis of a 33 mm diameter elevator bolt during a pull-off test shows that bending is negligible and hence the stress beneath the bolt is uniform.

When embedded and glued dolly methods are compared, it can be concluded that a dolly glued to the liner surface is more practical. In an embedded dolly method, first, a layer of liner is placed on the substrate and dolly is applied to the top of the liner, and a second layer of liner is then placed on top of dolly. If an underground field test is taken in to consideration, it is very difficult to hold the dolly on top of the first layer and spray the next layer to embed the dolly. This procedure becomes less practical especially for back of excavations. Another drawback of using the embedded dolly is that the dolly is stuck to the first layer of the liner before curing and some force is applied to it to make sure that it sticks to the liner. This procedure may cause internal defects and cracks, which may cause incorrect adhesion values. Therefore, it is better to let the liner cure before any external effects or body forces are applied.

Timing of dolly application is completely free when using the glued dolly method.

Given consideration to fixture size, desire for uniform stresses beneath the fixture, practicality, and cost, a suggested loading fixture is a standard elevator bolt with a 33 mm base. This size is smaller than previous devices used to measure adhesion with thin spray-on liners, but lies within the range of fixture diameter to coating thickness ratios used by other industries to measure adhesion.

The effect of steel dolly diameter on the stress distribution at the liner rock interface was studied using a finite element program, and results are presented in Appendix A. It was found that using a 33 mm diameter steel dolly gives constant stress distribution under the liner rock interface and therefore it is an ideal dolly diameter size for adhesion testing.

CHAPTER 3 PULL-OFF TEST PROCEDURE FOR MEASURING ADHESION

3.1 Scope and Overview of Test Method

This test method covers a procedure for evaluating the pull-off strength (commonly referred to as adhesion) of a thin spray-on liner by determining the greatest tensile stress that a surface area can bear before a plug of material is detached. The test is destructive and failure will occur along the weakest plane within the system comprised of the test fixture, epoxy, spray-on liner, and substrate. The fracture surface is exposed by the test. The test yields the adhesion of the liner-substrate interface only when debonding occurs at this interface. If failure occurs elsewhere, the test only provides a lower bound on the adhesion of the interface.

The general pull-off test is performed by securing a loading fixture (elevator bolt) normal (perpendicular) to the surface of the spray-on liner with an epoxy. After the epoxy is cured, the specimen is clamped into a tensile loading apparatus. The loading fixture is carefully positioned such that a tensile force is created normal to the liner-substrate interface. The loading fixture is gradually pulled away from the clamped specimen while loads and displacements are recorded. The test continues until a plug of material is detached. When a plug of material is detached, the exposed surface represents the plane of limiting strength within the system. The nature of the failure is described and the pull-off strength is computed based on the maximum indicated load and the original surface area stressed. Detailed information can be found in Tannant and Ozturk (2004).

3.2 Test Specimen Preparation and Procedure

Test specimen preparation involves the following steps before the pull-off test is conducted.

- Select appropriate specimen shapes and sizes
- Prepare substrate surface and record surface characteristics
- Apply liner material
- Allow liner material to cure
- Overcore at selected location(s)
- Affix elevator bolt and let epoxy cure
- Carefully connect the adapters, shackles and joint ball end bearing to the elevator bolt
- Align elevator bolt with loading device, using shims if required
- Clamp test specimen in vice; ensure that vertical alignment (±1%) is provided

The selected area for overcoring and testing must be flat relative to the elevator bolt size. If more than one test is conducted on the specimen, each test site should be separated by more than 10 mm. The liner overcoring should extend deeper than the liner-substrate interface by about 0.5 mm to guarantee that the plug of liner material is fully separated from the rest of the liner. The recommended speed of the drill press is 400 rpm to decrease sample disturbance. During drilling, coring must be done by manual feeding the drill bit up and down to decrease disturbance to the sample and to see the penetration depth in the substrate.

After coring, all dust and liner/rock particles must be gently wiped or blown from the surface. As with the elevator bolt, it is important not to touch the liner plug to prevent transfer of oils on fingers to the surface of the liner.

Prepare the epoxy according to the manufacturer's recommendations and apply a thin coating of epoxy over the clean elevator bolt surface. Press and centre the bolt over the liner plug and let the epoxy cure. Be certain to apply the epoxy across the entire surface. If necessary, carefully remove excess epoxy around the testing area.

Note the approximate temperature, relative humidity, and date and time of preparation.

3.2.1 Substrate preparation

Various types of substrate were used for the tests. These included concrete, limestone, granite and sandstone. The substrate surface was either created using a tensile fracture or a saw cut. To create a fresh tensile fracture surface, cores of the substrate material were loaded to failure using a Brazilian test setup. Small, thin rock wedges are a by-product of the Brazilian splitting method and may not have been removed by the cleaning with a steel brush. Figure 28 show a sandstone core after it was split. A steel brush was used to clean the surface of the split specimen. A circular diamond saw blade with water as a cutting/cooling fluid was used to create sawn surfaces.

Standard Brazilian tensile test specimens were also prepared and tested to measure the tensile strength of the various substrate materials.

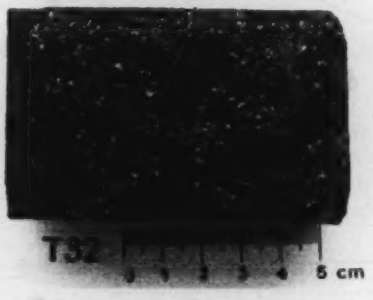

Figure 28 A typical sample after splitting.

3.2.2 Thin spray-on liner preparation and application

The liner materials were prepared according to the manufacturer's suggested method. A number of liner materials were prepared in the laboratory. For example, for Tekflex liner material, the dry powder and the liquid components were measured by weight at a ratio of 1 powder to 2.5 liquid. The components were poured into a commercial food mixer and mixed at medium speed for about 15 minutes (Figure 29). This resulted in a smooth sticky material. As soon as the mixing was completed, the Tekflex material was immediately spread onto the test surfaces using spatulas. The material spread easily and it was possible to create a fairly smooth surface using the spatulas. The specimen preparation was completed within about 25 minutes after the mixing started. Only small numbers of test specimens were prepared at a time because the Tekflex became more difficult to work with after roughly 25 minutes from the start of mixing. During lining application, liner thickness was estimated by eye; the thickness was later determined after testing.

Figure 29 Preparation of spray-on liner in the laboratory.

3.2.3 Coring of test samples before adhesion test

After complete curing of liner materials, in order to isolate the area to be tested for adhesion the liner layer was cored with a diamond core barrel (Figure 30). It has a 33 mm inner diameter and 35 mm outer diameter.

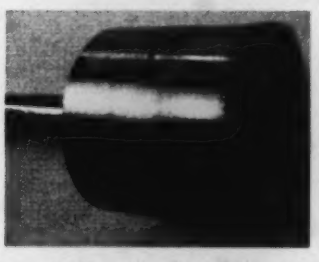

Figure 30 Core barrel used for coring.

In order to decrease the disturbance to the liner material and rock surface a very slow rotation rate (400 rpm) was used for coring using the drill press coring machine (Figure 31). The coring depth was arranged to penetrate the rock about 0.5 mm.

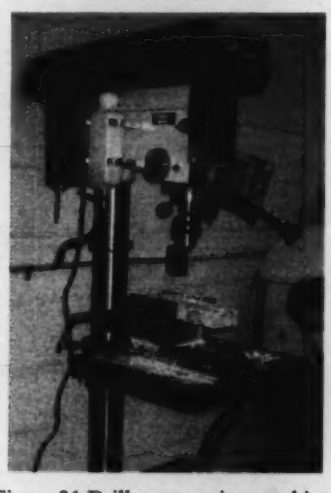

Figure 31 Drill press coring machine.

3.2.4 Epoxy

The loading fixture (elevator bolt) must be firmly attached to the liner. Various epoxies were used for testing, such as, Devcon 5 Ton, Devcon 60 sec, Devcon 5 min, and Araldite 2011. Testing of various adhesives by pulling away two elevator bolts sandwiching (Figure 32) various types of epoxy indicated that Araldite 2011 epoxy gave the highest adhesion to dolly surfaces in half of all test cases.

Figure 32 Back to back elevator bolt tension test.

All tests were carried out with sandblasted elevator bolts. Epoxies were cured as suggested by their manufacturers. Devcon 60 second is cured for 60 seconds, Devcon 5 minute for 5 minutes, Devcon 2 Ton and Araldite 2011 were cured for 24 hours. Results are presented in Figure 33.

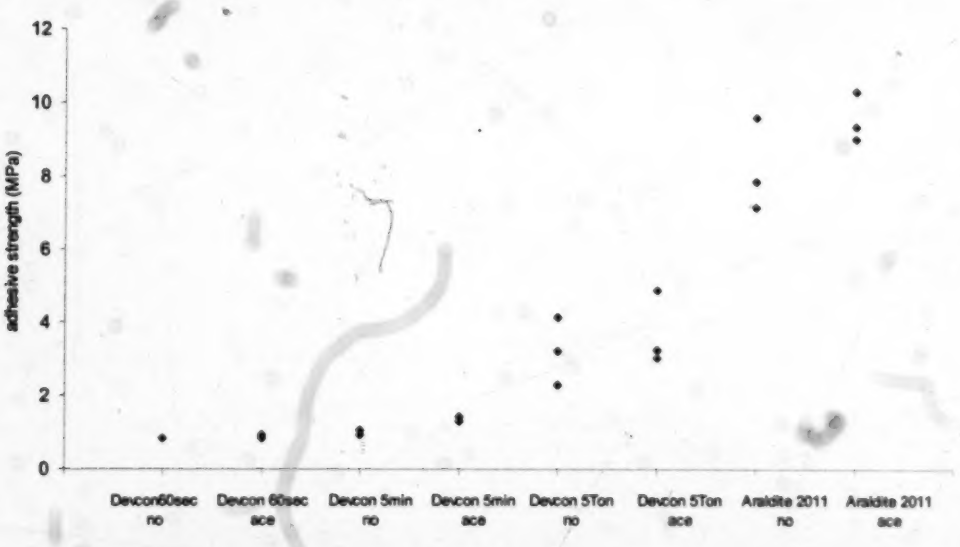

Figure 33 Epoxy adhesion test results (ace: acetone cleaned, no: no acetone cleaned).

As can be seen from Figure 33, Araldite 2011 on acetone cleaned elevator bolt surfaces gives the highest adhesions reaching 10 MPa. Therefore, Araldite 2011 epoxy was selected as a bonding agent between elevator bolt and TSL interfaces. It should be noted that the smoothness of the TSL surface or texture may change the adhesion strength of epoxies.

Various techniques for treating the flat steel surface of the elevator bolts were tested to determine the method giving the highest adhesion with the epoxy. These included treatment of elevator bolt surfaces with sand paper, a rock tumbler, sand blasting, and use of alcohol and acetone. Sand blasting the elevator bolts before their use with Araldite 2011 epoxy achieved the strongest interface strength.

The interface between the elevator bolt and the epoxy can form a potential weakness plane and it is important that the elevator bolt surface be completely clean (achievable by sand blasting). The sandblasting also has an advantage in that the process also creates thousands of micro-pits and scratches on the steel surface that enhances the adhesive bond.

After the elevator bolt is sand blasted and wiped clean with a cloth, it is important to not touch the flat portion of the bolt. Touching the elevator bolt can transfer oils from fingers to the surface and thus reduce the adhesive bond.

3.2.5 Application of dollies on the cored samples

After the coring process, dollies were glued to the samples (Figure 34) with Araldite 2011, and left for curing as suggested by the epoxy manufacturer. During this process, care was taken to make sure that coarse sand blasted dolly surfaces are free of any contaminant, such as finger prints. Therefore, acetone was applied to dolly surfaces in half of all test cases as shown in Figure 33.

Figure 34 Sample after application of dollies.

One important application care is the amount of epoxy applied to the dolly surface. In order to make sure that the epoxy will not flood or wrap around the liner, rock or dolly itself during curing, suitable amounts of epoxy were determined after trial and error testing.

3.3 Test Apparatus

3.3.1 Tensile testing machine and instrumentation

A device to gradually pull on the load fixture must be capable of a constant displacement rate of 2 mm/min and must be able to record loads with 2 N accuracy up to a maximum load of about 4 kN. A suitable screw driven tensile strength machine is shown in Figure 35. A typical recording rate is 10 measurements per second during the test. A test should take from 30 to 100 s to complete.

Figure 35 Screw drive tensile strength machine.

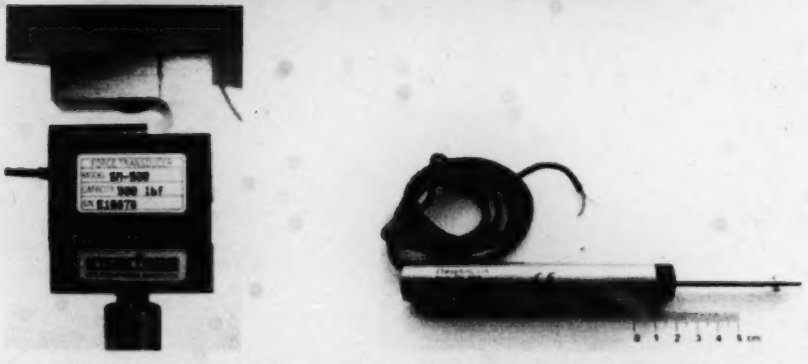

Figure 36 (a) 500 lbf load cell with with <±0.03% non linearity and with <±1% zero balance (b) 0-6.25 mm LVDT with 0.25% linearity and 0.125% stability to measure displacement.

3.3.2 Loading fixture (elevator bolt)

An elevator bolt has been found to be a suitable loading fixture. They are an off-the-shelf item with minimal cost ($0.5 each). An elevator bolt having a flat surface on one end with a diameter of 33 mm and 3/8" #16 male thread size on the other end (Figure 37) has been found to work well. Detailed finite element elevator bolt modelling is presented in Appendix A. The diameter of the flat elevator bolt surface is smaller than for other devices used in liner adhesion tests. However, the diameter is suitable when testing thin liners and makes placement and overcoring of the loading fixture on rough rock surfaces easier. The diameter typically exceeds 10 times the largest grain size of the rock surface, which is a desirable characteristic.

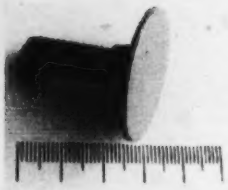

Figure 37 Elevator bolts used as load transfer fixture.

A solid cylindrical steel disk with a threaded hole at one end could be also be used. The advantage of using the elevator bolt is the lower cost and lower mass. The lower mass is helpful when using loading fixtures on inclined to vertical test surfaces.

3.3.3 Devices to connect test fixture to a load cell

Eliminating or minimizing bending moments during the pull test is important. Selection of appropriate connection fixtures can help keep the loading in a pure tensile mode. A ball joint end bearing (Figure 38) connected to the elevator bolt by a threaded adapter on one end, and to the load cell by a shackle on the other end works well.

Figure 38 Ball joint end bearing.

3.3.4 Test specimen restraint

The test specimen consisting of the block of substrate material coated on one surface with liner material must be held securely during the pull-off test. For large specimens, a loading device may simply react against the surface of the test specimen using any of the techniques described in ASTM 4541-02. Smaller specimens are most easily tested if they are clamped into the proper position within a tensile testing frame.

A drill press vise mounted to the tensile loading machine (Figure 39) that can be translated into different positions permits unlimited adjustment of the specimen position and orientation. It is essential to have the flexibility to align test specimens with different sizes and shapes directly below the load cell and loading device.

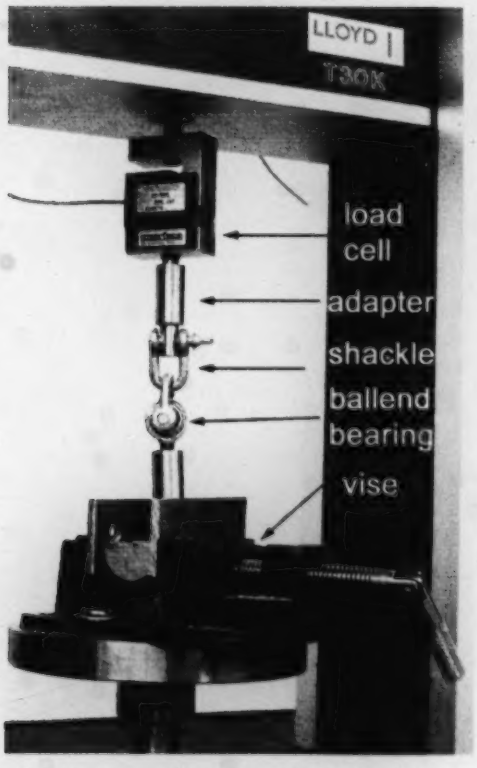

Figure 39 Typical test set-up showing a moveable vise mounted on test machine platen, connecting devices, shackle and load cell.

3.4 Test Procedure and Interpretation of Results

The pull-off test procedure is as follows:

- Pull on the elevator bolt at a constant rate of 2 mm/min
- Failure should occur in less than 100 s
- Record the force and displacement during test
- When a plug of material becomes detached, label and store sample of the failed surface
- Report any unusual behaviour, such as possible misalignment, sliding between jaws and sample, etc.

The measured force is converted into stress using:

$$\sigma = \frac{4F}{\pi d^2} \tag{10}$$

Where σ is the adhesive strength achieved at failure, F is the maximum force applied to the test surface and d is diameter of the elevator bolt (33 mm). This equation assumes that the force is uniformly carried over the full interface area defined by the overcore. The effect of eccentric loading can be seen in Section 2.3.3.

The shape of the recorded load-displacement curve during the test and visual observation of the eventual failure mode provide quality control information about the test. Unusual behaviour must be noted and the test results may be discarded if the results seem suspicious.

Visual examination of the failure surface will show which materials failed. An ideal test occurs when the failure occurs only at the liner-rock interface. Under this scenario, the substrate surface that was beneath the liner would not contain any liner material and the liner plug would not have any fragments of substrate material. However, failure often will occur partially through the substrate and/or the liner. In this case, the measured force results from a combination of adhesion at the interface and tensile strength of the liner or substrate. When the percentage material failing in tension exceeds about 10 to 15% of the overcored area, the interpretation of adhesion becomes less reliable and the test results yield a lower bound on the true intrinsic adhesion.

Figure 40 shows a photograph of a granite substrate and liner after a pull-off test. Only a few small fragments of granite remain attached to the failed liner plug and no liner material remains on the granite surface, thus indicating that failure was dominated by adhesion between the liner and the granite.

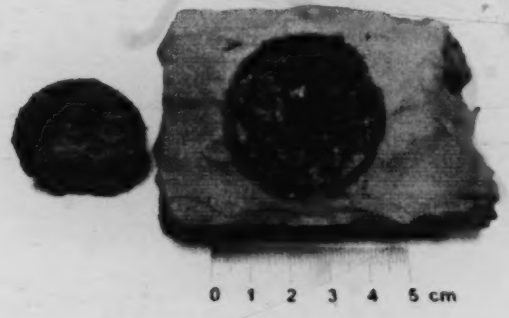

Figure 40 Substrate and liner after a pull-off test.

CHAPTER 4 IMPACT OF SUBSTRATE AND LINER TYPE ON ADHESION

4.1 Substrates

Various types of substrate were used for the tests. These included cinder block, paving stone, limestone, granite and sandstone (Table 3). The substrate surface was either created using a tensile fracture or a saw cut. To create a fresh tensile fracture surface, cores of the substrate material were loaded to failure using a Brazilian test setup. Detailed information on substrate preparation and physical property determination is presented in Appendix B.

Table 3 Substrate tensile strength, porosity, density, surface roughness and average grain/crystal size.

Sample	Tensile strength (MPa)	Average grain size (mm)	Porosity (%)	Bulk density (g/cc)	Surface condition	Roughness
Concrete cinder block	1.6	2	20	2.02	Natural	Flat
Concrete paving stone	3.7	3	11	2.21	Sawn or natural	Flat
Sandstone	1.5	0.2	20	2.02	Split	Rough
Granite	10.4	1.8	1	2.59	Split	Rough
Limestone	2.7	0.2	9	2.42	Split	Rough

It should be noted that cinder block substrate was used for only Tekflex and CS 1251 2k liner materials. When the testing first began, cinder block was selected as one of the substrates. As testing progressed, it was noticed that due to the weak tensile strength of the material, adhesive strength values could not be measured because the cinder block failed in tension before the liner-block interface. For further testing, the use of cinder blocks was discontinued and stronger paving stones were used as the standard substrate.

Tests were performed using six TSL products as listed in Table 4. Most of the testing was done using Tekflex because other products were weak in tension, adhesion values could not be measured. Detailed liner properties are presented in Appendix C. For each group of parameters, at least four tests were done.

Table 4 Test parameters used in the tests.

TSL Products	Substrate Type	Roughness
Tekflex	Paving stone	Flat
	Sandstone	Rough
	Granite	Flat, Rough
	Cinder block	Flat
	Limestone	Rough
Tekflex PM	Paving stone	Flat
	Sandstone	Rough
	Granite	Flat, Rough
	Limestone	Rough
Castonite	Paving stone	Flat
	Sandstone	Rough
	Granite	Flat, Rough
	Limestone	Rough
MBT CS 1251 2K	Sandstone	Rough
	Granite	Flat, Rough
	Limestone	Rough
	Cinder block	Flat
Tunnelguard	Paving stone	Flat
	Sandstone	Rough
	Granite	Flat, Rough
	Limestone	Rough
Rock Web	Norite	Rough

4.2 Tekflex

Tekflex is a two-component, cement-based, fibre-reinforced TSL material. Preparation of Tekflex liner is explained in section 3.2.2. Detailed Tekflex information is presented in Appendix C. It has been used for various geotechnical and mining applications (Figure 41).

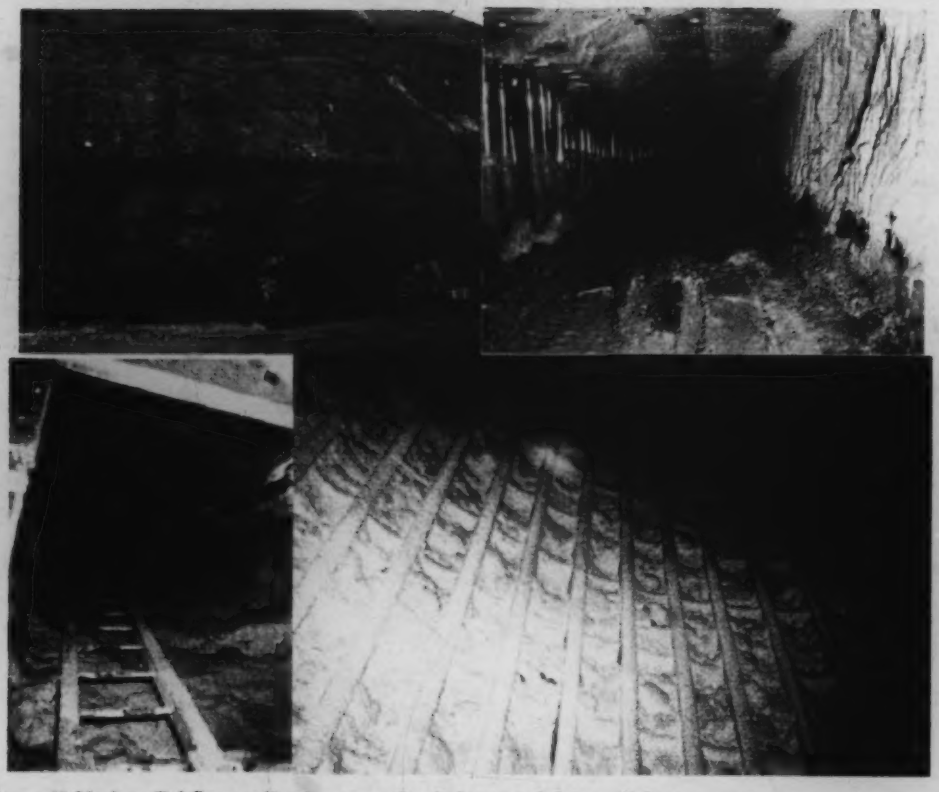

Figure 41 Various Tekflex application examples (mine portal, longwall face support, escape raise support, and ore bin maintenance support) (www.minova.com).

One of the substrates was cinder block sawn in 50 cm by 50 cm size (Figure 42). The average adhesion of clean cinder block substrate to Tekflex is 2.2±0.2 MPa with 95% confidence. Paving stone substrates (Figure 43) were sawn for testing too. The average adhesion of clean paving stone to Tekflex is 1.9±0.2 MPa with 95% confidence.

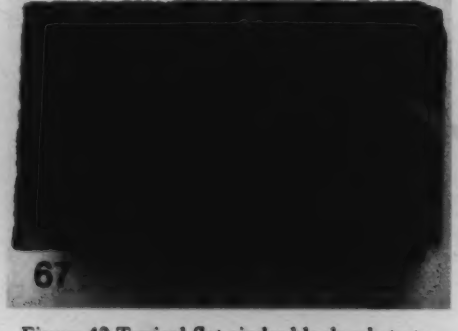

Figure 42 Typical flat cinder block substrate.

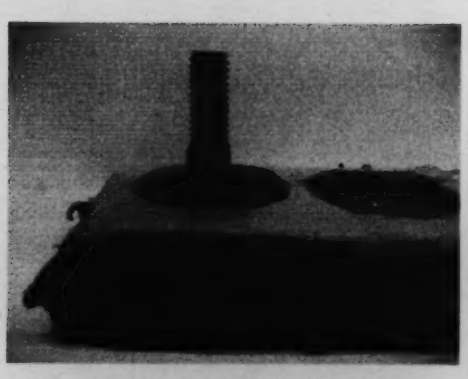

Figure 43 Tekflex cast paving stone substrate.

Three rock types were used for testing: granite, limestone, and sandstone. The average adhesion of Tekflex on saw-cut granite is 1.3±0.2 MPa and average strength on split granite is 1.5±0.4 MPa with 95% confidence. The average adhesion of Tekflex on split limestone is 1.6±0.5 MPa with 95% confidence. All failure types for the sandstone tests were within the substrate. Therefore, the inferred average strength of Tekflex on split sandstone is greater than 0.9±0.2 MPa. Detailed test results are presented in Appendix D.

Application of a fixed liner thickness on the substrates was a big challenge in the sample preparation. Due to the sticky and fast curing nature of the Tekflex, applying a fixed standard thickness on the substrates with spatulas in a short period of time was difficult. As more samples were prepared, a standard thickness application was achieved with experience. Liner thickness variations in the range of 3 to 6 mm may be seen in Appendix D.

For comparison of results, adhesion values were normalized with respect to a liner thickness of 4 mm, the reason being the inverse proportionality of adhesion to thickness, which is explained in Chapter 7. Equation 56 was used to normalize the adhesion and the justification for using this equation is also explained in Chapter 7. Table 5 lists the normalized adhesions. According to normalized adhesion values, the highest adhesion is obtained from the paving stone substrate, and the other substrates are ranked in decreasing adhesion strength order as split granite, split limestone, saw cut granite, cinder block substrates, and split sandstone. From these results, it is concluded that rough surfaces give higher adhesion.

Table 5 Comparison of Tekflex adhesive tests on different substrates.

Substrate	Average adhesion (MPa)	Average normalized adhesion (MPa)
Cinder block	2.2±0.2	0.8±0.1
Paving stone	1.9±0.2	1.8±0.2
Split granite	1.5±0.4	1.4±0.1
Sawn granite	1.3±0.2	1.3±0.3
Split limestone	1.6±0.5	1.4±0.3
Split sandstone	>0.9±0.2	>0.7±0.1

The effect of substrate tensile strength, grain size, porosity, density and grain size on the normalized adhesion was examined. The details of determination of these parameters and test results are explained in Appendix B.

As can be seen from Figure 44, which was plotted using the average values shown in Table 5, there is poor correlation between adhesion and the substrate parameters of tensile strength, grain size, porosity, density, and matrix density. The tests results from the split sandstone were not plotted because the test specimens failed in the substrate.

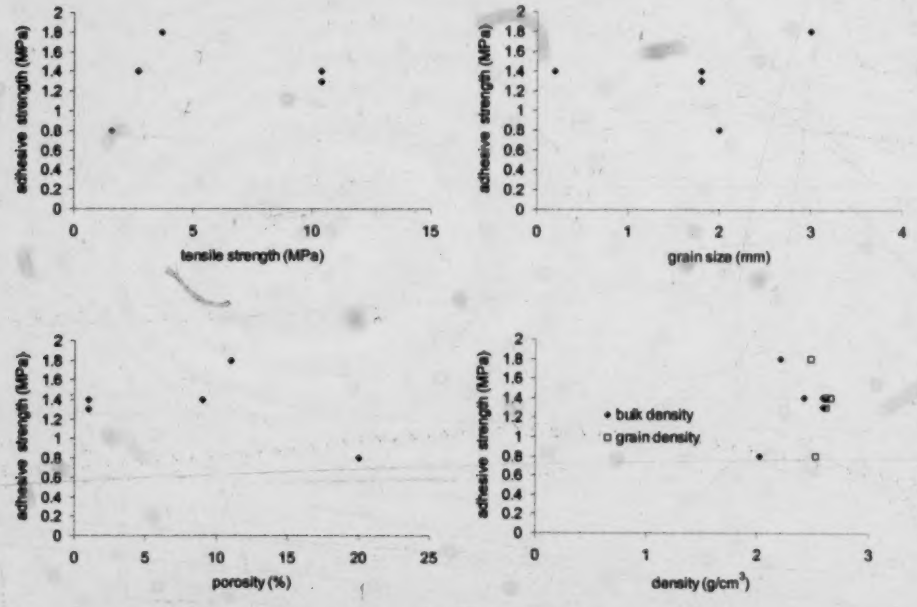

Figure 44 Normalized average adhesion versus substrate properties using Tekflex.

The same analysis was carried for rough and smooth surfaces separately. Figure 45 presents charts for rough surfaces (split granite and limestone). For flat substrates (sawn granite, cinder block, and paving stone), charts are presented in Figure 46. Unfortunately, there is not a sufficiently wide range in substrate properties to assess the role of substrate property on adhesion. It was expected that grain size and porosity would affect adhesion. More tests on different substrates with varying porosities and grain sizes are needed to evaluate the role grain size or porosity play. In the literature, it was concluded that mineral composition plays an important role in shotcrete adhesion (Malmgren et al. 2005).

The tests conducted using sandstone or cinder block clearly demonstrate that if the substrate itself is weak, then it is impossible to generate high adhesion with a TSL as the substrate will always fail in tension first.

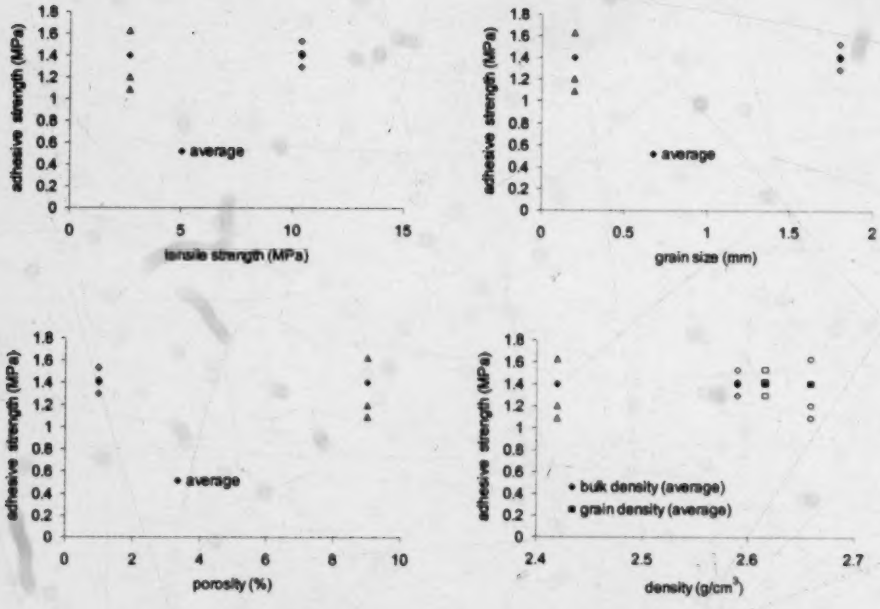

Figure 45 Normalized adhesion versus rough substrate properties.

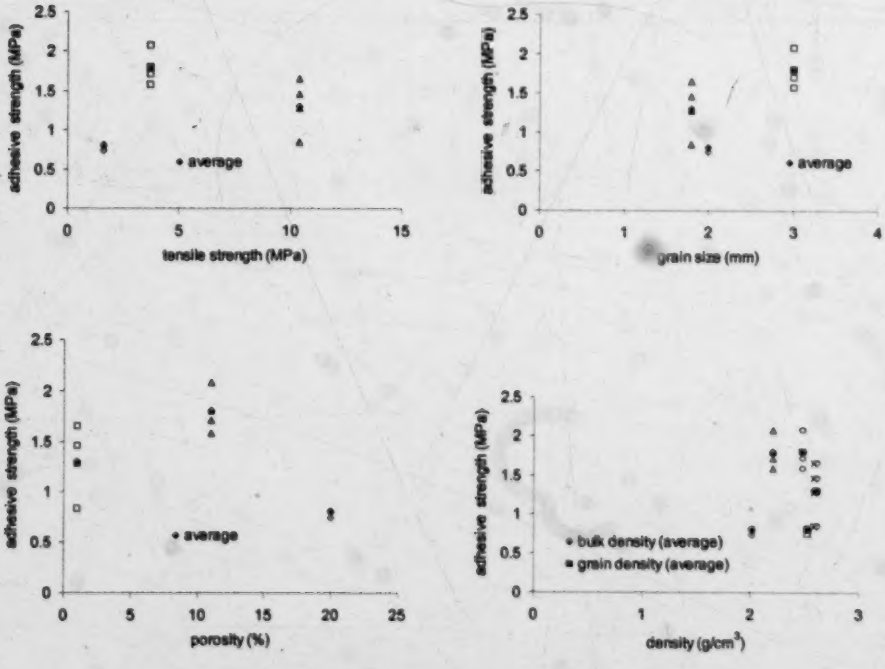

Figure 46 Normalized adhesion versus flat substrate properties.

4.3 Tekflex PM

Tekflex PM is two-component cement-based, non-shrinking cement. Tekflex PM is different and more flexible than Tekflex at low temperatures and unlike conventional Tekflex there is no problem with it freezing in transit to the mine. Detailed information about this product is presented in Appendix C. the two components, water and polymer-modified cement powder were mixed in the laboratory according to manufacturer's suggestions (0.20 water to solid ratio by weight). The mixture is grey in color and the working life of the product is about 30 minutes (Figure 47).

Figure 47 Tekflex PM mixture prepared in the lab.

Substrates were coated with 4-5 mm Tekflex PM material layers (Figure 48). Saw cut granite samples popped out during coring and thus no test data were obtained. For the paving stone substrate, five samples were tested (Figure 49). From these results, it was found that the average adhesion strength of clean paving stone substrate to Tekflex PM is 0.2±0.0 MPa with 95% confidence.

Figure 48 Tekflex PM cast paving stone sample.

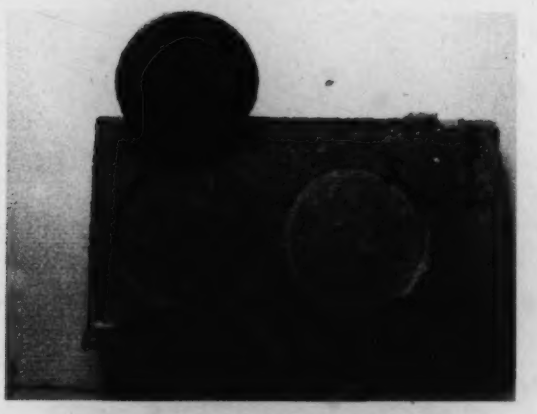

Figure 49 Adhesive failure after the test.

The average adhesive strengths of Tekflex PM on split limestone and split granite (Figure 50) substrates is 0.2±0.0 MPa with 95% confidence.

Figure 50 Typical adhesive failure for Tekflex PM cast split granite substrate.

For comparison of results (Table 6), adhesion values were normalized for a thickness of 4 mm, the reason being an inverse proportionality of adhesion to thickness, which is explained in the theory section. According to normalized adhesion values, paving stone and split granite have the highest adhesion values followed by split limestone. A rough granite substrate increases the adhesion compared to sawn granite substrates, in which fixtures popped off during coring. Rough limestone samples also have an adhesion value close to rough granite samples.

In comparison with Tekflex, Tekflex PM has much lower adhesive strength, so much so that it is unlikely that this product would be viable as a TSL for rock support applications.

Table 6 Comparison of Tekflex PM adhesive tests on different substrates.

Substrate	Average adhesion	Average normalized adhesion
	(MPa)	(MPa)
Paving stone	0.2±0.1	0.5±0.1
Split granite	0.2±0.0	0.5±0.1
Saw cut granite	Popped out	Popped out
Split limestone	0.2±0.0	0.2±0.0
Split sandstone	0.02±0.01	0.0±0.0

4.4 Castonite

Castonite is a two (liquid) component fast setting spray-on liner product that is water-based using acrylic polymer and gypsum. Detailed information for this TSL is included in Appendix C. Components A and B are mixed in a 1:1 volume ratio. The mixing time is 45 seconds and application to the substrate should be finished in 2 minutes. The mixture was prepared in the lab and it was cast to the concrete, granite (saw cut and split), sandstone, and limestone substrates. A typical Castonite product after test is presented in Figure 51.

Figure 51 Typical Castonite product.

For paving stone substrates, all failure types are tensile failure within Castonite. Therefore, it was concluded that the adhesion of Castonite to the clean paving stone substrate must be greater than 1.9±0.3 MPa. Similarly, for split granite, because of tensile failure within Castonite, the lower bound of average adhesion is greater than 1.3±0.3 MPa. Saw cut granite substrate tests also failed within Castonite, with the lower bound of average adhesion as 1.3±0.4 MPa.

Additional tests were conducted using sandstone (Figure 52). For these tests, tensile failure was observed within all the sandstone samples (Figure 53). From these results, it was concluded that the average adhesion of Castonite to sandstone must be greater than 1.2±0.2 MPa with 95% confidence. One other substrate used was limestone, but all test samples popped off during coring, therefore no test results were obtained. Detailed test results are presented in Appendix D.

Figure 52 Sandstone test picture.

Figure 53 Tensile failure within sandstone substrate after the test.

For comparison of results (Table 7), adhesion values were normalized for a TSL thickness of 4 mm, the reason being the inverse proportionality of adhesion to thickness, which is explained in Chapter 7.

Table 7 Comparison of Castonite adhesive tests on different substrates.

Substrate	Average Adhesive Strength (MPa)	Average Normalized Adhesion (MPa)
Paving stone	>1.9±0.3	>1.6±0.3
Split granite	>1.3±0.3	>1.1±0.2
Sawn granite	>1.3±0.4	>1.3±0.4
Split sandstone	>1.2±0.2	>1.2±0.3

Because of TSL tensile or substrate failure occurrences, actual adhesion values of Castonite on different substrates were not quantified. Therefore, lower bounds were found for all tests. Castonite appears to yield good adhesion but the tensile strength of the product is low.

4.5 Tunnelguard

Tunnelguard is a two-component (powder and liquid) product, containing a cement powder with fibres and a liquid polymer. It is a non-reactive liner and slightly green in color (Figure 54). Powder and liquid polymer mixed in 4kg:1l ratio. A ribbon type mixer was used and first 80%of the liquid was added to powder and rest was added slowly. Detailed information is presented in Appendix C.

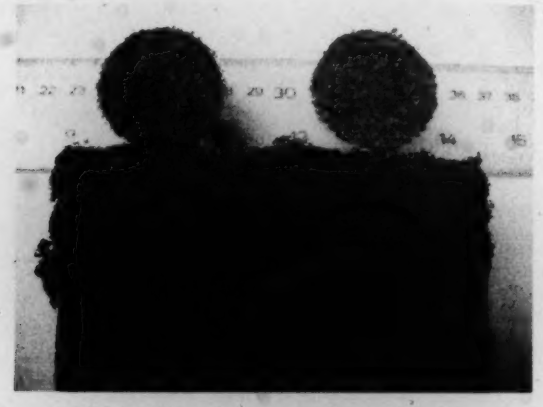

Figure 54 Typical Tunnelguard sample cured on the substrate.

The average adhesion value of Tunnelguard to clean paving stone is greater than 0.4±0.1 MPa. This value is a lower bound because cohesive failure of the TSL occurred within the Tunnelguard and thus did not allow measurement of the true adhesion of the Tunnelguard to paving stone. Similarly, due to cohesive failure within Tunnelguard, adhesion of Tunnelguard to split or sawn granite must be greater than 0.4 MPa. Detailed test results are presented in Appendix D.

The average adhesion strength of Tunnelguard to split limestone is greater than 0.3±0.1 MPa with 95% confidence. Split sandstone substrates (Figure 55) are the only ones that resulted in adhesive failures. The average strength of Tunnelguard to sandstone is 0.3±0.1 MPa with 95% confidence. Detailed test results are presented in Appendix D.

Figure 55 Adhesive failure of Tunnelguard on split sandstone.

For comparison of results (Table 8), adhesion values were normalized with thickness of 4 mm, the reason is being the inverse proportionality of adhesion to thickness, which explained in the theory section.

Table 8 Comparison of Tunnelguard adhesive tests on different substrates.

Substrate	Average adhesion (MPa)	Average normalized adhesion (MPa)
Paving stone	>0.4±0.1	>0.5±0.1
Split granite	>0.4±0.1	>0.5±0.1
Sawn granite	>0.4±0.0	>0.4±0.1
Limestone	>0.3±0.1	>0.3±0.1
Split sandstone	0.3±0.1	0.4±0.1

The cohesive failures within the Tunnelguard test specimens indicate low tensile strength for Tunnelguard.

4.6 MBT CS1251 2k

CS 1251 2k is a two component elastic polymer membrane for spray application onto rock and soil. The product is cement free and gels in less than 3 minutes at 20°C. Detailed information about this TSL is presented in Appendix C. Test substrate specimens were shipped to the United States to get them sprayed (Figure 56).

Figure 56 MBT CS 1251 2K sprayed substrate samples.

For cinder block, split granite, and split limestone since all failure types are tensile within the liner material, an average value for adhesion is calculated as being greater than 0.2 MPa. For sandstone, all failure types are interface failures, therefore, an average value for adhesion of MBT CS 1251 2k to sandstone is 0.1±0.0 MPa with 95% confidence. Detailed test results are presented in Appendix D. In all cases, it is clear that CS 1251 2k has low tensile strength and at best can only generate minor adhesive strength.

Average and normalized adhesion values are presented in Table 9.

Table 9 Comparison of CS 1251 2k adhesive tests on different substrates.

Substrate	Average adhesion (MPa)	Average normalized adhesion (MPa)
Cinder block	>0.3±0.1	>0.2±0.1
Split granite	>0.2±0.0	>0.2±0.0
Limestone	>0.2±0.0	>0.2±0.0
Split sandstone	0.1±0.0	0.1±0.0

4.7 Rock Web

Rock Web is a two component, one to one ratio, polyurea liner material. Detailed information is presented in Appendix C. Rock Web samples were shipped from Inco Copper Cliff Mine, Ontario. Block norite samples were sprayed in the field and were shipped to the university. Rock Web was sprayed on both clean and dusty norite surfaces. The amount of dust present could not be measured. The samples were sawn at the university and tested. Therefore, laboratory controlled adhesive strength tests on different substrates could not be conducted.

For clean norite substrates, interface failure results gave an average adhesion of 1.3±0.8 MPa reaching upper values of 3.0±1.5 MPa with 95% confidence. Detailed test results are presented in Appendix D.

4.8 Summary

Summary of adhesions of the liners are presented in Table 10. For some liners (Tekflex, Tekflex PM, Tunnelguard, and Rock Web) adhesion values are not reported in the product specification sheets, which can be seen in Appendix C. Therefore, a comparison between manufacturer reported and tested values of adhesion is not possible. For Castonite, Appendix C gives adhesion values of 0.5 and 1.8 MPa for 1 day cured and 28 day cured samples, respectively. From this study, adhesion of Castonite to paving stone substrate was found to be greater than 1.9 MPa after 7 days curing. Therefore, there is a good agreement between tested and reported adhesion values. For MBT CS 1251 2K, the specimens typically failed in tension (cohesive failure) through the liner material at a stress of about 0.3 MPa. The reported adhesion value for MBT CS 1251 2K is 1 MPa and based on the test results presented here it raises the question as to how a value as high as 1 MPa could be measured. After testing, MBT CS 1251 2K was pulled off the market.

In the literature, Espley et al. (1999) stated that good adhesion (>0.5 MPa) may be achieved with latex-cement based liners. From Tekflex (latex-cement based liner) adhesion tests, adhesion values reaching 2 MPa were found, which is consistent with the published values. The Tekflex PM adhesion was markedly lower than Tekflex (0.2 versus 1.9 MPa for paving stones). Clearly, although both products are classified as two-component, cement-based liner materials, the Tekflex PM results in lower adhesion. During preparation of dog-bone specimens, it was noted that Teklfex PM is weaker and more brittle than Tekflex, resulting in the fact that no specimens could be made for tensile tests.

Tannant (1997) reported adhesion values greater than 0.5 MPa for polyurea and polyurethane liner materials. Similarly, Archibald (2001) found adhesion values of polyurea and polyurethane

liners ranging between 0.4 and 0.6 MPa. For Rock Web, a polyurea liner, test results on norite substrate show that it has high adhesion, reaching 3 MPa. Archibald (2001) found that adhesion between Rock Web and paving stone to be 0.4 MPa. It is very low compared to the 3 MPa adhesion found from this study, the difference is most probably because he used a much larger (100 mm diameter) loading fixture that was embedded within the liner. It is likely that during the test progressive debonding occurred, which means that the surface area carrying the measured peak load was much smaller than the assumed 100 mm diameter loading fixture.

As can be seen from Table 10, tensile strength of the liners is always greater than the adhesive strength. If tensile strength is less than adhesive strength, the liner will rupture before debonding. Therefore, if 1 MPa adhesion is taken as a desirable bench mark, the tensile strength of liner should be at least 2 MPa to allow for variability in tensile strength and liner thickness.

Table 10 Adhesion test results compared to reported values.

TSL	Substrate	Adhesion (7 days) (MPa)	Adhesion reported (MPa)	Tensile strength (MPa)
Tekflex	cinder block	2.2±0.2	-	-
	paving stone	1.9±0.2		
	split granite	1.5±0.4		
	saw cut granite	1.3±0.2		
	split limestone	1.6±0.5		
	split sandstone	0.9±0.2		
Tekflex PM	paving stone	0.2±0.0	-	-
	split granite	0.2±0.1		
	saw cut granite	popped out		
	split limestone	0.2±0.0		
	split sandstone	0.02±0.01		
Castonite	paving stone	>1.9±0.3	0.5-1.8*	0.4-3.5**
	split granite	>1.3±0.3		
	saw cut granite	>1.3±0.4		
	split sandstone	>1.2±0.2		
Tunnelguard	paving stone	>0.4±0.1	-	-
	split granite	>0.4±0.1		
	saw cut granite	>0.4±0.0		
	split sandstone	0.3±0.1		
MBT CS 1251 2K	cinder block	>0.3±0.1	>1	>2
	split granite	>0.2±0.0		
	split limestone	>0.2±0.0		
	split sandstone	0.1±0.0		
Rock Web	norite	3	-	18

* 1 day - 28 day curing
** 1 hr - 28 day curing

CHAPTER 5 IMPACT OF SURFACE CONTAMINANTS ON ADHESION

5.1 Dust

Rock surfaces underground often become coated in rock dust carried by the ventilation system. To study the effect of dusty surfaces on adhesion, rock flour generated by diamond drilling was sprinkled on the surface of saw-cut paving stone substrates. The amount of dust applied was quantified by measuring the weight of the sample before and after the application of dust. Dust was sprinkled on the substrates by hand as uniformly as possible and pictures were taken. For Tekflex, a series of tests was carried out using varying quantities of dust. For other products, 0.005 g/cm^2 of dust was applied to paving stone substrates and the test results were compared with clean paving stone substrates.

Dust contamination tests were only conducted on paving stone substrates to avoid problems associated with variable surface conditions when using rock slabs. In addition, the substrate must have a higher tensile strength value as compared to the adhesive strength of the liners. Paving stones are strong in tension, off-the-shelf items, cheap, and they do not show variable surface conditions. Cinder blocks could have been chosen as a substrate, but because of their weak tensile strength, they were not used.

Additional tests were conducted using Rock Web applied to norite substrates. The Rock Web test specimens were shipped directly from the mine and the amount of dust present could not be quantified.

5.1.1 Tekflex

Paving stones were used as the substrate for all tests and different quantities of dust were sprinkled on the test sample surfaces before the Tekflex was applied. The dust quantities are listed in Table 11.

Table 11 Dust quantities.

Description	Dust (g/cm^2)
Highly Dusty	0.005
Moderately Dusty	0.0025
Lightly Dusty	0.00084

Test specimens with varying amounts of rock dust can be seen in Figure 57. This figure also shows how much dust ends up on a finger that is wiped across the surface of the substrate.

Figure 57 Saw-cut paving stones with varying amounts of dust (a) highly dusty, (b) moderately dusty and (c) lightly dusty.

Dust controlled test results are summarized in Table 12. Detailed test results are presented in Appendix D (Figures D24-D31).

Table 12 Comparison of Tekflex adhesive tests on dusty paving stone substrates.

Substrate	Dust	Average adhesion	Average normalized adhesion	Decrease in adhesion	Decrease in normalized adhesion
	(g/cc^2)	(MPa)	(MPa)	(%)	(%)
Highly dusty	0.005	0.3±0.1	0.2±0.1	84	85
Moderately dusty	0.0025	1.0±0.1	0.9±0.1	40	41
Lightly dusty	0.00084	1.4±0.1	1.5±0.1	14	8
Clean	none	1.6±0.1	1.6±0.2	-	-

The presence of dust on the substrates can significantly reduce the adhesion; highly dusty samples caused an 84% decrease in adhesion while, moderately and lightly dusty samples caused 40% and 14% decreases in adhesion, respectively. The significance of the test is addressed in Table 13 by the procedure that is explained in Appendix E.

Table 13 Comparison of significance of test results for Tekflex on dusty paving stone substrate.

Sample	Mean	Conf.	T	Student	Significance	
	(MPa)	(%)		Dist.	Adhesion	Normalized Adh
Clean Lightly Dusty	1.6±0.1 1.4±0.1	95	3.45	2.45	significant	not significant
Clean Moderately Dusty	1.6±0.1 1.0±0.1	95	8.67	2.45	significant	significant
Clean Highly Dusty	1.6±0.1 0.3±0.1	95	21	2.45	significant	significant
Lightly Dusty Moderately Dusty	1.4±0.1 1.0±0.1	95	7.19	2.45	significant	significant
Lightly Dusty Highly Dusty	1.4±0.1 0.3±0.1	95	26	2.45	significant	significant
Moderately Dusty Highly Dusty	1.0±0.1 0.3±0.1	95	13.9	2.45	significant	significant

For highly dusty cinder block substrates (0.005 g/cm^2), the average strength of Tekflex was 0.8±0.2 MPa with 95% confidence. Detailed test results are presented in Appendix D.

5.1.2 Rock Web

The amount of dust present could not be measured. The samples were sawn at the university and tested.

For clean norite substrates, interface failure results gave an average adhesion of 1.3±0.8 MPa reaching upper values of 3.0±1.5 MPa with 95% confidence. For dusty norite substrates, interface failure results gave adhesion values of 2.3±0.6 MPa reaching upper values of 3.1±1.4 MPa with 95% confidence. Detailed test results are presented in Appendix D.

When some dusty samples were closely observed, it was concluded that Rock Web material is not homogeneously mixed or dust was mixed with the Rock Web material during spraying action. Therefore, the effect of dust on this product was not able to be reliably determined.

5.1.3 Other products

Three dusty Castonite samples were popped off during coring, therefore, only one sample was tested and 0.5 MPa adhesive strength was recorded. This value can be taken as the upper bound for the adhesion of Castonite to the dusty concrete substrate. For Tekflex PM, eight samples were prepared and all of them popped off in coring.

5.1.4 Summary

A summary of the dust-controlled tests is presented in Table 14.

Table 14 Summary of dust-controlled tests.

TSL	Substrate	Ave. adhesion (MPa)	Ave. normalized adhesion (MPa)	Decrease in normalized adhesion (%)
Tekflex	Clean paving stone	1.6±0.12	1.6±0.2	
	Highly dusty paving stone	0.3±0.05	0.2±0.1	85
Tekflex PM	Clean paving stone	0.2±0.05	0.5±0.1	
	Highly dusty paving stone	0.00±0	0.00±0	100
Castonite	Clean paving stone	1.9±0.32	1.6±0.3	
	Highly dusty paving stone	0.1±0.24	0.2±0.1	94
Rock Web	Clean norite	1.3±0.8	1.0±0.6	
	Dusty norite	2.3±0.9	1.6±0.6	na

Highly dusty substrates can cause a substantial decrease in adhesion for Tekflex and Castonite. For the Rock Web, a reduction in adhesion when spraying the product on dusty norite was not observed.

5.2 Oil

Oil contamination of the rock surface can occur in underground mines. To evaluate the impact of oil contamination on adhesion, hydraulic oil was applied on the surface of saw-cut paving stone substrates. The amount of oil present was quantified by measuring the volume of the oil applied to a unit area of the substrate surface. For Tekflex, a number of tests were conducted with varying amounts of oil. For other TSL products, 0.1 cc/cm^2 of oil was applied to paving stone substrates and the test results were compared with clean paving stone substrates.

5.2.1 Tekflex

For the oil-controlled tests, varying amounts of hydraulic oil were spread using syringe on the paving stone substrates. The quantity of oil used is classified according to Table 15.

Table 15 Oil classification table.

Description	Oil (cc/cm^2)
Highly Oily	0.1
Moderately Oily	0.03
Lightly Oily	0.008

A saw-cut paving stone with lightly oily surface is shown in Figure 58. The photo also shows a small piece of tissue paper, which was wiped across the surface of the substrate.

Figure 58 Lightly oily paving stone surface.

A liner thickness of 3.5 to 4 mm was used for the tests. Detailed test results are presented in Appendix D (Figure D32). All highly and moderately oily samples and two lightly oily samples popped off during the overcoring, therefore just two lightly oily samples were able to provide test data. The average adhesion based on the two tests was 0.8±0.0 MPa. This represents a drop by 50% from the adhesion measured on clean saw-cut paving stone surfaces. If the adhesion values of popped off samples are taken as zero, it can be concluded that as the amount of oil applied goes up, the adhesion drops even further.

For oily cinder block substrates (0.1 cc/cm^2), the average adhesion was 1.1±0.5 MPa with 95% confidence. The drop in adhesion caused by the presence of the oil on the cinder blocks was not as dramatic compared to the paving stones. A possible explanation for this observation is that the much more porous cinder block can absorb the oil into its pores leaving less oil on the surface to affect the adhesive bond to the TSL.

5.2.2 Other products

For all TSL products, the presence of oil on paving stone substrates significantly decreases the adhesion. For Castonite, all the samples popped off during coring. Therefore, it is concluded that the adhesion of Castonite to an oily concrete substrate is very low, although it could not be quantified. For Tekflex PM and Tunnelguard, many tests specimens were prepared, but all of them popped off before testing.

5.3 Moisture

A potentially important contaminant is the presence of water on the substrate. To evaluate the impact of moisture on the measured adhesion, tap water was used to create damp substrates

consisting of saw-cut paving stones. The substrates were placed under tap water for one minute and they were left at room temperature for a half a minute before application of the liners. Four TSL materials were tested: Tekflex, Tekflex PM, Tunnelguard, and Castonite. It should be noted that CS 12512k and Rock Web liners were not used in moisture-controlled tests. Due to uncontrollable shipment conditions, moisture quality control of Rock Web and CS 12512k liners was impossible.

The average value of adhesion of Tekflex to damp paving stone was 2.1±0.2 MPa with 95% confidence. Average adhesion of Tekflex PM to damp paving stone was 0.2±0.2 MPa with 95% confidence. The lower limit for adhesion of damp paving stone substrates to Tunnelguard was 0.5±0.1 MPa with 95% confidence. For Castonite, cohesive failure within the liner was observed. From these results, it was concluded that the average adhesion of Castonite to damp concrete must be greater than 1.8±0.4 MPa with 95% confidence. Epoxy failures were not taken into consideration in averaging values. Detailed test results are presented in Appendix D.

A summary of the test results is presented in Table 16. The presence of moisture on the paving stone surface may increase adhesion for some cement-based products. The increase in adhesion for Tekflex appears to be significant based on the results of a significance test using the procedures described in Appendix E.

Table 16 Summary of tests to evaluate the effect of moist substrate surfaces on adhesion

TSL	Substrate	Ave. adhesion (MPa)	Ave. nor. adhesion (MPa)
Tekflex	Clean paving stone	1.6±0.1	1.6±0.2
	Damp paving stone	2.1±0.2	2.1±0.3
Castonite	Clean paving stone	1.9±0.3	1.6±0.3
	Damp paving stone	1.8±0.4	1.4±0.2
Tekflex PM	Clean paving stone	0.2±0.2	0.2±0.1
	Damp paving stone	0.2±0.2	0.3±0.2
Tunnelguard	Clean paving stone	0.4±0.1	0.5±0.1
	Damp paving stone	0.5±0.1	0.5±0.2

CHAPTER 6 IMPACT OF CURING TIME, LOADING RATE, CREEP AND LINER THICKNESS ON ADHESION

6.1 Curing Time

The effect of curing time was studied by comparing Tekflex specimens cured for one week and one month. The other products were not tested because of their weak tensile strength values. Saw cut granite and paving stone (clean or damp) were used for substrates. The results presented in Table 17 show that an increase in curing time can significantly increase the adhesion. This is to be expected with a cement-based liner material.

Table 17 Measured adhesion (mean & standard deviation in MPa) after 1 week and 1 month of curing time.

Sample	No. of tests	1 week	No. of tests	1 month
Saw cut granite	4	1.3 (0.1)	3	2.5 (0.3)
Clean paving stone	5	1.9 (0.2)	4	3.4 (0.2)
Damp paving stone	2	2.1 (0.2)	3	2.5 (0.6)

6.2 Loading Rate

To test the effect of different loading (displacement) rates, saw-cut paving stones were used with Tekflex liner material. Loading rates of 0.1, 0.5, 1, and 2 mm/min were used. The specimens were cured for 7 days under laboratory room conditions and the liner material was about 3 mm thick. A plot of loading rate versus adhesion is presented in Figure 59. Although there may be some impact of the loading rate on the measured adhesion, the effect is negligible for the loading rates that were used.

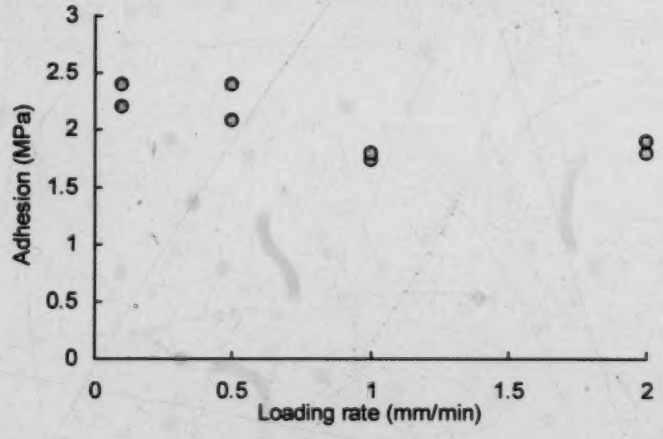

Figure 59 Loading rate versus adhesion.

6.2.1 Creep

One concern with polymer liners is their creep characteristics. Simple tests have demonstrated that most liner materials will creep and rupture at stresses much less than the values quoted for

their tensile strengths. The impact of creep on the load capacity of a liner in conditions where a liner is supporting the gravitation load from loose broken rock is unknown (Tannant 2004).

Creep test samples are prepared using a method similar to the standard adhesion test explained earlier, the only difference being the use of elevator bolts for both top and bottom parts of the substrate (Figure 60). Sawn paving stone was used as a substrate.

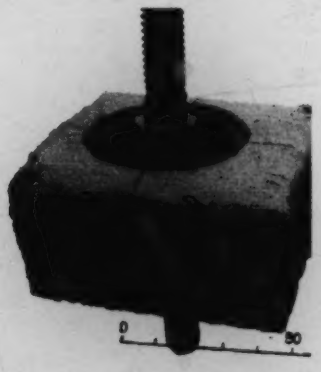

Figure 60 Typical creep test sample.

For creep tests, a new testing setup was prepared, which is based on applying dead loads to samples (Figure 61).

Figure 61 Creep test set up

Dry Tekflex product that was at least 17 months old was mixed to create a coating 3 to 4 mm thick on the paving stones. The liner was allowed to cure for varying periods before the dead-weight loads were applied. Each test specimen was loaded with a different mass to generate a range of applied stresses over the overcore area. The test measured the time that it took for the adhesive bond to fail after application of a constant load. The test parameters are presented in Table 18 and Figure 62.

Table 18 Creep test parameters.

No. of tests	Curing time (days)	Applied stress range (MPa)
6	7	0.66 – 1.1
18	45 to 62	0.43 – 1.6

Figure 62 shows, as anticipated, that as the magnitude of the dead-weight decreases, the adhesive bond lasts longer before it ruptures. Important practical implications from this test are that adhesive strengths obtained from the standard adhesion test can over-predict the long-term adhesion between a substrate and a liner. In a field situation where a liner carries loads from loose rock, the liner may fail weeks to months after the load is applied. After 500 to 1000 hours of sustained loading, the adhesive bond strength between old Tekflex and paving stones drops to less than 0.5 MPa, a reduction of at least 50% compared to adhesion measured under loading conditions that cause failure within 60 seconds.

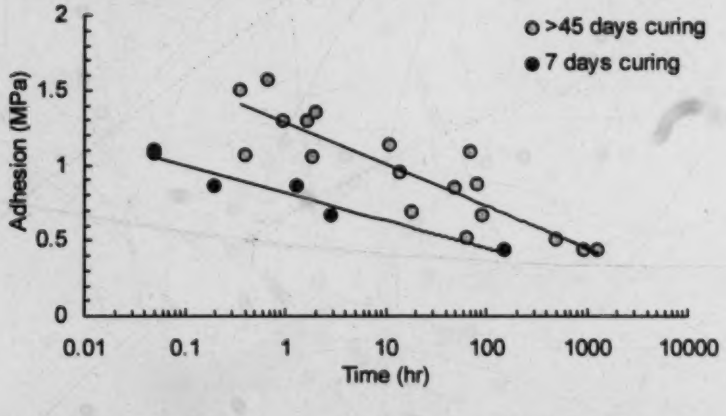

Figure 62 Adhesion versus time to failure after application of the load.

Figure 62 also shows that at any given failure time, the seven-day cured samples have lower adhesion compared to the test specimens that were cured for more than a month. These results are consistent with those presented earlier. Therefore, it appears that Tekflex would function better as long-term support when it has the chance to cure fully before it begins to carry load from loose rock.

6.3 Liner Thickness

During the adhesion testing, it was noted that the Tekflex liner thickness appeared to influence the magnitude of the measured pull-off force. Therefore, the effect of liner thickness was studied using Tekflex liner material on saw-cut granite and clean paving stones. Samples were cured for 7 days. Table 19 shows the parameters used in testing. For all tests, a 2 mm/min loading rate is used. The effect of changing liner thickness on a clean paving stone substrate is presented in Figure 63.

Table 19 Thickness test variables and substrates.

Sample	Thickness of liner (mm)
Paving stone	1, 2.25, 2.5, 3.25, 3.5, 5, 7, 7.75, 8, 9.5, 15
Saw cut granite	1, 3, 3.25, 4.25, 4.5, 4.75, 6.5, 6.75, 7.75, 8.75

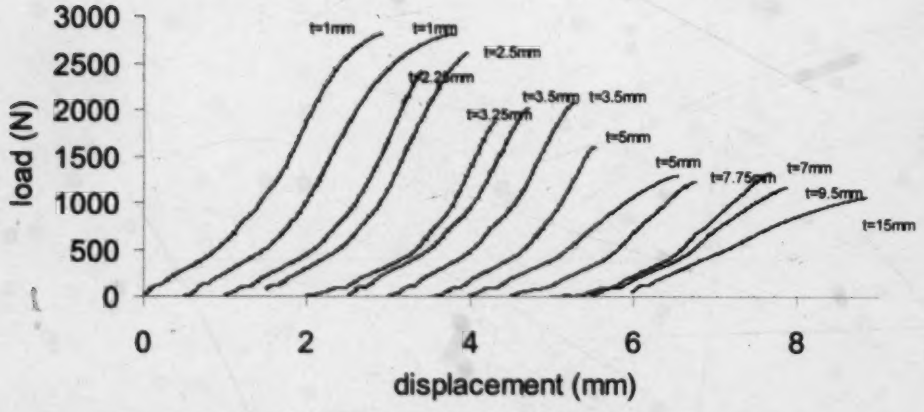

Figure 63 Effect of changing liner thickness on clean paving stone substrate.

As can be seen from Figure 63, thicker liners applied to paving stones result in a decreasing pull off force or adhesion. The same effect was obtained when using clean saw cut granite substrates (Figure 64).

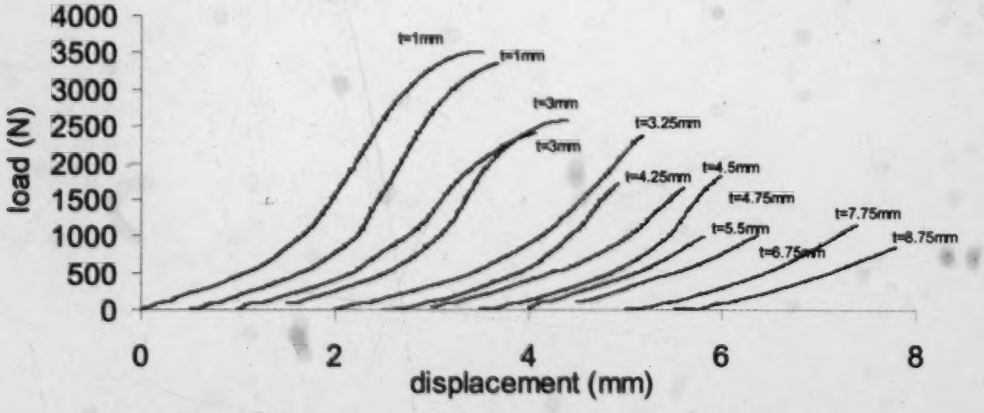

Figure 64 Effect of changing liner thickness on clean saw cut granite substrate.

Another observation from these tests is that as liner thickness increases, the load displacement curve becomes more linear, rather than the 'S' shape that occurs for relatively thin liner thicknesses. With thicker liners, the more compliant layer, which is the liner itself, dominates the load-displacement curve. When the first part of the load-displacement curve for all tests is examined, it can be seen that the slopes are the same up to almost 700 N after which slopes become steeper, suggesting an equivalent stiffness value (elevator bolt, epoxy and liner) for the tests. In addition, comparison of load-displacement behaviour of thicker liner tests with relatively

thinner ones shows that the first linear part of the curves is liner dependent (more compliant) rather than representative of deformation of the system. Therefore, each pull-out test is unique having a unique load-displacement behaviour and stiffness value. However, it can be concluded that, for up to 700 N of loading, the liner material dominates the load-displacement behaviour for all thicknesses. After 700 N loading, the load-displacement curves become steeper, suggesting an equivalent stiffness (elevator bolt, epoxy and liner) value for the system for liner thicknesses from 1 mm to 8 mm. This result can be seen clearly from the softening behaviour of load-displacement curves as the thickness increases.

The relationship between the measured adhesion and liner thickness using the data in Figure 63 and Figure 64 is presented in Figure 65.

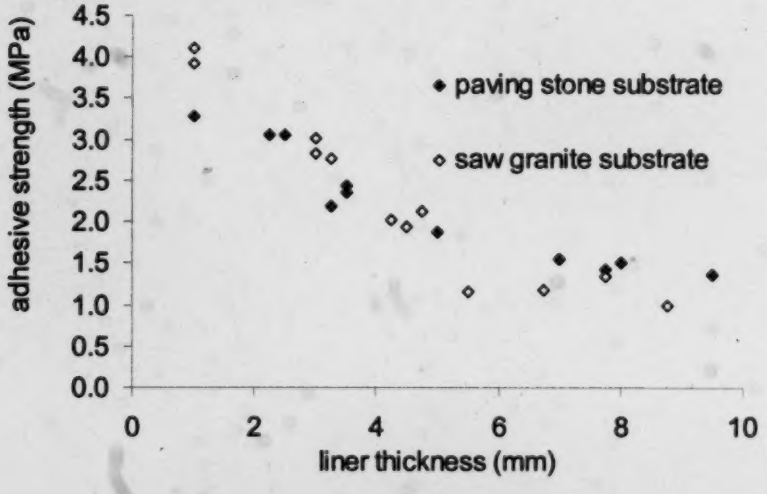

Figure 65 Relationship between the adhesion and thickness of liner.

As can be seen from Figure 65, adhesive strength and liner thickness are inversely proportional. The next chapter explores the theoretical relationship between adhesion and liner thickness and explains the trend seen in Figure 65.

CHAPTER 7 ADHESION THEORY

7.1 Introduction

The aim of this chapter is to analyse the work of adhesion (the work required to separate a unit area of the contacting surfaces) analytically and to compare test results with closed-form solutions. This chapter starts with behaviour of elastic material loaded by a circular punch, which is required to find the load-displacement behaviour of the liner that will be used in driving the work of adhesion equation. It is also important to analyse the behaviour of crack propagation at the liner rock interface. This chapter continues with the derivation of the work of adhesion equation. Later, depending on the testing geometry, deformation map of debonding liners is introduced. Then, comparison of test results with closed-form solutions is given. Finally, methodology to calculate the work of adhesion from test results and normalization of adhesion is introduced.

7.2 Elastic Material Loaded by a Circular Punch

7.2.1 Half space model

Consider the case of a rigid disc of diameter $2a$ making perfect contact with an infinite plane of elastic material of Young's Modulus E (Figure 66) and ν is the Poisson's ratio of the elastic material. When a detaching force P is applied to the disc, the elastic material deforms according to the Boussinesq's (1885) equation

$$\delta = \frac{P(1-\nu^2)}{2Ea} \tag{11}$$

where δ is the movement of the disc normal to the surface.

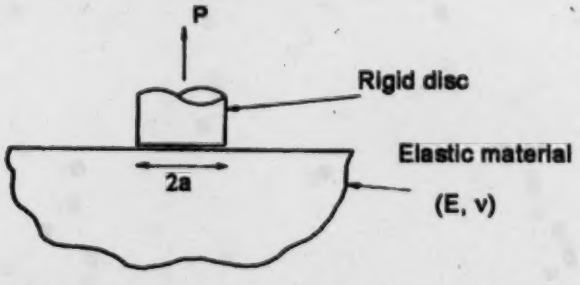

Figure 66 Contact between a rigid disc and an infinite elastic medium.

Boussinesq gives the normal stress distribution of half space loading as a function of radius r as

$$\sigma_z = \frac{2E\delta}{\pi a(1-\nu^2)}\left(\frac{1}{\sqrt{1-r^2/a^2}}\right) \tag{12}$$

7.2.2 Thin layer model

For a thin layer relative to the punch diameter (Figure 67), the imposed force gives the following vertical stress distribution (Lindsey 1967):

$$\frac{\sigma_z}{E\varepsilon} = \frac{\nu}{(1+\nu)(1-2\nu)}\left(1-\frac{I_0(\kappa r)}{I_0(\kappa a)}\right)+\frac{1}{1+\nu}\left(1+\frac{1}{2}\frac{I_0(\kappa r)}{I_0(\kappa a)}\right) \tag{13}$$

with

$$\kappa = \frac{2}{t}\sqrt{3(1-2\nu)} \tag{14}$$

where I_0 is Bessel's function of the order zero, ε is average macroscopic deformation of the film δ/t, and t is layer thickness.

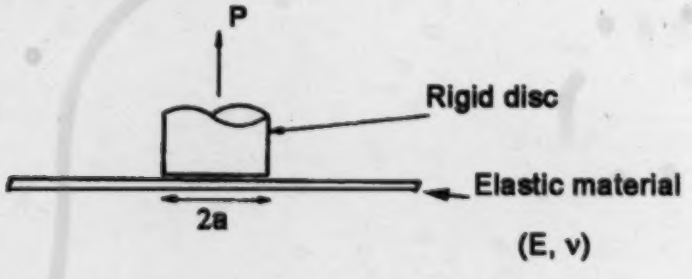

Figure 67 Contact between a rigid disc and elastic thin film.

When Equations (12) and (13) are compared (Figure 68), it can be seen that for both equations, maximum vertical stress under the punch occurs at the edge of the punch and it decreases and becomes minimum at the center of the punch. The same conclusion also can be seen in finite element modelling (Appendix A). Therefore, for both cases, propagation of a tensile rupture during an adhesion test will first occur from the outside of the punch and progress toward the center.

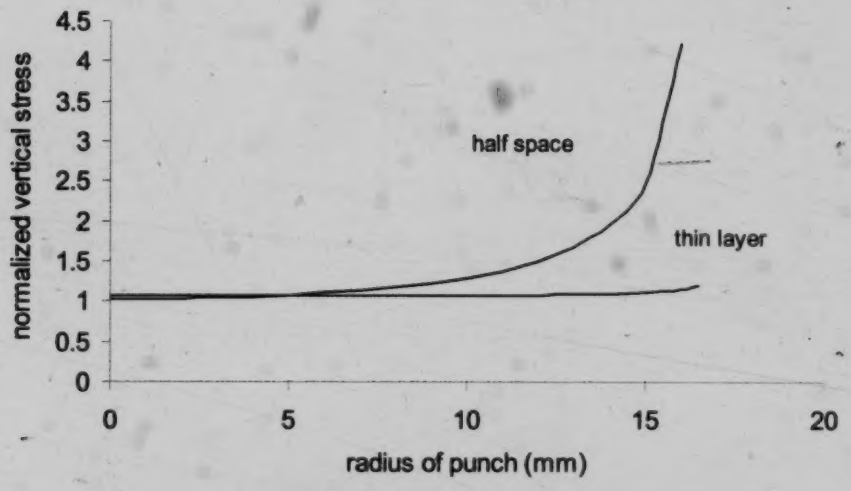

Figure 68 Vertical stress under a 33 mm diameter punch on a 4 mm thick liner (ν =0.25)

7.3 Work of Adhesion

The work required to separate a unit area of the contacting surfaces is called work of adhesion. Kendall (1971) first formulated the adhesion of elastic solids based on the energy of the system (elastic solid and rigid substrate). If the total energy which is the sum of adhesion energy, stored elastic energy, and potential energy of the applied load in a strained pull-out test of dimension a is U_T then adhesive rupture is possible when

$$\frac{dU_T}{da} \geq 0 \tag{15}$$

This equation is merely a statement of the fact that the total energy of the pull-out system cannot rise as fracture occurs.

When

$$\frac{dU_T}{da} > 0 \tag{16}$$

surplus energy is produced as fracture of the adhesive bond proceeds. This surplus energy may appear as an acceleration of a propagating crack or may be dissipated in viscous processes dependent on the rate of separation of the molecular bonds. When

$$\frac{dU_T}{da} = 0 \tag{17}$$

the work done in breaking the adhesive bonds is exactly compensated by the gain in surface energy of the system.

A condition for peeling of two adhesively bonded surfaces may be derived by considering the total energy U_T in the system. The total energy is made up of three terms, the surface adhesive energy U_S, the stored elastic energy U_E in the deformed material and the potential energy U_P in the applied load.

The adhesive energy is

$$U_S = -\pi a^2 \gamma \tag{18}$$

where γ is the work of adhesion defined as the energy required to separate a unit area of the contacting surfaces, a is the radius of the pull out test. Work of adhesion is a material property and is the product of effective bond thickness and adhesive strength.

The stored elastic energy is

$$U_E = \int P d\delta \tag{19}$$

Using Equation (11)

$$U_E = \frac{(1-\nu^2)P^2}{4Ea} + A \tag{20}$$

where E is Young's Modulus, ν is Poisson's ratio, P is pull out load, δ is displacement, and A is an arbitrary constant.

The potential energy of the load is

$$U_P = -P\delta + B \tag{21}$$

where B is an arbitrary constant. From Equation (11)

$$U_P = -\frac{(1-\nu^2)P^2}{2Ea} + A + B \tag{22}$$

Equilibrium peeling is possible at constant load P when Equation (17) is satisfied.

$$P^2 = \frac{8\pi}{(1-\nu^2)} E\gamma a^3 \tag{23}$$

Kendall (1971) gives the peeling load for a thin film of elastic material of thickness t sandwiched between an infinite rigid plane and a rigid disc of radius a (Figure 69). He suggests that the result of sandwiched layer solution can be used for pull-off testing of paint films and evaporated coatings. For relatively thick, low modulus coatings, where most of the deformation occurs in the film itself, Equation (23) applies. However, for very thin films of high elastic modulus it is clear that most of the deformation will take place in the substrate and Equation (24) applies.

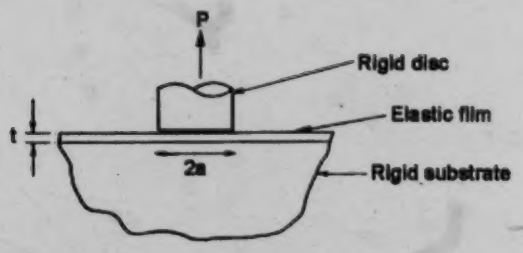

Figure 69 Elastic glue film sandwiched between rigid plane surfaces.

Using the same energy summation procedure above, he gives the peeling force by

$$P^2 = \frac{2\pi^2 K \gamma a^4}{t} \tag{24}$$

where K is bulk modulus. This equation is wrong because his assumption of the force-displacement relationship for thin film under tensile loading Equation (25) is invalid.

$$P = \frac{K\pi a^2 \delta}{t} \tag{25}$$

The correct force-displacement relationship is derived in the next section.

7.3.1 Force-displacement relationship of thin film

The force-displacement relationship for an elastic thin disc of radius a under tensile loading can be found as follows:

Let us cut out a thin disc with a radius 'a' from the thin film under the dolly (Figure 70).

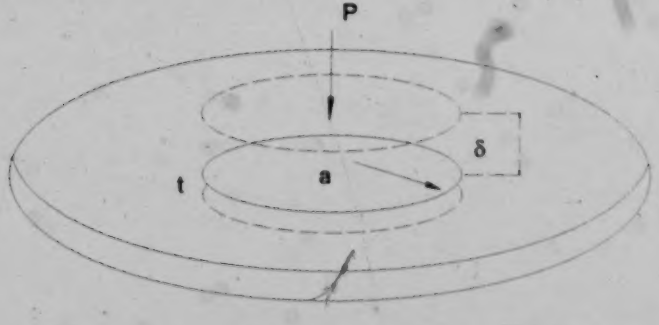

Figure 70 Thin disc film under loading.

The disc will expand, (Figure 71) which can be found from Equation (26) (Timoshenko and Goodier 1969).

Figure 71 Thin disc cut out from the liner.

$$\varepsilon_{\theta\theta} = \frac{\sigma_{\theta\theta}}{E} - \frac{\nu\sigma_{rr}}{E} - \frac{\nu\sigma_{zz}}{E} = \frac{m}{a} \Rightarrow m = \frac{\nu a\sigma}{E} \tag{26}$$

where, ε_{tt} is tangential strain, σ_{tt}, σ_{rr}, and σ_{zz} are tangential, radial, and axial stresses, ν is Poisson's ratio, E is Young's Modulus, m is expansion, and a is the radius of thin disc.

If we put the enlarged disc back in the hole, in the film a pressure 'R' will develop around the periphery of the disc (Figure 72). This pressure 'R' will shrink the disc in the radial direction by Equation (27).

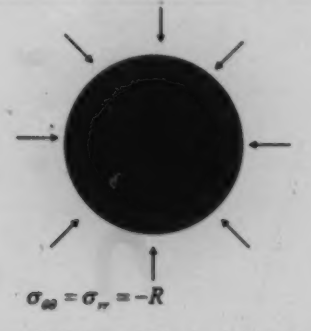

Figure 72 Enlarged film back in the hole.

$$\varepsilon_{\theta\theta} = \frac{\sigma_{\theta\theta}}{E} - \frac{\nu\sigma_{rr}}{E} - \frac{\nu\sigma_{zz}}{E} = \frac{r}{a} \Rightarrow r = \frac{-aR(1-\nu)}{E} \tag{27}$$

The same pressure will enlarge the hole (Figure 73) by (Equation (28))

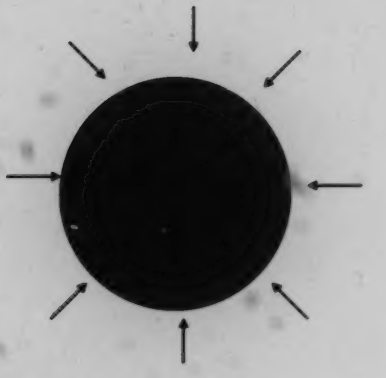

$$\sigma_{\theta\theta} = -\sigma_{rr} = R$$

Figure 73 Enlarged hole.

$$\varepsilon_{\theta\theta} = \frac{R}{E} + \frac{\nu R}{E} = \frac{k}{a} \Rightarrow k = \frac{aR(1+\nu)}{E} \tag{28}$$

To fit the disc back into the hole

$$k - r = m = \frac{\nu a \sigma}{E} \Rightarrow \therefore R = \frac{\nu \sigma}{2} \tag{29}$$

Axial strain (ε_{zz}) can be written as

$$\varepsilon_{zz} = \frac{\delta}{t} = \frac{\sigma}{E} - \frac{\nu^2 \sigma}{2E} - \frac{\nu^2 \sigma}{2E} \Rightarrow \frac{\delta}{t} = \frac{\sigma}{E}\left(1 - \nu^2\right) \tag{30}$$

Therefore, correct load-displacement behaviour of a thin disc can be written as

$$P = \frac{E \pi a^2 \delta}{t\left(1 - \nu^2\right)} \tag{31}$$

This equation differs from the incorrect equation presented by Kendall (1971), Equation (25).

The stored elastic energy can be expressed as

$$U_E = \int P d\delta \tag{32}$$

Using Equation (31)

$$U_E = \frac{\left(1 - \nu^2\right) P^2 t}{2E\pi a^2} + A \tag{33}$$

where A is an arbitrary constant.

The potential energy of the load is

$$U_P = -P\delta + B \tag{34}$$

where B is an arbitrary constant. From Equation (31)

$$U_P = -\frac{\left(1-\nu^2\right)P^2 t}{E\pi a^2} + A + B \tag{35}$$

The surface energy is

$$U_S = -\pi a^2 \gamma \tag{36}$$

Equilibrium peeling is possible at constant load P when Equation (17) is satisfied; therefore, the peeling force required for separation is given by

$$P^2 = \frac{2\pi^2 E\gamma a^4}{t\left(1-\nu^2\right)} \tag{37}$$

As can be seen from Equation (37) work of adhesion can be found if elastic properties of the liner are known. In the next section, debonding of a liner from the substrate is analyzed.

7.4 Debonding Approach

Crosby et al. (2000) define three main deformation modes that can be used to categorize the early stages of the debonding processes of a compliant layer from a rigid substrate. These three modes are described below.

1. Edge crack propagation [Figure 74a]:

This failure mechanism is simple adhesive failure. The contact perimeter decreases uniformly as the compliant layer separates from one of the rigid substrates. The energy applied to the system is shared between propagating the interfacial crack and any viscoelastic losses in the bulk of the compliant layer. This mechanism of debonding can be effectively characterized using a fracture mechanics analysis.

2. Internal crack propagation [Figure 74b]:

In some situations, stress at the interface develops to a point where a penny-shaped, internal crack will grow. If this defect remains at the adhesive/substrate interface, the growth of the penny-shaped crack is controlled by the same material properties controlling simple edge crack propagation. Typically, many internal cracks will nucleate and eventually coalesce when final failure occurs.

3. Cavitation [Figure 74c]:

This mode of deformation is similar to internal crack propagation, but the cavity expands into the bulk of the compliant layer instead of propagating at the interface. Growth of these bulk cavities corresponds to the early stages of fibrillation, which must take place in order for large deformations to be achieved. In addition to these three main classes of deformation, the

following two subclasses, related to the shape of the edge of the compliant layer, can also be defined.

4. Edge crack fingering:

This failure mode is analogous to simple edge crack propagation with the exception that the contact perimeter does not decrease uniformly in all directions.

5. Bulk fingering [Figure 74d]:

Bulk fingering is visually similar to edge crack fingering. However, with bulk fingering the shape instability exists within the bulk of the compliant layer and not at the interface with the rigid indenter. Bulk fingering is closely related to cavitation, with the difference being that the cavity-type defect forms at the edge of the compliant layer. Once nucleated, these defects grow parallel to the adhesive/substrate interface.

The interfacial deformation modes (1, 2, and 4) are governed by the energy release rate describing the driving force for crack propagation, whereas the bulk deformation modes (3 and 4) are governed by the stress within the layer. The relationship between the average stress within the layer and the energy release rate is, in turn, determined by the degree of lateral confinement. This degree of confinement is defined by a representative dimension of the contact area in the stressed region, in comparison to the thickness of the compliant layer. The degree of confinement is defined by the ratio of the contact radius a to the thickness of the layer t.

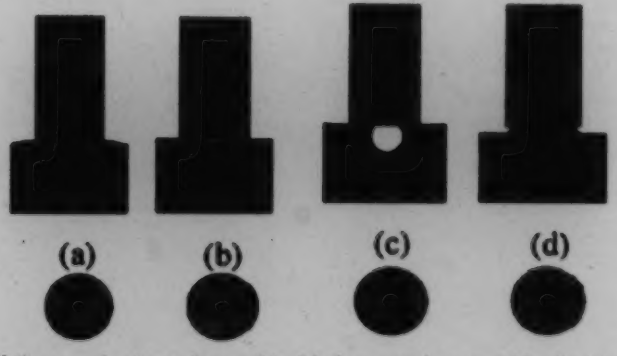

Figure 74 The basic failure mechanisms observed in thin layers under normal loads: (a) Edge crack propagation; (b) internal crack propagation; (c) cavitation; (d) bulk fingering (Crosby et al. 2000).

For low values of a/t there is a lateral Poisson contraction of the cylinder as it is extended. As a/t increases, the lateral strains are restricted. These lateral constraints will dramatically alter the stress distribution within the sample and effectively increase its stiffness. Therefore, the sample will attempt to change its configuration to a more compliant geometry where less energy is required to strain the sample.

Fracture mechanics analysis can be used to derive the driving force for motion of an edge crack or internal crack. Assuming a linearly elastic response for the compliant layer, which is the same energy approach described in the previous section, the driving force for propagation of an edge crack, γ_{edge}, is given by the following expression:

$$\gamma_{edge} = \frac{-(P' - P)^2}{4\pi a}\frac{dC}{da} \tag{38}$$

where a is the contact radius, P' is the load required to establish a contact radius without adhesive forces (which is zero in this case), P is the experimental load, and C is the compliance of the system. γ_{edge} represents the energy per area available to drive the crack forward, thereby reducing the contact area with the indenter and increasing the compliance.

The compliance is

$$C = \frac{(1-\nu^2)}{2Ea}\left\{1+\left[\frac{0.75}{(a/h)+(a/h)^3}+\frac{2.8(1-2\nu)}{(a/h)}\right]^{-1}\right\}^{-1} \tag{39}$$

Assuming the material is incompressible (ν=0.5), the driving force for edge crack propagation is given as

$$\gamma_{edge} = \frac{9(P'-P)^2}{128\pi Ea^3}\frac{\left\{0.75+2(a/t)+4(a/t)^3\right\}}{\left\{0.75+(a/t)+(a/t)^3\right\}^2} \tag{40}$$

By replacing P by average stress times area, $\sigma_{avg} A$, this becomes:

$$\frac{\gamma_{edge}}{Ea} = \frac{9\pi}{128}\left(\frac{\sigma_{avg}}{E}\right)^2\frac{\left\{0.75+2(a/t)+4(a/t)^3\right\}}{\left\{0.75+(a/t)+(a/t)^3\right\}^2} \tag{41}$$

The energy release rate for a penny-shaped crack is found as

$$\frac{\gamma_{cavity}}{Ea} = \frac{2(1-\nu^2)}{\pi}\left(\frac{\sigma_{avg}}{E}\right)^2\left(\frac{a_c}{a}\right) \tag{42}$$

This expression is valid for $a_c << a$ and $a_c << t$

In the following section, determination of elastic properties of thin spray-on liner materials is presented, in which case γ_{cavity} is dependent on a single geometric parameter, a_c. If σ_{avg}/E exceeds a critical value close to one, an interfacial defect will expand into the bulk of the compliant layer as illustrated in Figure 74 (c).

Assuming a_c/a=2x10^{-4}, a_c/t<<1, and where the sample is incompressible (ν=0.5) Crosby et al. (2000) give deformation maps (Figure 75).

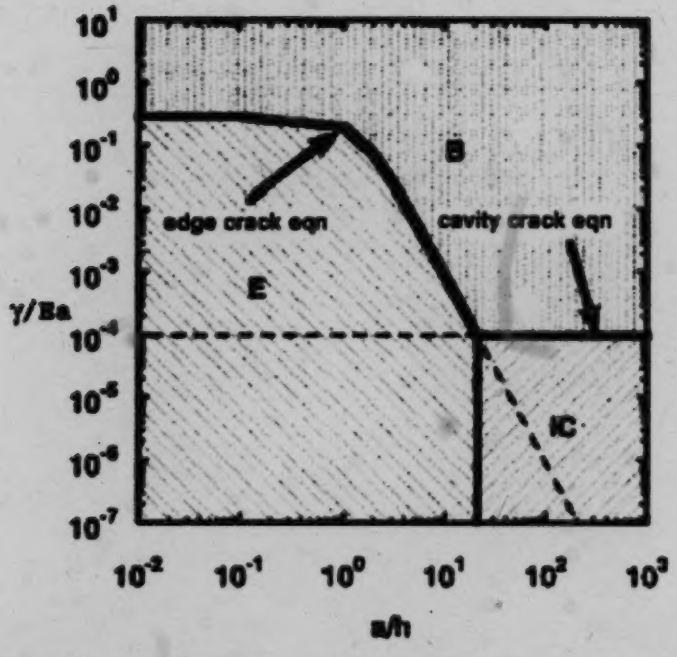

Figure 75 Deformation map for ν=0.5 and a_c/a=2x10^{-4} (Crosby et al. 2000).

The three different regions in this figure are edge crack propagation (E), bulk instability (B), and internal crack propagation (IC).

The same procedure was applied in developing the adhesion test geometry for the generic formulation of deformation graphs (changing Poisson's ratios). First γ_{edge} equation was derived for a generic case to give the following equation.

$$\frac{\gamma_{edge}}{Ea} = \frac{-\pi(1-\nu^2)}{8}\left(\frac{\sigma}{E}\right)^2 \left[\frac{\begin{array}{l} 5.6(1-2\nu)(a/t)^2\left(0.75+2.8(1-2\nu)\left(1+(a/t)^2\right)+(a/t)^3\right)- \\ (5.6(1-2\nu)(a/t)^2)\left(0.75+2.8(1-2\nu)\left(1+3(a/t)^2\right)\right)+2(a/t)+4(a/t)^3 \end{array}}{\left(0.75+2.8(1-2\nu)\left(1+(a/t)^2\right)+(a/t)^3\right)^2} \right] \quad (43)$$

which gives the Equation (41) for the incompressible case. The deformation curves can be seen in Figure 76, in which a_c was assumed as 0.25 mm.

The geometry of the developed test gives values smaller than 8 for a/t. A value of 1000 N/m is taken as γ, which is the calculated average value with Equation (37) for the tests carried out Similar values were reported in the literature for polymer composites on concrete (Karbhari & Engineer 1996, Lyons et al. 2002). Values of 13 MPa for E, and 0.25 for Poisson's ratio were found from elastic property determination tests and a is 16.5 mm; this gives γ/Ea equal to 4.6x10^{-3}, which corresponds to edge crack propagation for the test geometry used in this study (Figure 76, point A).

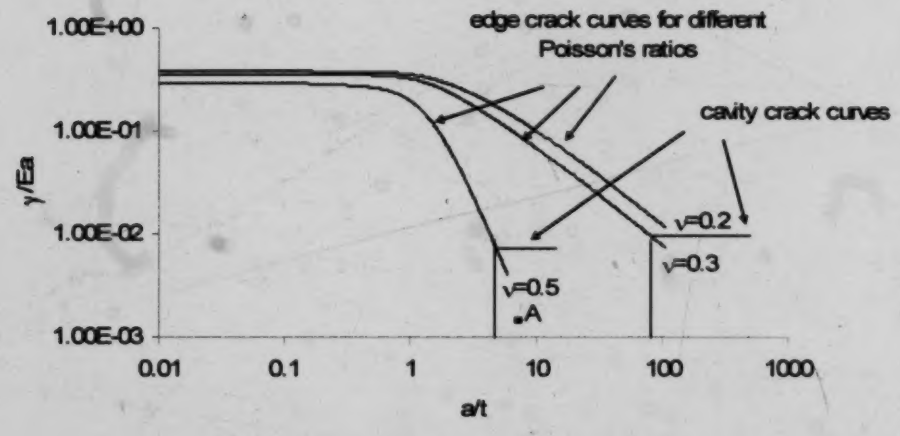

Figure 76 Deformation map for different Poisson's ratios and a_c/a=0.016.

Another compliance equation is given by Lin et al. (2000) and is based on the analytic expression of compliance for the Poker Chip test,

$$C = \frac{\delta}{P} = C_\infty \left[1 - \frac{\nu^2}{(1-\nu)^2} \frac{2I_1(\lambda)}{\lambda I_0(\lambda) - \frac{1-2\nu}{1-\nu} I_1(\lambda)} \right]^{-1} \tag{44}$$

where

I_1 and I_0 are modified Bessel functions of order one and zero, respectively

$$\lambda = \sqrt{\frac{3(1-2\nu)}{2(1-\nu)}} \frac{a}{h} \tag{45}$$

$$C_\infty = \frac{(1+\nu)(1-2\nu)h}{(1-\nu)E\pi a^2} \tag{46}$$

$$I_o(\lambda), I_1(\lambda) \cong \frac{e^\lambda}{\sqrt{2\pi\lambda}} \tag{47}$$

Therefore, when the new compliance equation is used, the peeling force required for separation is found as

$$P^2 = \frac{\gamma 2\pi^2 a^4 E \left[(1-\nu)^2 \lambda - (1-2\nu)(1-\nu) - 2\nu^2 \right]^2}{t(1+\nu)(1-2\nu)\left[(1-\nu)\lambda \left((1-\nu)^2 \lambda - 2(1-2\nu)(1-\nu) - 2\nu^2 \right) + (1-2\nu)(1-3\nu+4\nu^2) \right]} \tag{48}$$

The analysis made in all these derivations assumes that the liner is linearly elastic whereas, in reality, liners are viscoelastic. But still, elastic solutions have good relevance to actual

experiments. For example, Creton et al. (2000), and Crosby et al. (2000) successfully used an elastic analysis to interpret their experimental data.

7.5 'Elastic' Properties of Liner Materials

To compare theoretical equations with the adhesion test results, two important TSL material properties, Young's Modulus E and Poisson's ratio ν, are required. Uniaxial compression tests were used to measure these properties since no standard test method exists for thin liners. Cylindrical test specimens with a 2.3:1 height to diameter ratio (38 mm diameter) were made from the Tekflex material poured into a mold. After curing for 7 days, these were tested under cyclic loading (Figure 77). A typical stress strain curve obtained from the test is presented in Figure 78.

Figure 77 Cylindrical liner specimen under uniaxial loading.

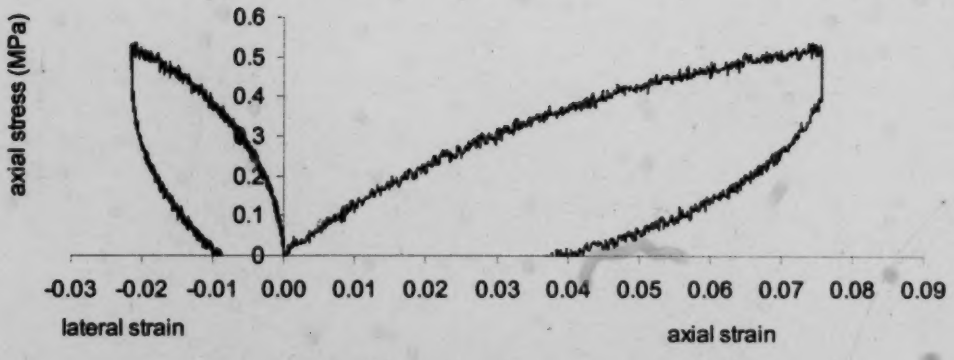

Figure 78 Stress strain curve for cylindrical Tekflex specimen.

From three uniaxial compression tests on cylindrical specimens, tangent Modulus (at 0.02 strain) and Poisson's ratio were found as 13±3 MPa and 0.25, respectively. As seen in Figure 78, there is hysteresis, therefore, the material shows viscoelastic behaviour.

Three "dog-bone" tensile tests were also conducted. Testing standards exist for measuring the tensile properties of plastic sheets. Perhaps the most relevant standard is ASTM D638 - Standard Test Method for Tensile Properties of Plastics. This test standard describes a testing method for use on "dog-bone" shaped pieces of plastic. Based on experience with property testing of TSL materials, a specimen with Type 1 dimensions is recommended. This specimen is the largest size allowed within the range specified by the testing standard. The dimensions of this specimen are shown in Figure 79. The test specimen should be about 3 mm thick.

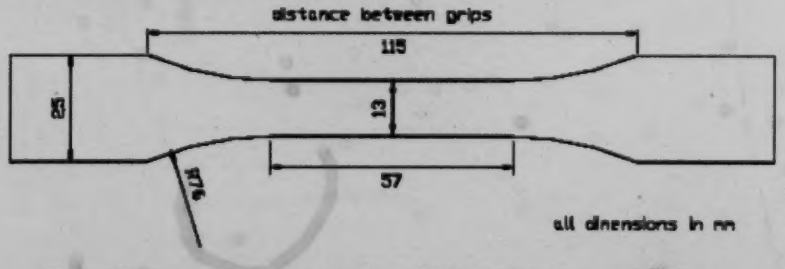

Figure 79 Shape and dimensions of an ASTM D638 Type 1 test specimen.

The ASTM D638 test involves clamping the specimen into a tensile testing machine and then pulling on the specimen at a displacement rate of 5 to 50 mm/minute, while measuring the loads and, if desired, the displacement or elongation. The specimen should break into two pieces in 30 to 300 seconds after loading begins. As with the adhesion tests, multiple tests are recommended on each material to obtain reliable measurements of the tensile strength.

Tekflex modulus of deformation is 52±6 MPa, which is calculated at 0.02 strain. The difference between Young's Modulus values from two different tests can be attributed to two different boundary conditions, loading rate and the viscoelastic property of the material. A typical load-displacement curve for dog-bone specimen is presented in Figure 80. The tensile strength of Tekflex cured for 7 days was 3.2±0.1 MPa.

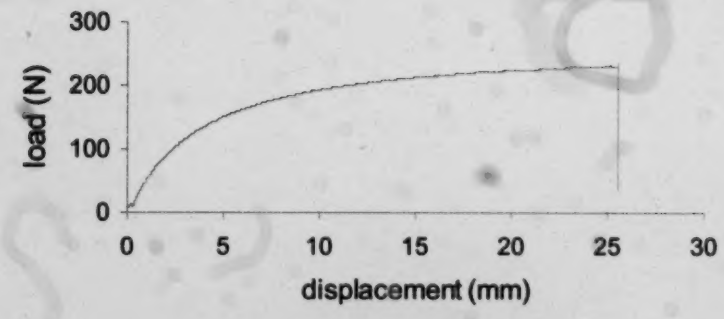

Figure 80 Dog-bone test results.

Similar tests were done for Castonite. It was very challenging to prepare dog-bone samples because of the brittle nature of the material. Three dog-bone tests were carried out and tensile strength was averaged as 3.9±0.6 MPa and Young's Modulus was found as 81±16 MPa. Only one cylindrical sample could be prepared and tangent Modulus (at 0.02 strain) and Poisson's ratio are found as 55 MPa and 0.2, respectively. For Tekflex PM and Tunnelguard, samples were very brittle and the dog-bone samples could not be prepared.

7.6 Comparison of Theoretical Studies with Tekflex Adhesion Test Results

To determine a representative load-displacement curve for Tekflex, the load-displacement curves of all the adhesive strength tests were plotted on one graph and regression fit was applied.

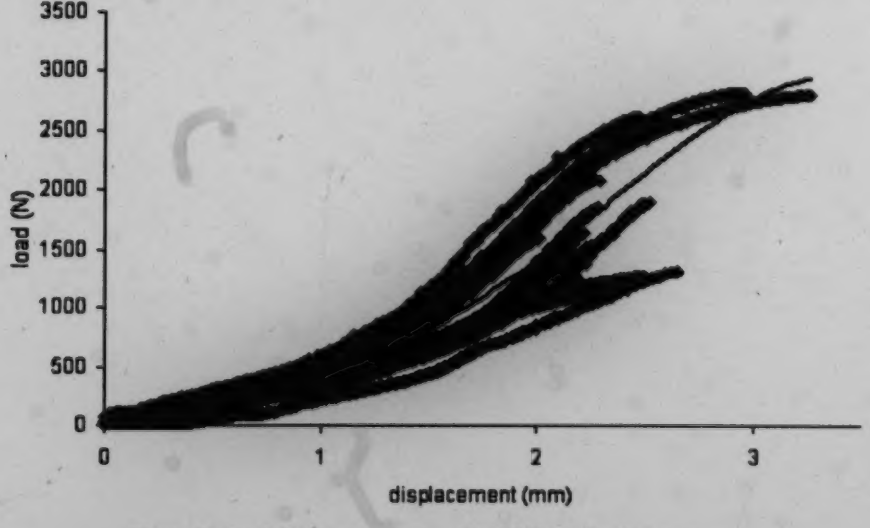

Figure 81 Load displacement curve for Tekflex adhesion tests.

To compare theoretical equations with the best-fit curve from the experiment results, the following graph was drawn. In Figure 82, Poisson's ratio and Young's Modulus were taken as 0.25 and 13 MPa, respectively for the analytical equations.

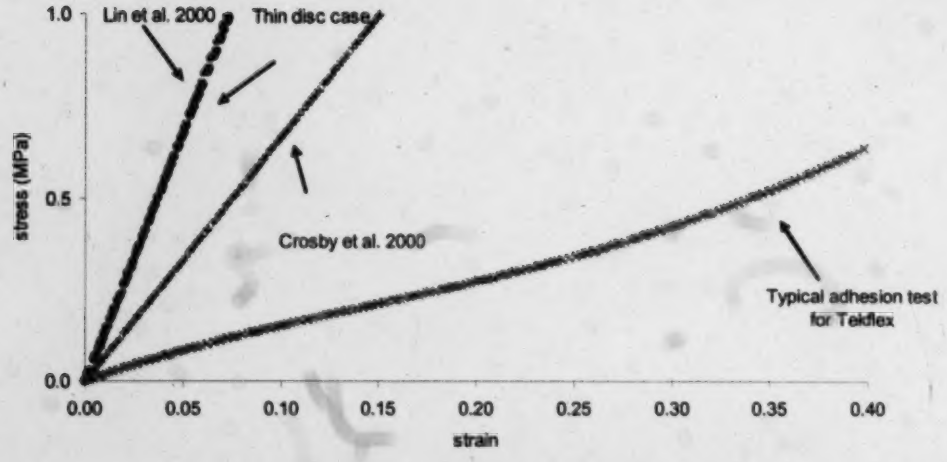

Figure 82 Comparison of analytical results with Tekflex results for E = 13 MPa.

For another comparison, 2 MPa for Young's Modulus and 0.25 for Poisson's ratio was used (Figure 83).

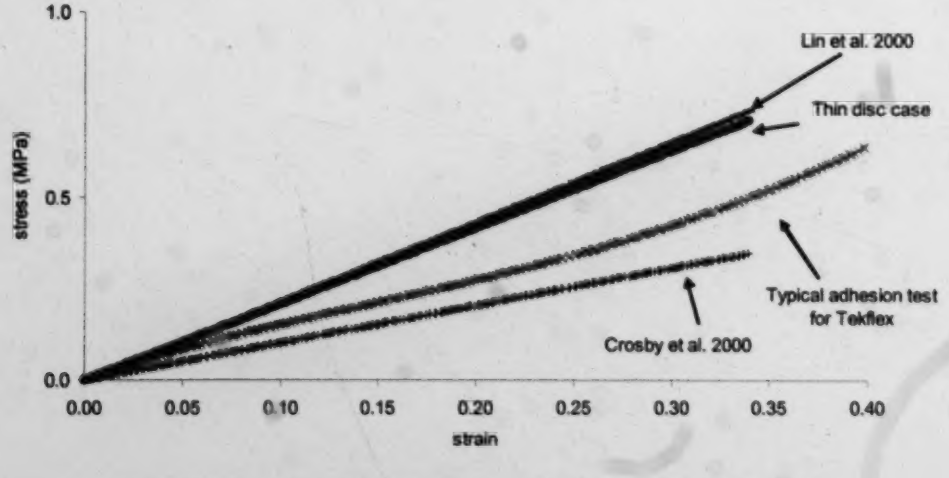

Figure 83 Comparison of analytical results with Tekflex results for E= 2 MPa.

As can be seen from Figure 82, laboratory adhesion test results differ from the analytical equations. The same kind of behaviour was also observed for Castonite product. The difference between analytical test results and typical adhesion tests show that equivalent stiffness (slope of the curves) of the adhesion test system (elevator bolt, epoxy and liner) is softer than the liner material stiffness, which was used for the closed-form solutions plotted on the graph. It should be noted that the other products (CS 1251 2k, Tekflex PM, Rock Web, and Tunnelguard) could not be compared with closed-form equations, due to an inability to measure elastic properties.

7.7 Methodology for Work of Adhesion Calculation

To estimate the work of adhesion γ, the area under the load-displacement curve measured during the adhesion tests can be used. This area represents the work performed during the adhesion test. It includes both the work of adhesion at the liner-substrate interface and the elastic energy stored elsewhere in the testing fixtures.

To compensate for the energy stored in the testing fixtures, some extra tests were conducted. The goal of these tests was to determine the energy required to deform the liner material itself as well as the steel-epoxy-liner interfaces. To estimate the energy stored in the steel elevator bolt, the epoxy, and within the liner material itself, pull tests were conducted on liner material sandwiched between epoxy and elevator bolts as shown in Figure 84.

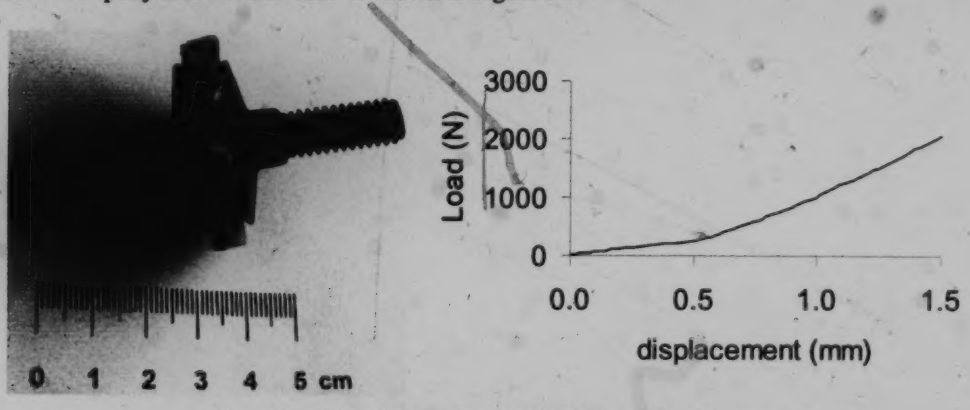

Figure 84 Back to back pull test with Tekflex liner and epoxy.

A schematic view of typical tests can be seen in Figure 85. In this figure, A is the area under a typical adhesion test load-displacement curve, B is the area under the back-to-back pull test curve over a load range up to the adhesive test failure load, and C is the area under the dog bone tensile test curve up to the adhesive test failure load.

$$
\begin{aligned}
C &= \text{liner} \\
B &= \text{liner} + 2*(\text{steel} - \text{epoxy} - \text{liner interface}) \\
A &= \text{Liner} + (\text{steel} - \text{epoxy} - \text{liner interface}) + \text{work of adhesion} \\
B &= C + 2K \\
A &= C + K + X
\end{aligned}
\tag{49}
$$

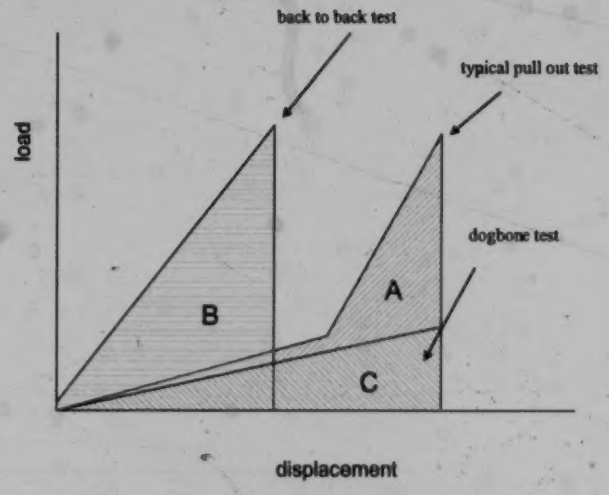

Figure 85 Schematic view of typical tests.

In the above equation, X is the unknown energy used to create a new surface between the liner and rock substrate (work of adhesion). Solving for X gives:

$$X = A - \frac{(B+C)}{2} \tag{50}$$

Work of adhesion for the liner can be estimated from this equation. For calculation of the energy or work under the measured load-displacement curves, the pull-off force from the adhesion test is used as a reference to find the corresponding areas under dog-bone and back-to-back tests. In addition, the tensile force data obtained from the dog-bone tests must be scaled to a cross-sectional area equal to that of the elevator bolt area.

One other important parameter is the loading rate used in these three different tests. Because of the viscoelastic behaviour of the liner and epoxy materials, dog-bone and back-to-back tests were carried out at the same strain rate as a typical pull out test, which is 0.5/minute. Typical test results are presented in Figure 86.

As can be seen from Figure 86, dog-bone and back-to-back tests have almost the same stiffness around the 1 MPa stress level. Before this stress level, the dog-bone test behaves stiffer and after this level, it becomes softer and ductile. The back-to-back test, however, has a constant stiffness value for the test. This result shows that the back-to-back test has its own characteristic stiffness value, which can be called an equivalent stiffness composed of steel, epoxy, and liner responses. However, the pull out test has a softer stiffness than back-to-back and dog-bone tests. It has also its equivalent stiffness value but it is not constant and after a stress level of 0.7 MPa, it shows strain hardening behaviour. One of the reasons for the softer behaviour of pull out tests compared to the other two tests is the commencing of debonding of the liner-rock interface at the very early stage of loading. As loading continues, after stress level of 0.7 MPa, strain hardening occurs, but the equivalent stiffness value is still softer than for the other two tests. This behaviour can be explained by the continuity of debonding of the liner-rock interface.

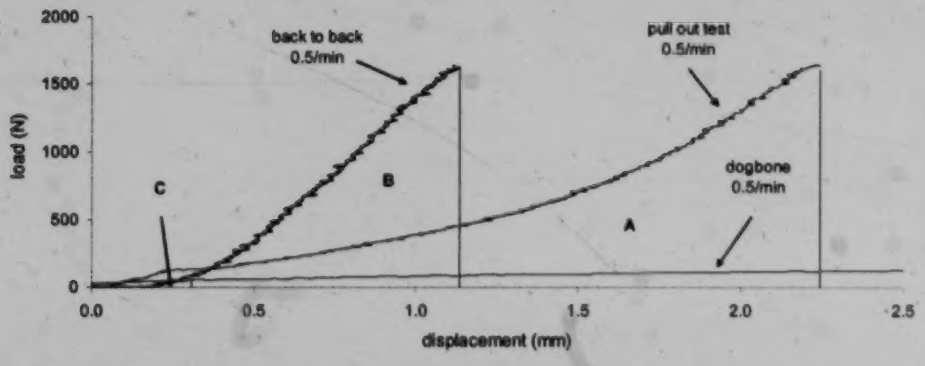

Figure 86 Dogbone, back-to-back and pull out tests for Tekflex for the same strain-loading rate.

An example work of adhesion calculation is given based on Figure 86. The area under the pull out test (A) is 1290 Nmm, the area under the back to back test (B) is 676 Nmm, and the area under the dog-bone test (C), corresponding to 35 N of dog-bone failure load as an equivalent of 1640 N pull out load, is 70 Nmm. When Equation (50) is applied, the energy spent to peel the liner is found as 917 Nmm, when it is divided by the testing area, the work of adhesion is 1072 N/m.

Using this approach, the work of adhesion was calculated using the load-displacement data obtained from the various adhesion tests and the overall results for Tekflex are presented in Table 20. The work of adhesion for Tekflex applied to various substrates ranges from nearly zero to as high as 3377 N/m. For clean strong substrates, the work of adhesion is typically larger than 1000 N/m. Similar work of adhesion values (300 to 1000 N/m) were reported in the literature for polymer composites on concrete (Karbhari & Engineer 1996, Lyons et al. 2002).

Table 20 Overall results for Tekflex work of adhesion.

Substrate	Work of adhesion (N/m)	Standard deviation
1 month cured paving stone	3377	719
1 month paving stone highly dusty	1031	111
1 month damp paving stone	2887	1006
1 month cured split granite	1366	275
1 month cured sawn granite	2376	284
1 week cured cinder b. clean	1034	235
1 week cured cinder b. highly dusty	445	141
1 week cured cinder b. highly oily	657	222
1 week cured sawn granite	967	186
1 week cured split granite	973	383
1 week cured limestone	933	238
1 week cured sandstone (substrate failure)	677	152
1 week cured damp paving stone	1049	67
1 week cured lightly oily paving stone	345	16
1 week cured clean paving stone	777	38
1 week cured highly dusty paving stone	73	23
1 week cured moderately dusty paving stone.	511	54
1 week cured lightly dusty paving stone	665	113

Overall results for Castonite are presented in Table 21.

Table 21 Overall results for Castonite work of adhesion.

Substrate	Work of adhesion (N/m)	Standard deviation
clean paving stone	>798	195
damp paving stone	>754	237
highly oily paving stone	0	0
highly dusty paving stone	127	0
split granite	>513	171
sawn granite	>525	155
split sandstone	>488	96
split limestone	0	0

The work of adhesion for Tekflex is plotted versus liner thickness in Figure 87. As can be seen from Figure 87, for paving stone substrate, it can be concluded that the work of adhesion is roughly constant. For saw cut granite substrate, if 3 mm thick test results are ignored, a roughly constant work of adhesion value is also observed. Given the difficulty involved in interpreting the test data and the influence of testing conditions on the resulting load-displacement curves, it is encouraging to observe that the work of adhesion is in fact roughly constant for a given liner-substrate interface.

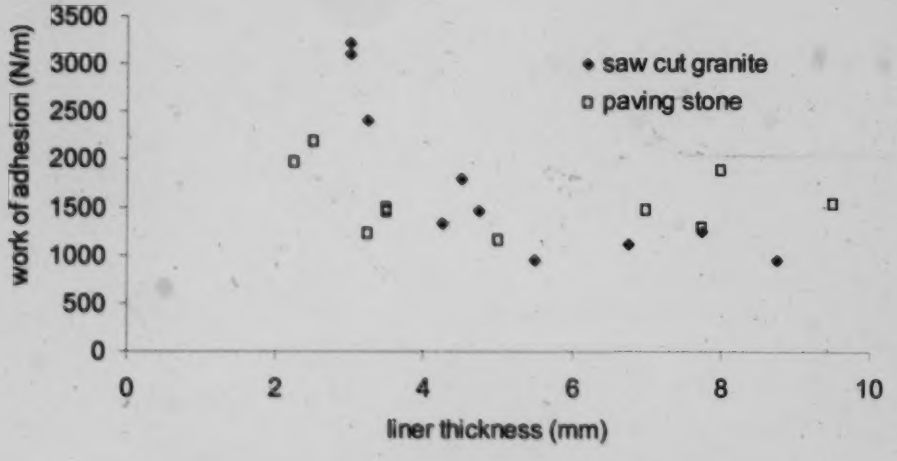

Figure 87 Work of adhesion versus liner thickness for Tekflex.

7.8 Adhesion Normalization

The influence of liner thickness on the measured adhesive strength was presented in Section 6.3.3. It was observed that an increase in liner thickness caused a decrease in the adhesive strength. To understand the mechanism better, effective bond width analyses were carried out and normalization of adhesion to a reference liner thickness (4 mm) was introduced as discussed next.

7.8.1 Effective bond width

The effective bond width of a Tekflex liner (Table 22) can be determined by dividing the work of adhesion value by the adhesive strength. The effective bond width of Tekflex on different substrates varies from 0.5 mm to 1 mm. For comparison, Tannant (2004) gave effective bond width values for Mineguard of 5.3 mm and 3.4 mm based on the back-calculation of laboratory test data.

Table 22 Effective bond width values for Tekflex.

Substrate	Work of adhesion (N/m)	Adhesion (MPa)	Effective bond width (mm)
1 month cured paving stone	3377	3.39	1.0
1 month cured split granite	1366	1.79	0.8
1 month cured sawn granite	2376	2.45	1.0
1 week cured sawn granite	967	1.32	0.7
1 week cured split granite	973	1.45	0.7
1 week cured limestone	933	1.63	0.6
1 week cured clean paving stone	777	1.63	0.5

Tannant (2004) also postulated that liner thickness affects effective bond width. Tekflex liner adhesion test results on paving stone and saw cut granite are presented in Figure 88 to see this effect. The regression curve belongs to paving stone and with the two 1 mm thick results excluded during the regression. There is wider scatter in the bond widths calculated for the thinner liners which is to be expected, as it was difficult to create a uniform thickness when applying the Tekflex to the substrates.

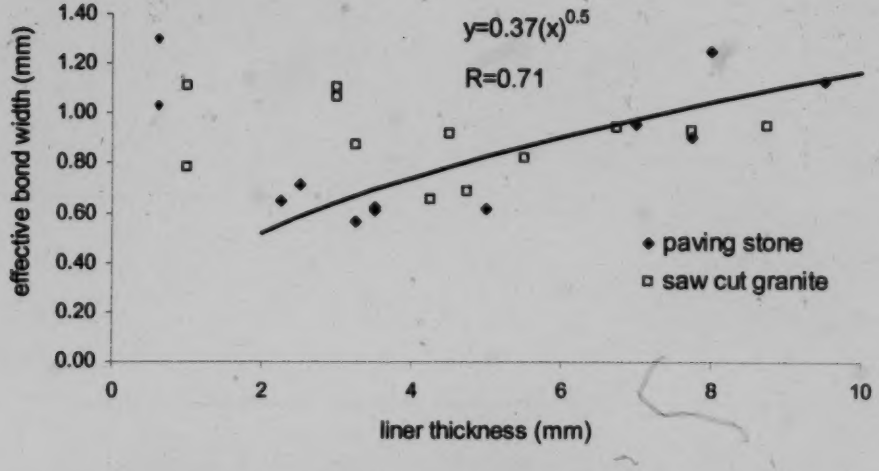

Figure 88 Effective bond width versus Tekflex thickness on paving stone and saw cut granite.

Based on the data plotted in Figure 88, it appears that the effective bond width increases with liner thickness, which was also shown by Tannant (2004). The bond width versus thickness roughly matches a square root relationship. Compare this figure with Figure 65, which shows

that adhesion is inversely proportional with the square root of liner thickness; a finding that is also consistent with the closed-form solution, Equation (37).

Figure 88 shows that for the saw cut granite substrate there is no good correlation between liner thickness and effective bond width.

These two parameters: adhesion and effective bond width, are both dependent upon the liner thickness and this relationship with thickness is studied below.

Work of adhesion γ being a material (constant) property specific to an interface between the liner and the rock and can be written as

$$\gamma = \sigma_a w_b \tag{51}$$

where, σ_a is adhesion and w_b is effective bond width. As Figure 88 shows, w_b is directly proportional with square root of liner thickness:

$$w_b \propto t^{0.5} \tag{52}$$

where, t is liner thickness. From this relationship, it can be concluded that to get a constant value from Equation (51), adhesion σ_a should be inversely proportional with square root of liner thickness t.

$$\sigma_a \propto \frac{1}{t^{0.5}} \tag{53}$$

Equation (53) agrees well with the closed-form solution, Equation (37), and the test results. Test results using Tekflex with varying thickness are presented in Figure 89.

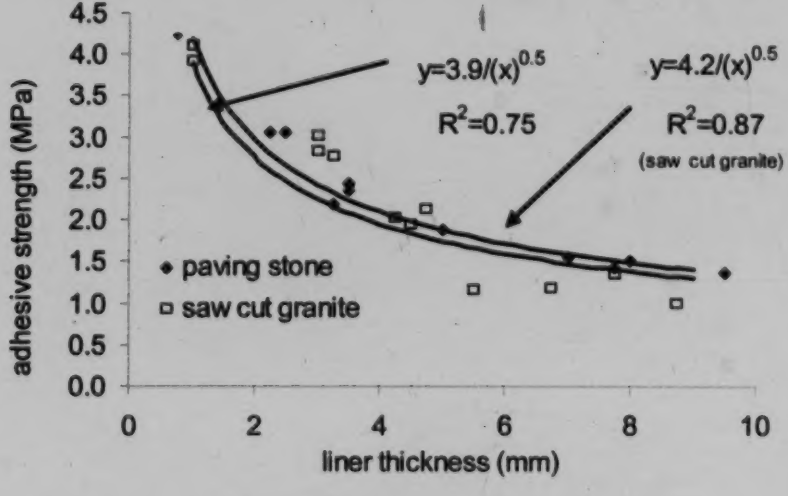

Figure 89 Liner thickness versus adhesive strength.

Based on the inverse square-root relationship between liner thickness and adhesion shown in Figure 89, adhesion test results (Chapter 4 and Chapter 5) are normalized for liner thickness of 4 mm. The choice of 4 mm to normalize the test data was based on observations that a practical liner thickness applied in the field is about 2-4 mm (Archibald, 2001). The normalization process enables comparison of test data obtained from different thicknesses of liner materials. Other researchers that have conducted adhesion tests on TSL materials have failed to recognize that adhesion is dependent upon thickness even though the work of adhesion is not.

The details of normalization procedure are explained below. From the regression in Figure 89, adhesion can be written as

$$\sigma_a = \frac{A}{t^{0.5}} \tag{54}$$

where, σ_a is the adhesive strength measured from the test, t is the liner thickness of the test, and A is a constant. From Equation (54), A can be written as

$$A = \sigma_a t^{0.5} \tag{55}$$

Therefore, normalized adhesion $(\sigma_a)_n$ can be found by inserting Equation (55) into Equation (54) for a reference liner thickness of 4 mm.

$$(\sigma_a)_n = \frac{\sigma_a t^{0.5}}{4^{0.5}} \tag{56}$$

Based on this analysis, it can be concluded that knowing adhesive strength for a particular liner on a particular substrate is not enough. The work of adhesion of a liner on a substrate captures both adhesive strength and effective bond width and is thus more valuable for liner design. It is a liner property that changes depending on the substrate. Therefore, it is suggested that liner materials should be tested on a standard substrate, such as paving stone, and work of adhesion value should be given instead of finding adhesive strength. In this manner, a more useful design parameter can be obtained from the testing.

CHAPTER 8 IMPLICATIONS FOR BETTER TSL DESIGN

To improve TSL design, potential liner failure modes have to be understood. In the following section, liner design based on tensile/shear and adhesive failure modes and parameters controlling these failure modes are explained.

8.1 Potential Liner Failure Modes

8.1.1 Tensile failure

The model shown in Figure 90 can be used to analyse the support capacity of a liner with thickness t holding a loose rock block that undergoes either small or large displacements. The surface area of the block coated by the liner is assumed square in shape with width s. The block is assumed to move vertically downward a distance d, thus inducing stress in the liner (Tannant 2004).

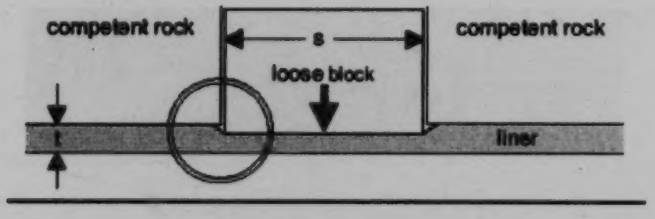

Figure 90 Model for rock support by a liner assuming a square block moving vertically downward (after Tannant 2004).

The first check is to determine whether the liner ruptures at small displacements due to either shear or diagonal tensile stresses around the perimeter of the block (Figure 91).

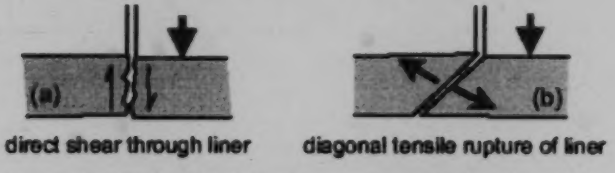

Figure 91 Liner failure modes at small block displacements caused either by shear rupture or diagonal tensile rupture (after Tannant 2004).

The liner can fail in two modes (Figure 91). It is assumed that failure of the adhesive bond does not occur. Given that a typical liner is only a few millimetres thick, direct shear failure or diagonal rupture of the TSL must occur within the first few millimetres of block movement and are most likely when the liner adhesion is similar to the tensile strength. Note that this is the situation for unreinforced shotcrete, which is why shear or diagonal tensile failure modes occur in shotcrete.

For the failure modes shown in Figure 91, the support capacity around the perimeter is a simple function of the liner thickness t and either the shear or tensile strength of the liner σ_t. Given a lack of test data, the shear strength will be assumed equal to the tensile strength.

$$F = \sigma_t * t \quad \textit{per metre} \tag{57}$$

8.1.2 Adhesive failure

When the adhesion is less than the tensile strength, the liner adhesive bond may progressively fail around the displacing block. By debonding, a section of liner rotates and begins to act in tension to resist the weight of the moving block as shown in Figure 92. Under these conditions, the liner can tolerate relatively large block displacements. Force equilibrium can be achieved when the vertical component of the tensile forces acting in the liner equals the weight of the block (assuming no frictional resistance along the sides of the block).

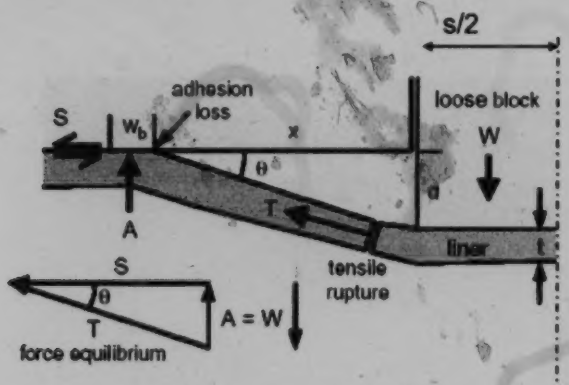

Figure 92 Interaction between liner adhesion and tensile strength to support the weight of a displaced block (only half of the model is shown) (Tannant 2004).

The model first looks at the adhesive capacity of the TSL. If the block movement causes progressive adhesive failure, the debonding will progress away from the edge of the block (Figure 92). In doing so, the area over which the adhesion acts grows because the perimeter length increases. It is assumed that the area eventually becomes large enough to create an adhesive force A that satisfies force equilibrium with the weight of the block. The width of the debonded zone x at equilibrium or when tensile rupture occurs is calculated from

$$A = 4\sigma_a w_b (s + 2x) = W \tag{58}$$

where W is the weight of the block, σ_a is the average adhesion of the membrane acting over the effective bond width w_b, and s is the width of the block. This equation is derived from the perimeter of the debonded square area multiplied by the adhesion and effective bond width. The top view of the same block is presented in Figure 93.

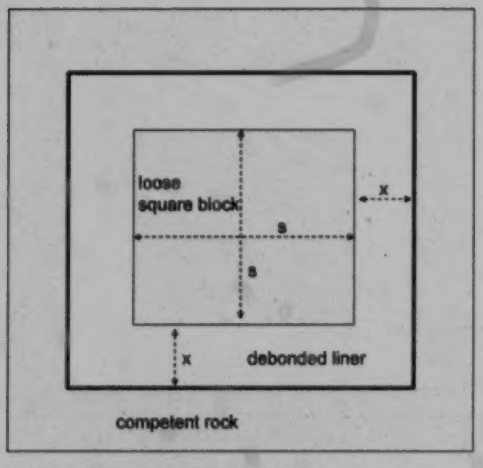

Figure 93 Top view of the debonded liner and loose square block.

In Equation (58), the loose block is assumed to be square. Where one can assume it to be circular with a diameter of s, Equation (58) becomes

$$A = \sigma_a w_b (s + 2x)\pi = W \tag{59}$$

Because of the nature of discontinuities in a rock mass, blocks are more likely to be square or rectangular, rather than circular. Therefore, Equation (58) is more applicable to underground liner design.

Adhesive support from the liner has now been fully mobilized so attention can now turn to the tensile strength of the liner. It is reasonable to assume that tensile rupture will occur near the perimeter of the block, in which case the maximum tensile force T that can be carried in the plane of the TSL is:

$$T = 4s * \sigma_t * t \tag{60}$$

The vertical component of the tensile force must equal the block weight at equilibrium. There is a geometric relationship between the block's weight and the tensile force in the liner. By estimating the block weight and knowing the maximum allowable force in the liner, the minimum angle, θ can be determined.

$$\theta = \arcsin(W / T) \tag{61}$$

This angle will determine the minimum vertical block displacement needed to ensure that the vertical component of T is equal to the block weight W. The vertical block displacement at equilibrium is

$$d = x \tan\theta \tag{62}$$

Based on the model shown in Figure 91, at tensile rupture the following equation must hold true

$$\sigma_t * s * t * \sin\theta = \sigma_a w_b (s + 2x) \tag{63}$$

It is useful to note that the greater the angle θ for larger displacements and liner elongation, the greater the capacity. However, there is a limit to the allowable displacement that is governed by the elongation capacity of the liner. In this model, the following relation must not be violated.

$$\sqrt{x^2 + d^2} < (1+e)x \tag{64}$$

The parameter e is the strain at peak strength for a given liner product determined from laboratory dog-bone tests. A typical value for e might be 0.4 for Tekflex, however, it can be quite large and > 0.5.

8.2 Parameters Affecting Liner Failure

As can be seen from Equation (58) and Equation (60), major parameters controlling the liner failure are adhesion, effective bond width, thickness of liner, tensile strength of liner, and loading rate which is actually included in the adhesion.

As can be seen from Equation (58), the only unknown parameter in this equation is the term $\sigma_a w_b$, which is basically the work of adhesion γ. The work of adhesion for different liner materials can be calculated either using closed-form solutions or laboratory test results that were explained previously. The closed-form solution based on linear elasticity explained in the adhesive theory section is:

$$\gamma = \frac{-P^2}{4\pi a}\frac{dC}{da} \tag{65}$$

where P is the pull out load, a is the radius of testing area, and C is the compliance of the liner. This equation is based on the assumption that work done during the adhesion test is fully used to debond the liner. A deformation map depending on the testing geometry and elastic material properties was derived earlier. This map can be used the see if work done by the testing system is gained by the interface or not.

The compliance of the liner may obey the disc case (Equation (31)), the one defined by Lin et al. (2000), (Equation (44)) or the one defined by Crosby et al. (2000) (Equation (39)).

Using the most appropriate compliance equation for the liner, the work of adhesion can be calculated using Equation (65). For example, if Equation (31) best matches the liner behaviour then the work of adhesion is given by

$$\gamma = \frac{P^2 t(1-\nu^2)}{2\pi^2 E a^4} \tag{66}$$

If compliance of the liner obeys Equation (44), work of adhesion is calculated as

$$\gamma = \frac{P^2 t(1+\nu)(1-2\nu)\left[(1-\nu)\lambda\left((1-\nu)^2\lambda - 2(1-2\nu)(1-\nu) - 2\nu^2\right) + (1-2\nu)(1-3\nu+4\nu^2)\right]}{2\pi^2 a^4 E\left[(1-\nu)^2\lambda - (1-2\nu)(1-\nu) - 2\nu^2\right]^2} \tag{67}$$

If compliance of the liner obeys Equation (39), work of adhesion is calculated as

$$\gamma = \frac{P^2(1-\nu^2)}{8Ea\pi^2}\left[\frac{\begin{array}{l}5.6(1-2\nu)(a/t)^2\left(0.75+2.8(1-2\nu)\left(1+(a/t)^2\right)+(a/t)^3\right)- \\ (5.6(1-2\nu)(a/t)^2)\left(0.75+2.8(1-2\nu)\left(1+3(a/t)^2\right)\right)+2(a/t)+4(a/t)^3\end{array}}{\left(0.75+2.8(1-2\nu)\left(1+(a/t)^2\right)+(a/t)^3\right)^2}\right] \quad (68)$$

If work of adhesion of the liner is known, either from the test result interpretation or from the closed-form solutions, Equation (69) which is a new form of Equation (58) can be used to find the weight of a frictionless block that can be held in place.

$$A = 4\gamma(s+2x) = W \quad (69)$$

Assuming a variety of block sizes in the range between 0.5 m and 2 m^2, and a density of 2600 kg/m^3, then the height of a block that a liner could theoretically hold can be calculated using the work of adhesion values calculated in the previous section. Block area versus block height curves for various work of adhesion magnitudes are plotted in Figure 94. Using test data for Tekflex, the height of a block that can be supported ranges between 0 and 1.6 m depending on the block's surface conditions.

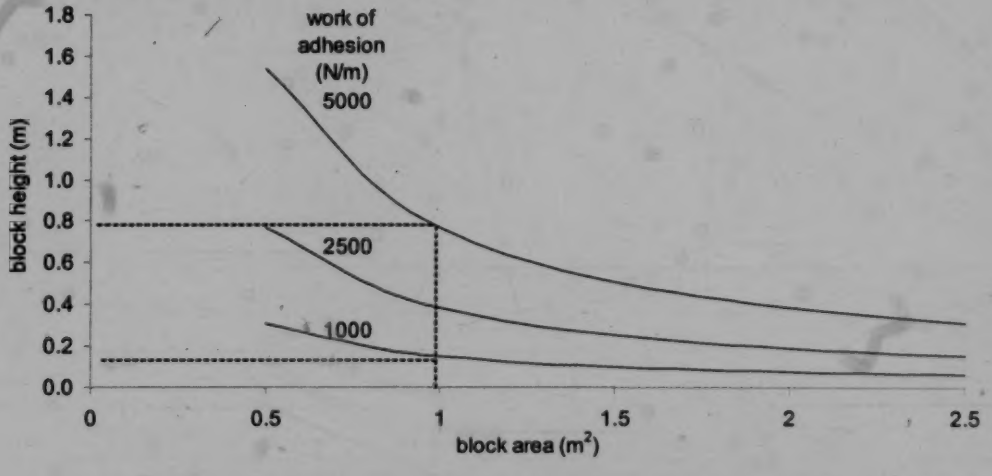

Figure 94 Block area versus block height for given work of adhesion.

An increase in work of adhesion increases the height of a block that a liner could theoretically hold. For example, for a 1 m^2 block, the height of the block that a liner with a work of adhesion value of 1000 N/m could carry is 17 cm, but for 5000 N/m it is 80 cm.

8.3 Thickness Based Liner Support Design

As explained earlier in this chapter, the two parameters controlling liner failure are work of adhesion and tensile/shear strength, Equations (69) and (60), respectively. Based on the tensile strength approach, the weight of rock that a liner can hold is directly proportional with the liner thickness, whereas, based on the work of adhesion approach; it does not change with the liner thickness. The relationship between Equations (60) and (69) were examined to maximize the weight of rock that a liner can carry, as shown in Figure 95.

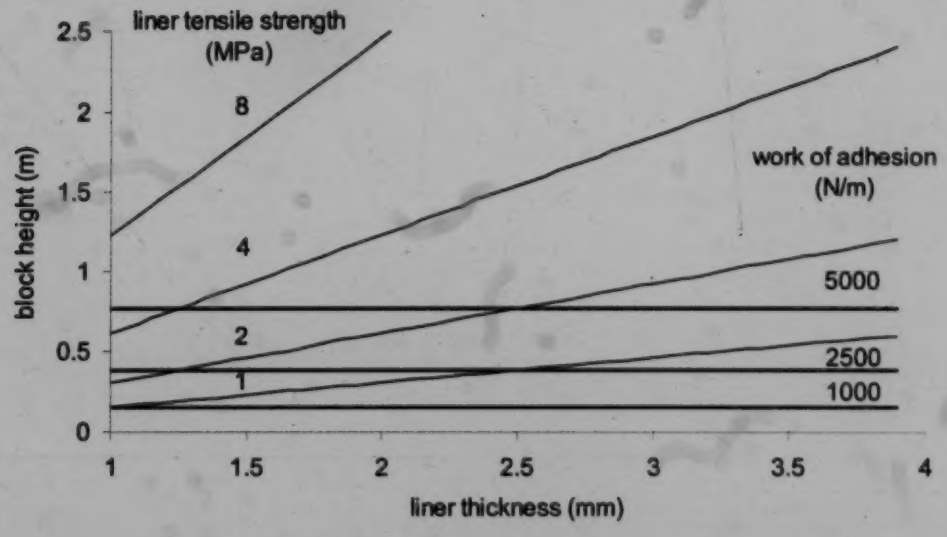

Figure 95 Supportable block height for a 1 m square block (density = 2600 kg/m^3) versus liner thickness based on work of adhesive and tensile failure modes.

In Figure 95, no debonding is assumed (x=0), and a 1 m by 1 m block of density of 2600 kg/m^3 is assumed. As can be seen from Figure 95, if work of adhesion is used, the block height that a liner can carry is constant and directly proportional to the value of work of adhesion, whereas, if tensile strength approach is used, block height that a liner can carry is directly proportional to liner thickness times tensile strength. The optimum value of the liner thickness that gives the maximum value for the block height is found from the intersection of the lines corresponding to the appropriate values of tensile strength and work of adhesion.

For example, if the tensile strength of the liner material is 2 MPa, and the work of adhesion is 5000 N/m, a liner thickness of 2.5 mm is the optimum value to get the highest support capacity and therefore block height. If a liner thickness greater than 2.5 mm is applied, adhesive debonding will occur and depending on the debonded length of the liner, it will carry a block height, which is controlled by the liner tensile strength. If the liner has a tensile strength greater than 5 MPa, there is no optimum solution for liner thickness, because for any thickness greater than 1 mm, adhesive debonding occurs first. Then depending on the debonding length of the liner, a block height range that a liner can carry can be found.

Most TSL products when sprayed on clean strong substrates will likely have work of adhesion values greater than 2000 N/m. Given a range in TSL tensile strength of say 1 to 10 MPa and typical liner thicknesses of 3 to 4 mm, an important conclusion arising from Figure 95 is that liner debonding should be the initial failure mechanism. Tensile rupture should only occur after a large debonded width is created.

CHAPTER 9 CONCLUSIONS

9.1 Test Method

A review of various adhesion test methods concluded that the following testing attributes were most important for adhesion testing of thin spray-on liners: (a) minimize eccentric loading and bending, (b) loaded area must be predefined by overcoring, (c) force versus displacement should be recorded, (d) method must be practical and inexpensive, and (e) method can be performed in the laboratory or the field. It was concluded that a direct pull-off method with a suitable loading fixture should work best for testing and a test method was developed to measure the adhesion strength of spray-on liners to rock and concrete substrates. The method is easy, practical and inexpensive.

The size of the loading fixture is an important consideration. A typical radius:thickness ratio used in the past for thin spray-on liners is 10. Assuming a reasonable upper limit is 10 and considering the design thickness for thin spray-on liners in the range of 2 to 6 mm, implies the need for loading fixtures no larger than 20 to 60 mm in diameter. If the loading fixture diameter is too large, there is greater chance the liner failure during a test will be progressive in nature. This means that the calculated adhesion will be less than the actual adhesion because the peak force is divided by an area that is larger than the true area carrying the measured load. If the loading fixture is too small, inherent variations in surface texture and roughness of the substrate may not be adequately reflected in a test result unless a large number of tests are completed at various locations.

Given consideration to fixture size, desire for uniform stresses beneath the fixture, and cost, a suggested loading fixture is a standard elevator bolt with a 33 mm base diameter. A single elevator bolt costs about $0.5. This size is smaller than previous devices used to measure adhesion with thin spray-on liners, but lies within the range of fixture diameter to coating thickness ratios used by other industries to measure adhesion. The advantages of this size are: (a) it matches a standard elevator bolt size, (b) the required size of substrates for laboratory testing are fairly small (two tests can be performed on a rock the size of a construction brick), and (c) the required over-core bit size (35 mm ID) is also fairly small, making it easier to over-core coated surfaces in the field.

The proposed test method covers a procedure for evaluating the pull-off strength (commonly referred to as adhesion) of a thin spray-on liner by determining the greatest tensile stress that a surface area can bear before a plug of material is detached. The test is destructive and failure will occur along the weakest plane within the system comprised of the test fixture, epoxy, spray-on liner, and substrate. The fracture surface is exposed by the test, permitting visual observation of where failure occurred.

The general pull-off test is performed by securing a loading fixture (elevator bolt) normal (perpendicular) to the surface of the spray-on liner with an epoxy. After the epoxy is cured, the specimen is clamped into a tensile loading apparatus. The loading fixture is carefully positioned such that a tensile force is created normal to the liner-substrate interface. The loading fixture is gradually pulled away from the clamped specimen while loads and displacements are recorded. The test continues until a plug of material is detached. When a plug of material is detached, the exposed surface represents the plane of limiting strength within the system. The nature of the failure is described and the adhesive strength is computed based on the maximum load and the original surface area stressed.

9.2 Adhesion Test Results

Most of the adhesion tests were conducted using Tekflex as the liner product. The effects on the adhesive strength of the substrate properties (tensile strength, roughness and grain size) and surface contaminants (oil or dust) were examined. In addition, the effect of liner thickness and loading rate on adhesive strength were studied. The results show that under room temperature and humidity conditions, the adhesive strength between the Tekflex liner and concrete paving stones is about 1.9 MPa. Where the surface of the substrate is contaminated with dust or the substrate is weak in tension, it may be difficult to reach adhesion of 1 to 1.5 MPa. Rock Web appeared to adhere well to either clean or dirty norite rock.

Adhesion tests on five other liner products showed an order of magnitude range in adhesive strengths between 0.2 and over 2.4 MPa. Some liner products are weak in tension and give low adhesive strengths. This will likely preclude their use in rock support applications.

For rock types such as granite, limestone and sandstone, larger grain size or a rougher surface increases the adhesive strength of a liner to the substrate. The substrate tensile strength probably needs to exceed 2 MPa to ensure good adhesion.

For Tekflex, a damp substrate slightly increases adhesion. The presence of oil on the substrate surface can significantly reduce the adhesion, in many cases, to essentially zero. One interesting observation was that the impact of oil was smaller when the oil was applied to highly porous cinder blocks, probably because the oil was absorbed by the substrate rather than remaining on the surface as it did with the other substrates.

Increasing the curing time for Tekflex from one week to one month, increases adhesive strength. Creep behaviour of a Tekflex liner on paving stone substrates was also studied. A different testing set up was developed for creep testing. Long-term creep tests showed that the adhesive strength could drop by at least 50% when the liner carries load for about a month.

The measured adhesive strength decreased significantly as the liner thickness increases. Adhesive strength and effective bond width both depend on liner thickness. Adhesion drops as thickness increases whereas bond width increases as thickness increases. Adhesive strength has an inverse square-root relationship with liner thickness.

9.3 Work of Adhesion and Implications for Better Liner Design

The design of a thin spray-on liner for rock support requires knowledge of the adhesive strength and the effective bond width of the liner. The product of adhesion times the bond width is essentially an interface material property known as 'work of adhesion'. A new methodology was developed to calculate the work of adhesion at the liner-substrate interface based on pull-off test data. This methodology is based on finding the energy needed to create the crack between a liner and interface. This involves taking the areas under the load-displacement curve measured during the pull-off test and subtracting work done to deform everything but the liner-substrate interface. Based on analysis, it can be concluded that knowing adhesive strength for a particular liner on a particular substrate is not enough. Work of adhesion of a liner on a substrate, which captures both adhesive strength and effective bond width, is more valuable. It is a liner property changing with the substrate. Therefore, it is suggested that every liner should be tested on a standard substrate, such as paving stone, and work of adhesion value should be given instead of finding adhesive strength.

Based on the calculated work of adhesion values, the effective bond width of Tekflex to different clean substrates ranges between 0.5 mm and 1 mm. There was a good correlation observed between liner thickness and effective bond width.

Two parameters controlling the failure of a liner functioning as rock support under field conditions are work of adhesion and tensile/shear strength. Based on a tensile failure mechanism, the weight of a rock block that a liner can hold is directly proportional to the liner thickness, whereas for the work of adhesion mechanism, the rock weight does not change with the liner thickness. For example, if the tensile strength of the liner material is 2 MPa, and the work of adhesion is 5000 N/m, a liner thickness of 2.5 mm is the optimum value to get the highest support capacity and therefore block height. If a liner thickness greater than 2.5 mm is applied, adhesive debonding will occur first. Most TSL products when sprayed on clean strong substrates will likely have work of adhesion values greater than 2000 N/m. Given a range in TSL tensile strength of 1 to 10 MPa and typical liner thicknesses of 3 to 4 mm, liner debonding should be the initial failure mechanism. Tensile rupture of the TSL should only occur after a large debonded width is created.

REFERENCES

Archibald, J. F., 2001. Assessing acceptance criteria for and capabilities of liners for mitigating ground falls. MASHA, Health and safety Conference, Sudbury, 31 pages.

Archibald, J. F. and Lausch, P., 1999. Thin spray-on linings for rock failure stabilization; 37th U.S. Rock Mechanics Symposium -Rock Mechanics for Industry, Vail, Colorado, Vol. 2, pp. 617-624, B. Amadei et al., Ed. Rotterdam: Balkema.

Archibald, J. F., and DeSouza, E. M., 1993. Mine Support Radiation and Ventilation Control with Spray-on Barriers; 4th International High Level Radioactive Waste Management Conference, Las Vegas, Nevada, pp. 1770-1777.

Archibald, J. F., Espley, S. J., and Lausch, P., 1997. Field and laboratory response of spray-on Mineguard polyurethane liners; International Symposium on Rock Support -Applied Solutions for Underground Structures, Lillehammer, Norway, pp. 475-490.

Archibald, J.F., DeSouza, E. M., and Emmerson, G., 1998. The effectiveness of spray-on Mineguard linings for post-yield failure stabilization in soft and hard rock mine environments. 7th International Symposium on Mine Planning and Equipment Selection (Balkema), Calgary, Alberta, pp. 191-197.

ASTM D3330/D3330M-02, 2004. Standard Test Method for Peel Adhesion of Pressure-Sensitive Tape. V. 15.09, Paper; Packaging; Flexible Barrier Materials; Business Imaging Products, pp. 340-345.

ASTM D4541-02, 2004. Standard test method for pull-off strength of coatings using portable adhesion testers. V. 06.02, Paint-Products and Applications: Protective Coatings; Pipeline Coatings, pp. 342-354.

ASTM D638, 1998. Standard test method for tensile properties of plastics. V. 8.01, Plastics(I): D256-D2343, pp. 46-58.

ASTM D903-98, 2004. Standard Test Method for Peel or Stripping Strength of Adhesive Bonds. V. 15.06, Adhesives, pp. 20-22.

ASTM F548-01, 2004. Standard Test Method for Intensity of Scratches on Aerospace Transparent Plastics. V. 15.03, Space Simulation & Applications of Space Technology: Aerospace and Aircraft: Composite materials, pp. 922-925.

Austin, S., Robins, P. and Pan Y., 1995. Tensile bond testing of concrete repairs. Materials and Structures, 28, pp. 249-259.

Barton N. and Choubey V., 1977. The shear strength of rock joints in theory and practice. Rock Mechanics, 10, 1-54.

Blank, L.T., 1980. Statistical procedures for engineering management and science. McGrawHill.

Borejszo, R. and Bartlett, P., 2002. Tunnel guard in the mining industry. 2nd International Seminar on Surface Support Liners, South African Institute of Mining and Metallurgy, Johannesburg, Section 18, 4 pages.

Boussinesq, J., 1885. Applications des Potentiels à l'Étude de l'Équilibre et Mouvement des Solides Élastiques. Gauthier-Villard, Paris.

Bungey, J. H. and Madandoust, R., 1992. Factors influencing pull-off tests on concrete. Magazine of Concrete Research, 44, No. 158, pp. 21-30.

Chalker, P. R., Bull, S. J., and Rickerby, D. S., 1991. A review of the methods for the evaluation of coating-substrate adhesion. Materials Science and Engineering, A140, pp. 583-592.

Cleland, D. J. and Long, A. E., 1997. The pull-off test for concrete patch repairs. Proc. Institution Civil Engineers Structures & Buildings, 122, Nov., pp. 451-460.

Creton, C. and Lakrout, H., 2000. Micromechanics of flat-probe adhesion tests of soft viscoelastic polymer films. Polymer Science: Part B: Polymer Physics, 38, pp. 965-979.

Crosby, A. J. and Shull, K. R., 1999. Adhesive failure analysis of pressure-sensitive adhesives. Journal of Polymer Science: Part B: Polymer Physics, 37, pp. 3455-3472.

Crosby, A.J., Shull, K.R., Lakrout, H., and Creton, C., 2000. Deformation and failure modes of adhesively bonded elastic layers. Journal of Applied Physics. Vol:88, 5, pp. 2956-2966.

Delgado, F. G., Cording, E.J., Mahar, J.W., and Van Sintjan, M. L., 1979. Thin Shotcrete Linings in Loosening Rock, Proceedings, Rapid Excavation and Tunneling Conference, Vol. 1, AIME, N.Y., pp. 790-814.

Erck, R. A., 1994. Pin-pull adhesion measurements of copper films on ion-bombarded alumina. Thin Solid Films, 253, pp. 362-366.

Espley, S. J., Gustas R., Heilig J., and Moreau L. H., 2001. Thin spray-on liner research & field trials at INCO. Int. Seminar and Field Ttrials on Surface Support Liners: Membrane, Shotcrete and Mesh, Perth, Australia, Section 25.

Espley, S. J., O'Donnell, J. D., Thibodeau, D. and Paradis-Sokoloski, P., 1996. Investigation into the replacement of conventional support with spray-on liners; CIM Bulletin, Vol. 89, No. 1001, pp. 135-143.

Ganghoffer, J. F. and Gent, A.N., 1995. Adhesion of a rigid punch to a thin elastic layer. Journal of Adhesion, 48, pp. 75-84.

Giurgiutiu, V., Lyons, J., Petrou, M., Laub D. and Whitley, S., 2001. Fracture mechanics testing of the bond between composite overlays and a concrete substrate. Journal of Adhesion Science and technology, 15 (11), pp. 1351-1371.

Gunter, M., 1999. The blister test to determine the bond strength between polymer coatings and concrete. Proc. of the 2nd Int. RILEM Symposium, Dresden, Germany, September, edited by Y. Ohama and M. Puterman. pp. 21-33.

Hadjigeorgiou, J. and Grenon, M., 2002. Rational design methodology for thin sprayed on liners. 2nd International Seminar on Surface Support Liners, South African Institute of Mining and Metallurgy, July 29-31, Johannesburg, Section 12, 16 pages.

Hepworth, N. and Lobato, J., 2002. Tekflex resin spray field trials-Neves Corvo Mine, Portugal. 2nd International Seminar on Surface Support Liners, South African Institute of Mining and Metallurgy, July 29-31, Johannesburg, Section 19, 8 pages.

Jankowski, A. F., 1987. Adhesion of physically vapour-deposited titanium coatings to beryllium substrates. Thin Solid Films, 154, pp. 183-198.

Karbhari, V.M. and Engineer, M., 1996. Investigation of bond between concrete and composite: use of a peel test. Journal of Reinforced Plastics and Composites. Vol. 15, pp. 208-227.

Katz, G., 1976. Adhesion of copper films to aluminum oxide using a spinel structure interface. Thin Solid Films, 33, pp. 99-105.

Kendall, K., 1971. The adhesion and surface energy of elastic solids. Journal of Physics D: Applied Physics, 4, pp. 1186-1195.

Kuijpers, J.S. and Toper, A.Z., 2002. Towards a better understanding of the support function of thin sprayed liners. 2nd International Seminar on Surface Support Liners, South African Institute of Mining and Metallurgy, July 29-31, Johannesburg, Section 11, 7 pages.

Lacerda, L and Rispin, M., 2002. Current ground support membrane applications in North American underground mines. 2nd International Seminar on Surface Support Liners, South African Institute of Mining and Metallurgy, July 29-31, Johannesburg, Section 17, 16 pages.

Laurence, D.C., 2001. Membrane Trials at an Australian Underground Coal Mine, 1st International Workshop on Surface Support Liners, Australian Centre for Geomechanics, Perth WA, August.

Lewis, B., 2001. Mondi Rock-Hold, the development of this structural membrane support. Int. Seminar and Field Ttrials on Surface Support Liners: Membrane, shotcrete and Mesh, Perth, Australia, Section 18.

Lin, Y. Y., Hui, C. Y. and Conway, H. D., 2000. A detailed elastic analysis of the flat punch (tack) test for pressure-sensitive adhesives. Journal of Polymer Science Part B: Polymer Physics, 38, pp. 2769-2784.

Lindsey, G.H., 1967. Triaxial fracture studies. Journal of Applied Physics, 38, pp. 4843-4852.

Lyons, J., Gurgiutiu, V., Petrou, M., and Salem, H., 2002. Effect of hydrothermal aging on the fracture of composite overlays on concrete. Journal of Reinforced Plastics and Composites. Vol. 21, 4, pp. 293-309.

Malmgren, L., Nordlund, E, and Rolund, S., 2005. Adhesion strength and shrinkage of shotcrete. Tunneling and Underground Space Technology (20) pp. 33-48.

Marti, O., 2001. Chapter 17: Measurement of adhesion and pull-off forces with the AFM. Modern Tribology Handbook, Bharat Bushman.

Maugis, D., 2001. Chapter 4: Adhesion of solids: mechanical aspects. Modern Tribology Handbook, Bharat Bushman.

Mercer, R.A., 1992. The investigation of thin polyurethane linings as an alternative method of ground control. M.Sc. Thesis, Department of Mining Engineering, Queen's University, Kingston, Ontario, Canada.

Nagel, M. and Joughin, W.C., 2002. Thin sprayed liner trials at south deep mine. 2nd International Seminar on Surface Support Liners, South African Institute of Mining and Metallurgy, July 29-31, Johannesburg, Section 20, 12 pages.

Ozturk, H. & Tannant, D., 2004. Influence of rock properties and environmental conditions on adhesive bond to a liner. Surface Support in Mining. Potvin, Y., Stacey, T.R. and Hadjigeorgiou, J. ACG., Chapter 11, pp. 135.

Paul, S., 1985. Surface Coatings. John Wiley & Sons, 741 pages.

Potvin, Y., 2002. Towards a common understanding of TSL application in mines. 2nd International Seminar on Surface Support Liners, South African Institute of Mining and Metallurgy, July 29-31, Johannesburg, Section A, 9 pages.

Rocscience, 2002. Phase2, Version 5, Finite Element Program.

Rosa, G., Oltra, R. and Nadal M., 2002. Evaluation of the coating–substrate adhesion by laser-ultrasonics: Modeling and experiments. Journal of Applied Physics, (91)10, pp. 6744-6753.

Spearing, A.J.S. and Gelson, J., 2002. Developments and the future of thin reactive liners since the previous conference in Australia. 2nd International Seminar on Surface Support Liners, South African Institute of Mining and Metallurgy, July 29-31, Johannesburg, Section 13, 10 pages.

Tannant, D.D., 1997. Interpretation on pull tests on Mineguard to estimate capacity. Report to INCO Limited, Ontario Division, Geomechanics Research Centre, Sudbury, Ontario.

Tannant, D.D., 2004. Thin spray-on liners for underground rock support-testing and design issues. Surface Support in Mining. Potvin, Y., Stacey, T.R. and Hadjigeorgiou, J. ACG Chapter 1, pp. 49.

Tannant, D.D. and Ozturk, H., 2004. Evaluation of test methods for measuring adhesion between a liner and rock. Surface Support in Mining. Potvin, Y., Stacey, T.R. and Hadjigeorgiou, J. ACG Chapter 10, pp. 125-134.

Tannant, D.D., 2001. Thin spray-on liners for underground rock support-testing and design issues, Int. Seminar and Field Trials on Surface Support Liners: Membrane, Shotcrete and Mesh, Perth, Australia, pp. 1-18

Tannant, D.D., Swan, G., Espley, S. and Graham, C., 1999. Laboratory test procedures for validating the use of thin spray-on liners for mesh replacement; Canadian Institute of Mining, Metallurgy and Petroleum 101st Annual General Meeting, Calgary, Alberta, published on CD-ROM, 8 pages.

Timoshenko, S., and Goodier, J.N., 1970. Theory of Elasticity, London: McGrawHill.

Wan, K.T. and Duan, J., 2002. Adherence of rectangular flat punch onto a clamped plate: transition from a rigid plate to a flexible membrane. Transactions of the ASME, 69, pp. 104-109.

APPENDIX A: FEM MODELS

To study the effect of steel dolly diameter on the stress distribution at the liner-rock interface, axisymmetric finite element Phase 2 (Rocscience 2002) models were run. The vertical loading was kept as 0.1 MN. The general modelling geometry and boundary conditions can be seen in Figure A1.

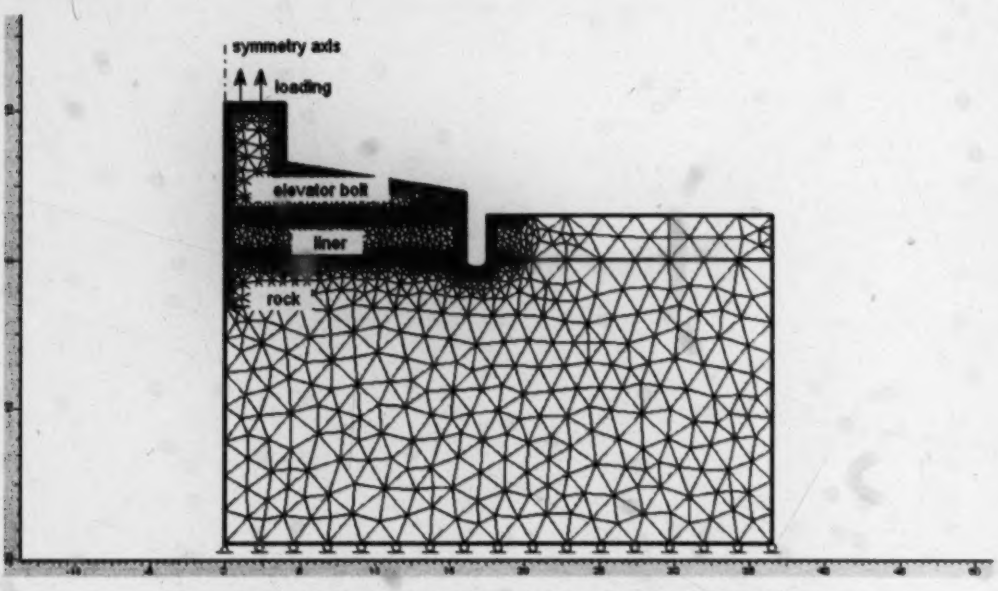

Figure A1 General geometry and boundary conditions of FE modelling.

A close-up view of the interface geometry and dimensions is presented in Figure A2.

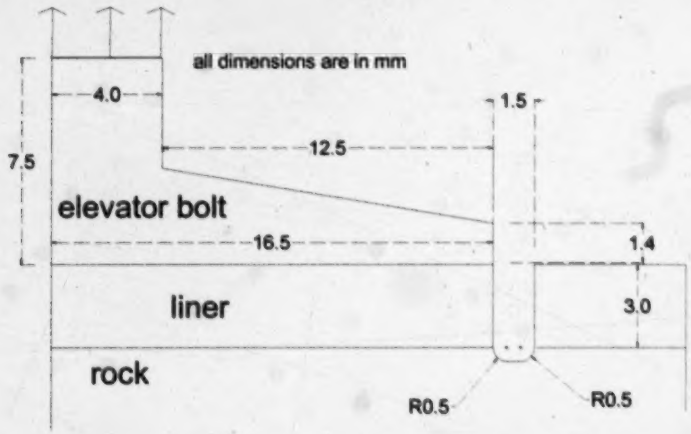

Figure A2 Close-up view of geometry of elevator bolt-liner-rock interfaces.

The input parameters for modelling are presented in Table A1.

Table A1 Mechanical properties of materials used in FEM modelling.

Material	Elastic modulus (MPa)	Poisson's ratio
Elevator Bolt	200000	0.3
Spray-on liner	13	0.25
Rock	20000	0.25

The vertical stress distribution at both interfaces and center of liner can be seen in Figure A3.

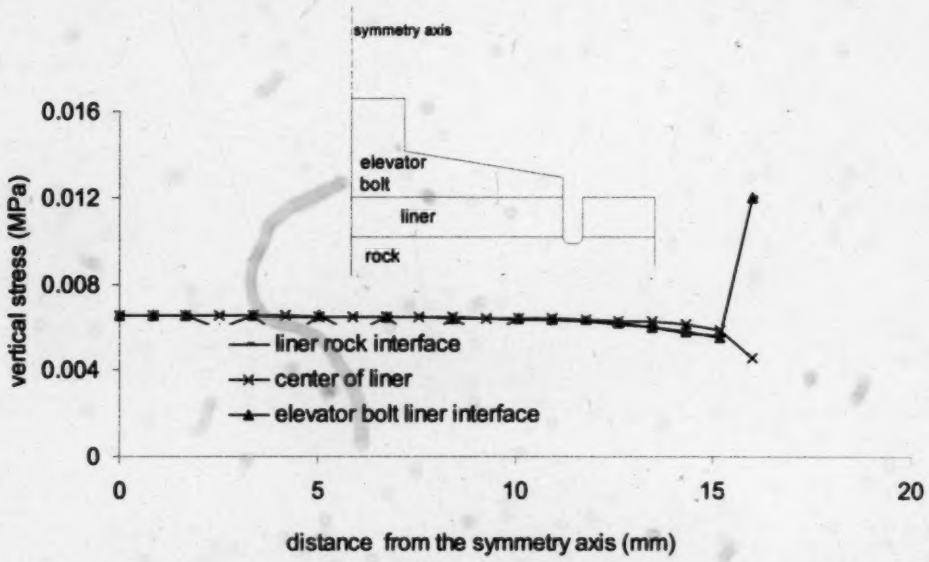

Figure A3 Vertical stress distribution at both interfaces and centre of liner.

As can be seen from Figure A3, vertical stress along the interface is tension, and constant for all the interfaces, except the end of the dolly boundary which makes a peak, which is most probably due to the stress concentration at the corner of the partial core and liner interface. So as can be seen from Figure A3, with the 16.5 mm dolly radius, getting a uniform stress distribution along the interface is possible.

To see the effect of a cylindrical dolly loading with the same diameter (Figure A4), a new FEM review was run with the same material properties. Vertical stress distributions along the both interfaces and at the center of liner can be seen in Figure A5.

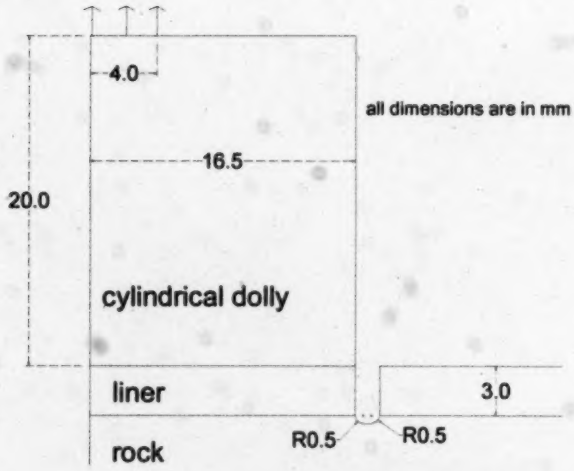

Figure A4 Cylindrical dolly loading geometry.

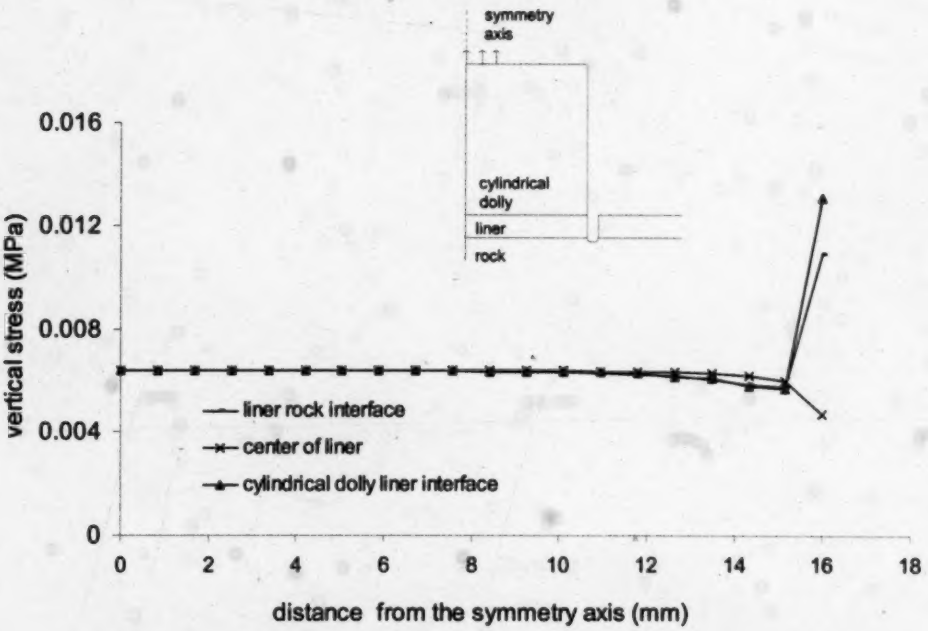

Figure A5 Vertical stress distribution along interfaces for cylindrical dolly loading.

As can be seen from Figure A5, both interfaces and center of liner give constant stress distributions, except at the edge of coring as in Figure A5, therefore, it was concluded that a steel dolly with 16.5 mm radius is sufficient to be used in the test.

To study the effect of increasing elevator bolt diameter, a 25 mm radius elevator bolt was modelled, and it was seen that tensile stress decreases towards the edge of the bolt (Figure A6). Therefore, it was concluded that a 16.5 mm radius elevator bolt is ideal for the test.

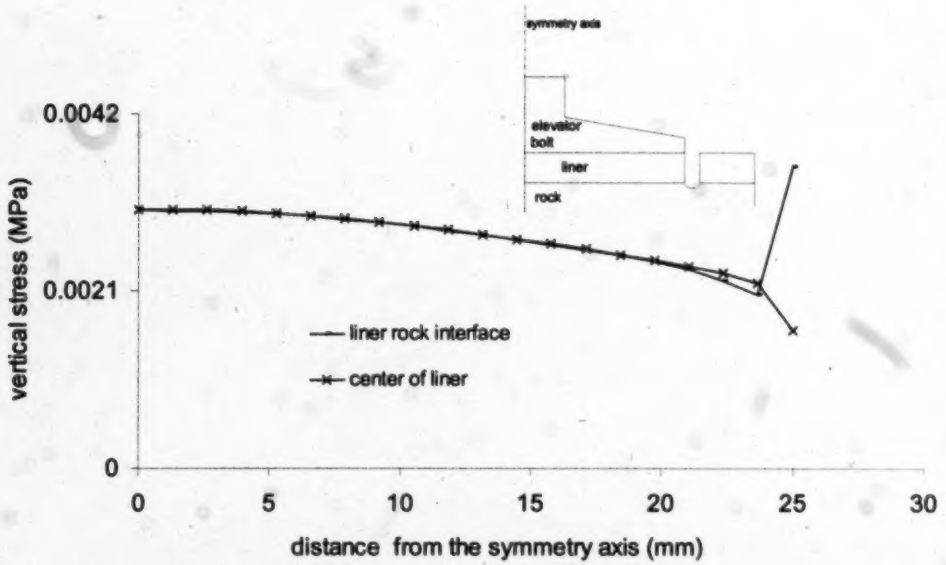

Figure A6 Vertical stress distribution along interfaces for 25 mm radius elevator bolt.

To study the effect of partial core depth on the mechanism of failure several FE runs were carried out with the geometry shown in Figure A7. The vertical stress distribution along the liner-rock interface with changing partial core depth is presented in Figure A8.

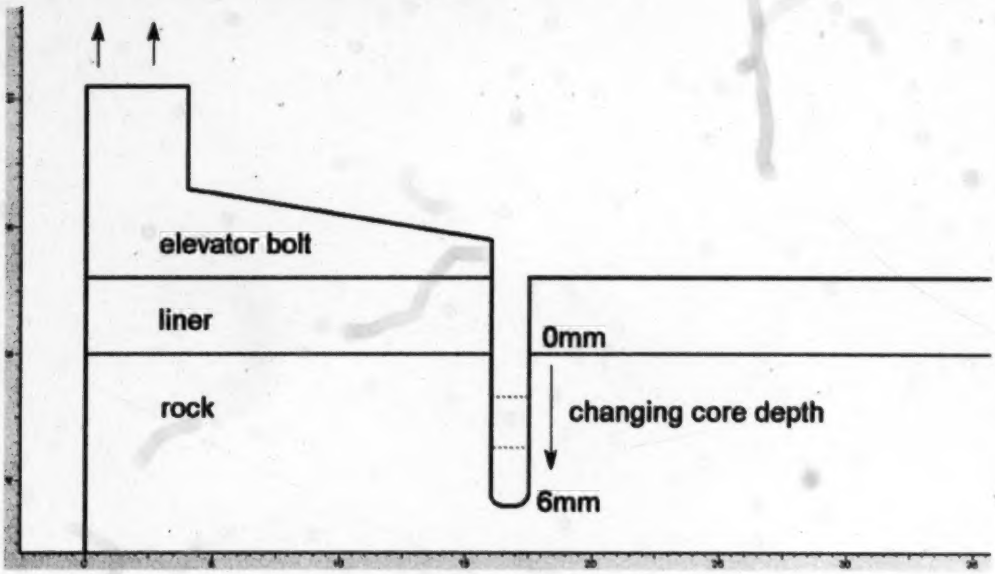

Figure A7 FE Modelling geometry of partial coring depth.

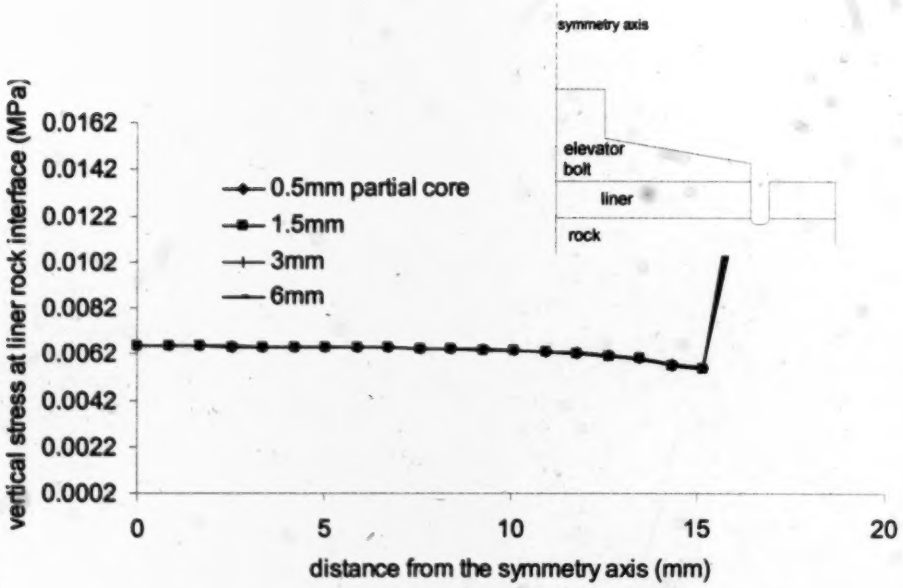

Figure A8 Vertical stress distribution along liner-rock interface.

As can be seen from Figure A8, partial coring depth has no effect on the vertical stress distribution along the liner-rock interface, therefore a 0.5 mm partial coring depth, which means just coring the lining material itself, was selected.

APPENDIX B: PHYSICAL AND SURFACE PROPERTY DETERMINATION

The roughness characteristics of the test surface were measured using a roughness profiler (Figure B9) and simple measurements of the average grain/crystal size. Profiles were taken along the length and width of each specimen and transferred onto paper by simply tracing over the edge of the profile with a pencil. Joint Roughness Coefficients (JRC) were estimated from the profiles using standard profiles provided by Barton and Choubey (1977). Digital photographs were also taken to document the surface condition.

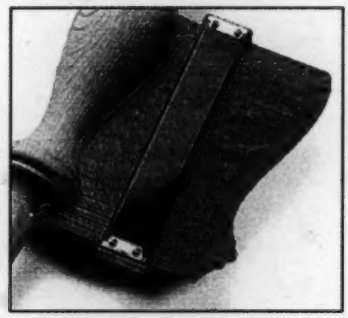

Figure B9 Roughness profile gauge.

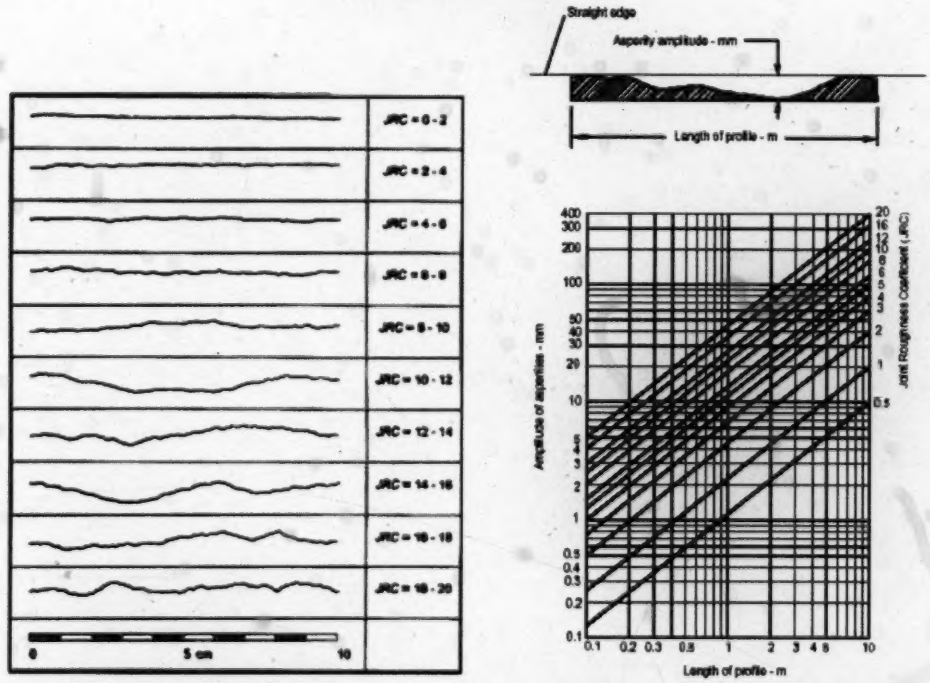
Straight edge
Asperity amplitude - mm
Length of profile - m
JRC = 0 - 2
JRC = 2 - 4
JRC = 4 - 6
JRC = 6 - 8
JRC = 8 - 10
JRC = 10 - 12
JRC = 12 - 14
JRC = 14 - 16
JRC = 16 - 18
JRC = 18 - 20
0
5 cm
10
Amplitude of asperities - mm
Joint Roughness Coefficient (JRC)
Length of profile - m

Figure B10 Roughness profiles and corresponding JRC values (Barton and Choubey 1977).

For grain size determination a magnifying glass (x10) was used. To check the grain sizes, a transparent scale (Figure B11) was formed using Photoshop. In Figure B11, each number

corresponds to the unit, dot, by knowing the resolution of the printer they were converted to usual scale, millimeter.

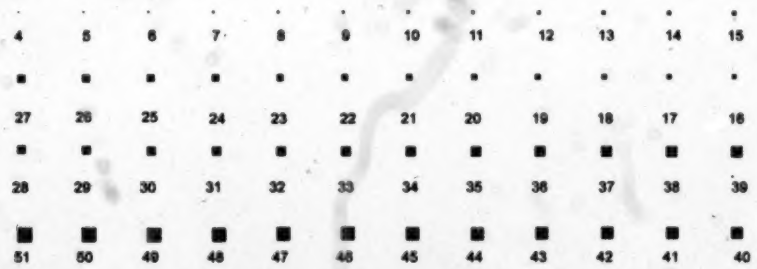

Figure B11 Grain size determination scale.

From each rock type, 4 to 5 samples were taken to measure density and indirect tensile strength (Brazilian test).

Various types of substrate were used for the tests. These included cinder block, paving stone, limestone, granite and sandstone (Table B2). The substrate surface was either created using a tensile fracture or a saw cut. To create a fresh tensile fracture surface, cores of the substrate material were loaded to failure using a Brazilian test setup.

Table B2 Substrate tensile strength, surface roughness and average grain/crystal size.

Sample	Tensile strength (MPa)	Ave. Tensile strength (MPa)	Average grain size (mm)	Surface condition	Roughness JRC
Concrete cinder block	1.6	1.6	2	Natural	0.5 (Flat)
Concrete paving stone	2.95, 4.35, 3.39, 3.75, 3,2, 4.48	3.7 (0.62)	3	Sawn or natural	0.5 (Flat)
sandstone	2.43, 0.99, 1.47, 1.66, 0.96	1.5 (0.6)	0.2	Split	20 (Rough)
Granite	11.81, 12.13, 7.08	10.4 (2.8)	1.8	Split	20 (Rough)
Limestone	2.71, 1.74, 3.32, 2.46, 3.14, 2.93	2.7 (0.6)	0.2	Split	20 (Rough)

Porosity of substrates was also determined (Figure B12), porosity values are presented in Table 3. Matrix densities were calculated using the following equation.

$$\rho_b = \phi\rho_a + (1-\phi)\rho_{ma} \qquad \text{(B1)}$$

where ϕ is porosity, ρ_b is bulk density, ρ_a is air density (1.2 kg/m^3), and ρ_{ma} is matrix density.

Figure B12 Porosity measurement set up (vacuum chamber and samples).

APPENDIX C: LINER PRODUCTS

Tekflex

MINOVA

Flexible, high-strength, membrane strata support

Uses
Tekflex coating is a patented high tensile strength sealant specially designed to permanently stabilize the integrity of rock structures accommodating the stresses associated with strata movement while providing a barrier to moisture degradation.

Advantages
- **Tough** - Ability to stretch, excellent tensile characteristics, and fiber reinforcing assure coating integrity even after strata deformation.
- **Simple Mixing** - Convenient packaging of two and one half parts liquid component to one part powder component minimizes mixing errors—no water or additional additives required.
- **Excellent Adhesion** - Special formulation enables superb adhesion to the rock, assuring a long-lasting coating.
- **Non-flammable** - No unusual storage or ventilation requirements, equipment clean-up procedures, or waste disposal.

Description
Tekflex coating, developed in response to customer-demand for a premium strata support membrane with famous Minova USA Inc. quality, is a cement-based spray material designed with superb flexibility, high tensile strength, and excellent adhesive qualities. The product enhances the structural integrity of the rock and forms an impervious barrier, which eliminates the degrading effects of weathering. Material coverage at a thickness of 1/6" varies from 1.2 to 2.7 sq ft per liter, depending on the roughness of the rock surface.

Packaging
Tekflex Liquid is available in 5 gallon pails, 36 pails per stretch-wrapped pallet. **Tekflex** Powder is available in 44 lb., 3 ply bags with one polyethylene layer, 43 bags to a stretch-wrapped pallet. Three pallets of liquid are consumed with each pallet of powder.

Instructions for Use
No unusual ventilation requirements are needed during application. Workers should take general precautions including protective clothing, gloves, dust masks, and adequate eye protection.

1. Remove or protect any objects that are not to be covered with **Tekflex** coating.
2. Remove as much dust and loose material as possible. Spraying onto a clean, dust-free substrate enables best results.
3. As **Tekflex** sealant material may be mixed and sprayed using various types of equipment, follow the instructions for the particular equipment you are using.
   Notes:
   a) The best time to spray is right after excavation, when fresh, solid rock is first exposed.
   b) Temperature should be 40°F, or higher. Ideal is roughly 60°F.
   c) The practical thickness achievable will depend somewhat on the orientation of the rock. Suggested thickness is 1/6" (4mm).
4. Pot life is approximately one half hour. Water may be used for clean up during this time.
5. Thoroughly purge all **Tekflex** material from the machine and lines with water when preparing for clean-up. Follow any machine manufacturer's recommendations for clean-up.

Shelf-Life
Both components: twelve months, in cool, dry conditions. Temperature of the **Tekflex** Liquid component must be kept above the freezing point.

Consult your local Minova USA Inc. representative for additional application and contracting information.

Rev 10 - 11/04

Tekflex PM

MINOVA

Polymer modified sprayable cement coating

Uses
Tekflex PM is specially designed for use in Minova USA Inc.'s Apex continuous placing machine. Alternately it may be batch mixed and applied via Minova's Air Red or Big Red machines. This high strength cement coating is ideal for quickly coating an entryway with a strong durable sealant. Uses include the prevention of spalling from moisture ingress and helping ensure the structural integrity of mine passages. An excellent alternative to gunite or shotcrete without the mess.

Advantages
- **Good Adhesion** – Contains polymer latex for superior adhesion.
- **Economical** – Coverage rate of 12 1/2 ft^2/bag at ½ inch thickness.
- **Attractive** – Dries off white.
- **Strong** – Over 4,000 psi.
- **Convenient – Tekflex PM** can be pumped over 400 feet through standard mine spray hose.
- **Simple** – Minova USA Inc.'s Apex unit automatically mixes in the right amount of water as it pumps. It also has an on board compressor and water tank.
- **Clean** - Minimal dust compared to dry process gunite.
- **Non-flammable** – No unusual storage or ventilation requirements, equipment clean-up procedures, or waste disposal.

Description
Tekflex PM was developed in response to customer demand for a more easily applied gunite with improved adhesion. **Tekflex PM** was specifically designed for pumping through our Apex. The Apex meters and mixes the proper amount of water and powder as it pumps **Tekflex PM**. **Tekflex PM** can also be pumped through Minova designed air-powered and hydraulic powered equipment.

Tekflex PM is a non-shrinking cement that dries to a durable off-white finish. **Tekflex PM** has a pumping life of up to 30 minutes and sets in 5 to 8 hours. **Tekflex PM** is especially suited for large remediation or preventative sealing. The convenience of the self contained Apex allows fast and easy application.

Instructions for Use
It is recommended that a consultant from Minova USA Inc. or an authorized contractor be at the site during pumping to aid in training on the equipment, mixing, and spraying

1. Spray clean the roof and ribs with water or air.
2. Run a 1 to 2 inch hose from the Apex to the job site.
3. Fill the Apex's water tank. Hook up either 460/575 volt AC power, start compressor, start water pump and grout pump. Add **Tekflex PM** to hopper and adjust water flow until pressure gauge reads 20-40 bar (300 to 600 psi).
4. Spray roof and ribs to desired thickness.

Apex
- Made in the USA by Minova USA Inc.
- Available on a lease arrangement.
- Multi-use can handle several of Minova USA Inc.'s cementitious products: **Tekflex PM**, Tekrok G, Tekflex All-Powder, Teklite.
- 10 horsepower AC motor; full load 14 amps @ 460V.
- Apex develops 870 psi pressure, and is capable of pumping **Tekflex PM** over 400 feet through a 1 1/2 inch hose.
- Cable size normally used - #6.
- Apex requires a clean source of water.
- See diagram for dimensions. Weight is approximately 2300 pounds.
- Integral compressor.

Packaging
55 lb., 3 ply bags with one polyethylene layer, 48 bags per stretchwrapped pallet.

Shelf-Life
Twelve months, in dry conditions. Consult your local Minova USA Inc. representative for additional information.

Rev. 4 - 09/04

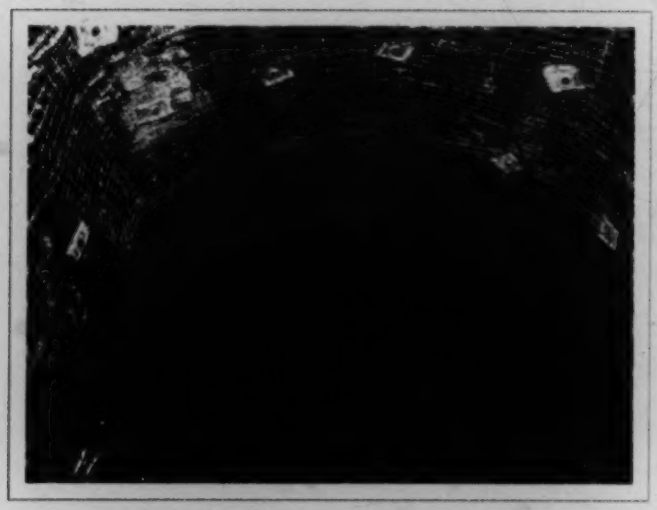

TUNNEL GUARD

THIN SUPPORT LINER FOR MINING AND CONSTRUCTION

- Tunnel Guard is a two component product, containing a cementitious powder with fibers and a liquid polymer.
- It is a non-reactive and rigid system
- It is non-toxic, non-flammable and has a pot life around 6 to 10 minutes
- There is a significant reduction in the amount of materials handled as compared to other liners such as shotcrete
- The current Tunnel Guard pump requires 250 cfm at 5 to 6 bars
- Tunnel Guard passes the ASTM E162 radiated heat test
- Specifications:
  - Components: A - Dry Powder B - Liquid Additive
  - Color: A - Brown B - White
  - Relative density: Approx. 1.8
  - Gel Time: Approx. 10 min
- Applications include:
  - Limits rock weathering
  - Helps limit rock scaling
  - Highwall (slope) support
  - Supplemental roof and rib support
  - Seals and consolidates rock
  - Contains surface dumps and stockpiles

STRATA

YOUR SUPPORT FOR LIFE

MASTER BUILDERS
POLYMER MEMBRANE

degussa.
Construction Chemicals

CS 1251 2K THIN SUPPORT MEMBRANE

Sprayable, two-component, elastic polymer membrane for immediate temporary surface reinforcement of soil and rock

Applications

Recommended for use in:

- Tunnelling and mining
- Temporary stabilization of soil and rock
- Immediate rock reinforcement just behind TBM cutterhead, or other areas with difficult accessibility
- Against hard rock strain bursting
- When large deformations are expected within short time
- To reduce air-slaking and rock weathering
- Alternative to mesh protection

Description

CS 1251 2K is a two-component membrane for spray-application onto soil and rock. The product is cement free, gels in less than 3 minutes at 68 °F (20 °C) and immediately forms a very ductile and strong surface reinforcement on the substrate. Through excellent bond, good elasticity and high failure stress, the ground stability and stand-up-time is substantially improved.

Features

- Effective reinforcement within minutes
- Excellent bond, high strength and elasticity
- Excellent shotcrete bond strength with CS 1251 2K as a substrate
- Air-"tight" after less than 5 minutes
- Solvent free
- Does not support fire, self-extinguishing

Benefits

- No setup time, 220 lb (100 kg) covers ~ 215-538 ft² (~20-50 m²)
- Placement possible in narrow space
- Spray applied using simple equipment

Performance Characteristics

Form		A & B: Gel
Color	A	Black
	B	White
Density mixed		(68 °F (20°C)) 10 ± 0.8 lb/gal (1.2 ± 0.1 kg/L)
Application thickness		0.1-.25 in. (2-6 mm)
Maximum thickness per pass		0.25 in. (6 mm)
Application temperature		50-95 °F (10-35 °C)
Maximum air humidity		65% (no strength loss)
Tensile failure stress (1 h)		> 290 psi 68 °F (> 2.0 MPa, 20 °C)
Failure strain (1 h)		> 100%, 68 °F (20 °C)
Bond to dry concrete (24 h)		> 145 psi (> 1 MPa)
Reaction time		< 3 min. 68 °F (20 °C)
Weight ratio A:B		Nominal 3:0:1
Flammability		self-extinguishing
Chemical resistance		acids and solvents

Guidelines for Use

CS 1251 2K must be used for strengthening of ground under the supervision of a qualified geotechnical engineer. The product should primarily be used to increase safety by application onto potentially unstable ground where other means cannot be applied due to space limitations or other restrictions. Depending on ground conditions the effect of CS 1251 2K will in many cases be of a temporary nature. The need for other support measures to supplement, and further strengthen the ground, must always be carefully considered.

The substrate should be free from dust, oil and other contamination prior to spraying. The product is not designed to be sprayed against running water. However, local point damage, or locally reduced properties due to water ingress will only partly reduce the stabilizing effect.

CASTONITE™

THIN SUPPORTLINER

SPECIFICATIONS

•	Tensile strength:	1 hour	58psi
		28 days	510psi
•	Bond strength:	1 day	73psi
		28 days	260psi

BENEFITS

- Excellent weathering protection
- Rapid strength development
- Rapid application (over 3yd³/minute)
- Helps improve illumination
- Can be applied in limited access areas
- Does not hinder other activities
- Reduction in materials handling compared to other liners (such as shotcrete/gunite)

SAFETY & PRECAUTIONS

- In ambient conditions and original sealed containers the shelf life is 12 months
- Should not be stored in freezing conditions
- Safe environment is required before application
- Gloves and goggles must be worn during application
- Prior to spraying, prewash surface thoroughly with high-pressure water
- Product not suitable for application in areas where freezing and thawing may occur
- No TSL can be applied over mobile/running water underground

STRATA MINE SERVICES

Strata Mine Services offers a full application service, technical assistance and training.

For more information, please contact your Strata Products (USA) Inc. representative, call 1-800-691-6601 or contact Strata Mine Services at 1-276-991-1003

© 2002 Strata Products (USA) Inc. Strata Products is a registered trademark of Strata Product (USA) Inc. Castonite is a trademark of the Rohm and Haas Company

TECHNICAL DATA SHEET
"Rock Web"

Spray-On Plastics two component, one to one ratio spray coating is a 100% solids, solvent free pure Polyurea for protective seamless finishing and plastic structures. This coating provides ground support while maintaining excellent adhesion with rock surfaces.

PHYSICAL PROPERTIES:
HARDNESS: 60 Shore D
TENSILE STRENGTH: 2674 psi
MODULUS @ 100% ELONGATION: 2353 psi
ELONGATION: 124%
TEAR STRENGTH:
(die C) 415 pli
(pant leg) 66 pli
SERVICE TEMP RANGE: -20 TO 400 ^{0}F
CHEMICAL RESISTANCE:
(ACIDS): Very Good
(BASES): Very Good

APPENDIX D: DETAILED TEST RESULTS

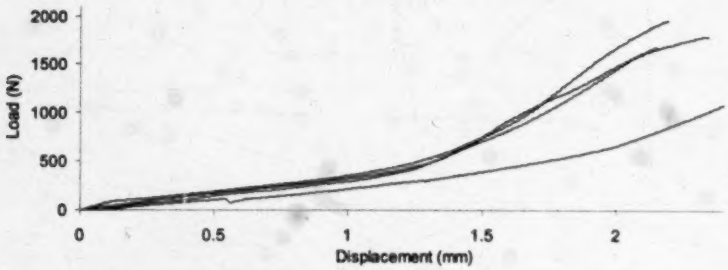

Figure D1 Load displacement curve for Tekflex on cinder block tests.

Table D1 Thicknesses, adhesion and failure type results of Tekflex on cinder block substrate.

Adhesion (MPa)	Thickness (mm)	Failure Type
2.10	0.5	Interface
2.29	0.5	Interface
1.96	0.5	Epoxy
1.38	0.5	Epoxy

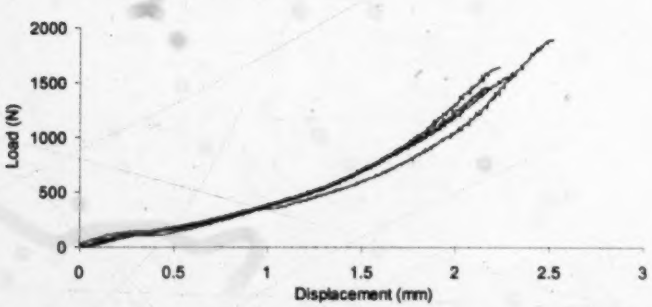

Figure D2 Load displacement curve for Tekflex on clean paving stone tests.

Table D2 Thicknesses, adhesion and failure type results of Tekflex on paving stone substrate.

Adhesion (MPa)	Thickness (mm)	Failure Type
2.22	3.5	Interface
1.71	4	Interface
1.92	3.5	Interface
1.82	3	Interface

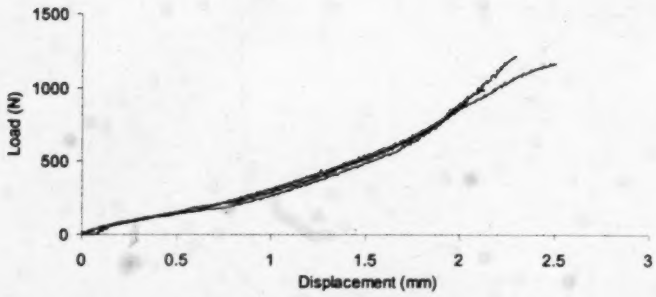

Figure D3 Load displacement curve for Tekflex on saw cut granite tests.

Table D3 Thicknesses, adhesion and failure type results of Tekflex on saw cut granite substrate.

Adhesion (MPa)	Thickness (mm)	Failure Type
1.16	5	Interface
1.42	4	Interface
1.37	5	Interface

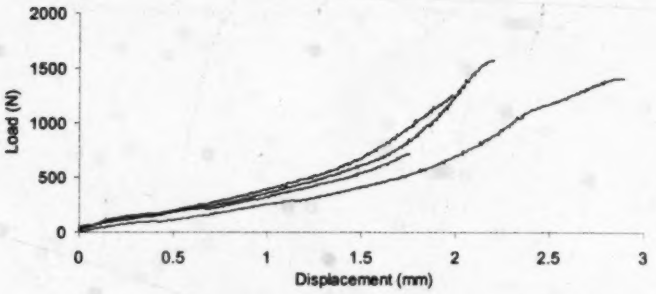

Figure D4 Load displacement curve for Tekflex on split granite tests.

Table D4 Thicknesses, adhesion and failure type results of Tekflex on split granite substrate.

Adhesion (MPa)	Thickness (mm)	Failure Type
1.85	2.5	Interface
0.84	4	Interface
1.48	3	Interface
1.65	4	Interface

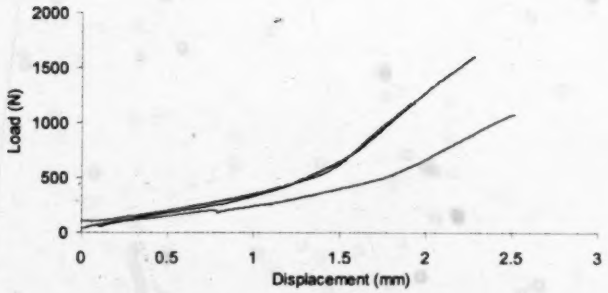

Figure D5 Load displacement curve for Tekflex on split limestone tests.

Table D5 Thicknesses, adhesion and failure type results of Tekflex on split limestone substrate.

Adhesion (MPa)	Thickness (mm)	Failure Type
1.38	3	Interface
1.26	3	Substrate
1.88	3	Interface

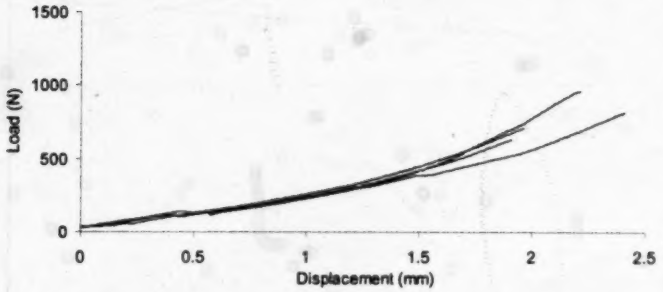

Figure D6 Load displacement curve for Tekflex on sandstone tests.

Table D6 Thicknesses, adhesion and failure type results of Tekflex on split sandstone substrate.

Adhesion (MPa)	Thickness (mm)	Failure Type
0.83	2	Substrate
1.00	3	Substrate
1.13	2	Substrate
0.74	3	Substrate

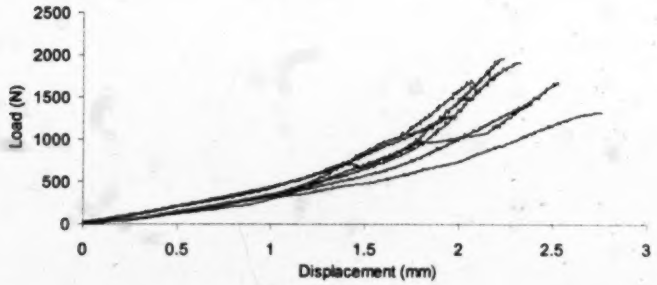

Figure D7 Load displacement curve for Castonite on paving stone substrate.

Table D7 Thicknesses, adhesion and failure type results of Castonite on paving stone substrate.

Adhesion (MPa)	Thickness (mm)	Failure Type
2.24	3	Cohesive
1.66	3	Cohesive
1.99	3	Cohesive
2.29	3	Cohesive
1.96	3	Cohesive
1.50	3	Cohesive
1.54	3	Cohesive

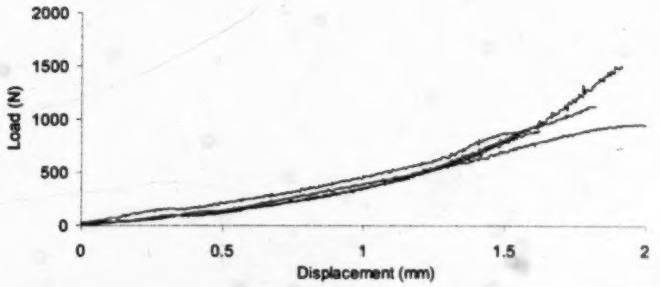

Figure D8 Load displacement curve for Castonite on split granite substrate.

Table D8 Thicknesses, adhesion and failure type results of Castonite on split granite substrate.

Adhesion (MPa)	Thickness (mm)	Failure Type
1.31	2.5	Cohesive
1.04	4.5	Interface
1.11	3	Interface
1.76	2.5	Cohesive

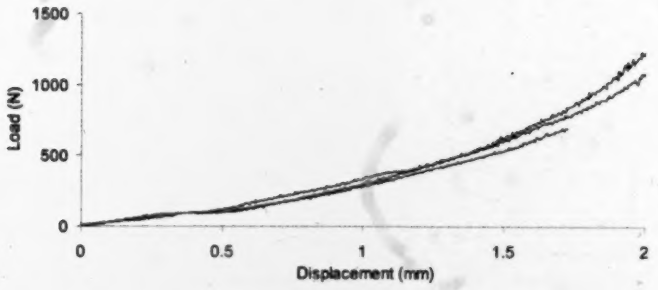

Figure D9 Load displacement curve for Castonite on sawn granite substrate.

Table D9 Thicknesses, adhesion and failure type results of Castonite on saw cut granite substrate.

Adhesion (MPa)	Thickness (mm)	Failure Type
1.43	4	Cohesive
1.61	4	Cohesive
0.81	5	Interface

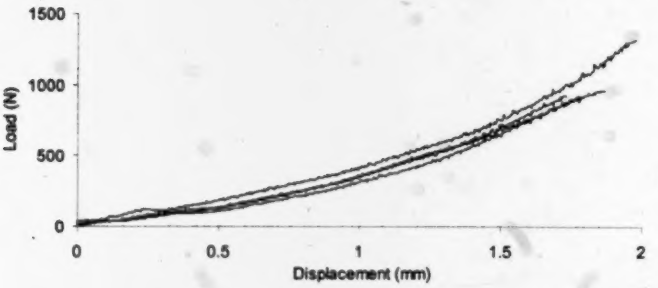

Figure D10 Load displacement curve for Castonite on sandstone substrate.

Table D10 Thicknesses, adhesion and failure type results of Castonite on sandstone substrate.

Adhesion (MPa)	Thickness (mm)	Failure Type
1.08	3	Substrate
1.08	3	Substrate
1.54	4.5	Substrate
1.12	4.5	Substrate

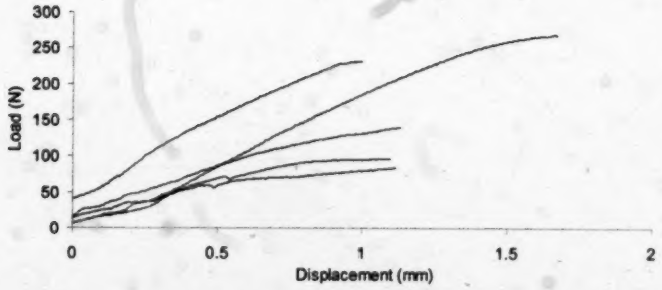

Figure D11 Load displacement curve for MBT CS1251 2K on cinder block substrate.

Table D11 Thicknesses, adhesion and failure type results of MBT CS1251 2K on cinder block substrate.

Adhesion (MPa)	Thickness (mm)	Failure Type
0.31	3	Cohesive
0.27	3	Cohesive
0.16	3	Cohesive
0.11	3	Cohesive
0.10	3	Cohesive

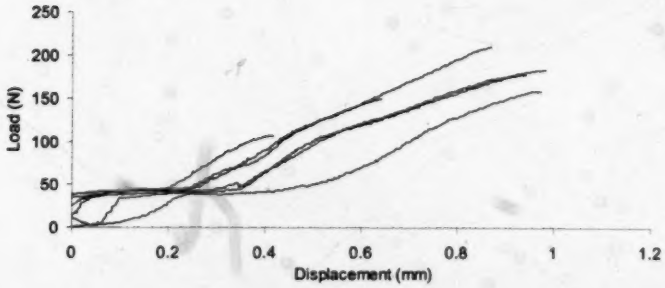

Figure D12 Load displacement curve for MBT CS1251 2K on split granite substrate.

Table D12 Thicknesses, adhesion and failure type results of MBT CS1251 2K on split granite substrate.

Adhesion (MPa)	Thickness (mm)	Failure Type
0.21	3	Cohesive
0.25	3	Cohesive
0.21	3	Cohesive
0.18	3	Cohesive
0.13	3	Cohesive
0.19	3	Cohesive

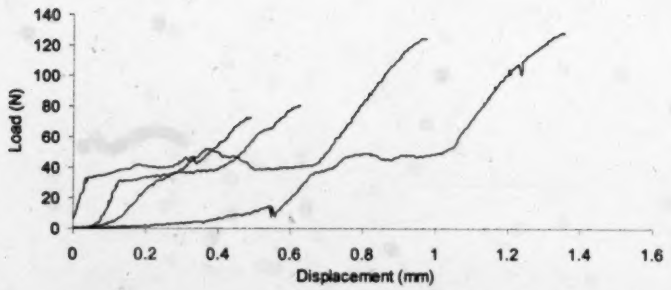

Figure D13 Load displacement curve for MBT CS1251 2K on split sandstone.

Table D13 Thicknesses, adhesion and failure type results of MBT CS1251 2K on split sandstone substrate.

Adhesion (MPa)	Thickness (mm)	Failure Type
0.15	3	Interface
0.15	3	Interface
0.09	3	Interface
0.08	3	Interface

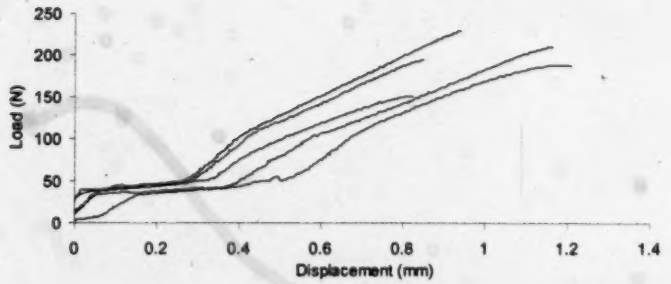

Figure D14 Load displacement curve for MBT CS1251 2K on split limestone.

Table D14 Thicknesses, adhesion and failure type results of MBT CS1251 2K on split limestone substrate.

Adhesion (MPa)	Thickness (mm)	Failure Type
0.23	3	Cohesive
0.27	3	Cohesive
0.18	3	Cohesive
0.25	3	Cohesive
0.22	3	Cohesive

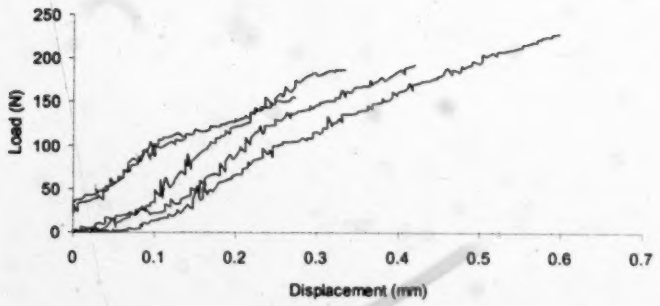

Figure D15 Load displacement curve for Tekflex PM on clean paving stone.

Table D15 Thicknesses, adhesion and failure type results of Tekflex PM on paving stone substrate.

Adhesion (MPa)	Thickness (mm)	Failure Type
0.23	4	Interface
0.27	4	Interface
0.18	4	Interface
0.13	4	Interface
0.22	6	Interface

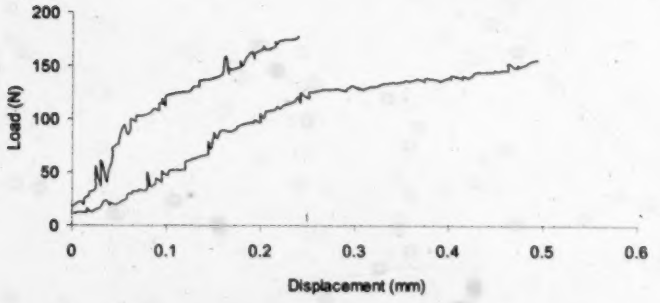

Figure D16 Load displacement curve for Tekflex PM on split limestone substrate.

Table D16 Thicknesses, adhesion and failure type results of Tekflex PM on split limestone substrate.

Adhesion (MPa)	Thickness (mm)	Failure Type
0.21	6	Interface
0.18	6	Interface

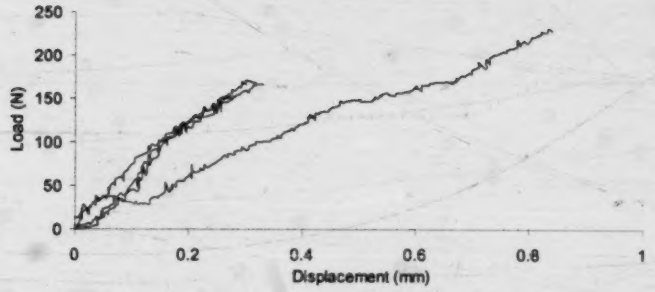

Figure D17 Load displacement curve for Tekflex PM on split granite substrate.

Table D17 Thicknesses, adhesion and failure type results of Tekflex PM on split granite substrate.

Adhesion (MPa)	Thickness (mm)	Failure Type
0.20	6	Interface
0.19	6	Interface
0.18	4	Interface
0.27	3	Interface

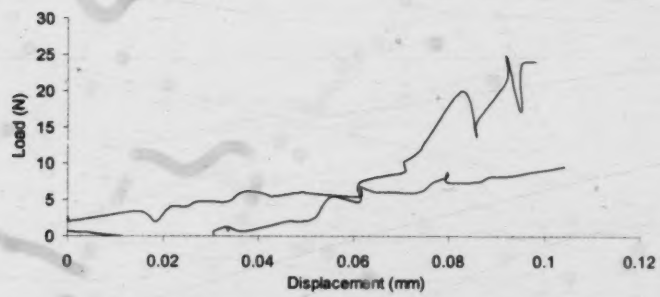

Figure D18 Load displacement curve for Tekflex PM on split sandstone substrate.

Table D18 Thicknesses, adhesion and failure type results of Tekflex PM on sandstone substrate.

Adhesion (MPa)	Thickness (mm)	Failure Type
0.03	3.5	Interface
0.01	6	Interface

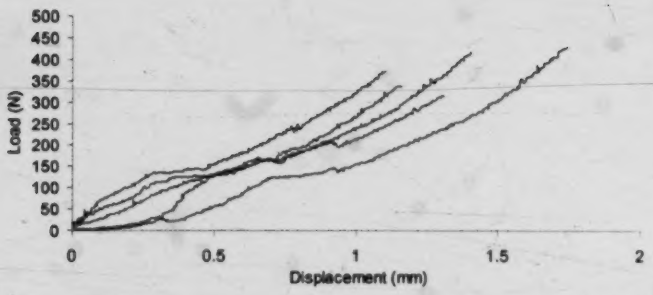

Figure D19 Load displacement curve for Tunnelguard on clean paving stone substrate.

Table D19 Thicknesses, adhesion and failure type results of Tunnelguard on paving stone substrate.

Adhesion (MPa)	Thickness (mm)	Failure Type
0.37	4	Cohesive
0.49	4	Cohesive
0.44	4	Cohesive
0.39	4	Cohesive
0.50	6	Cohesive

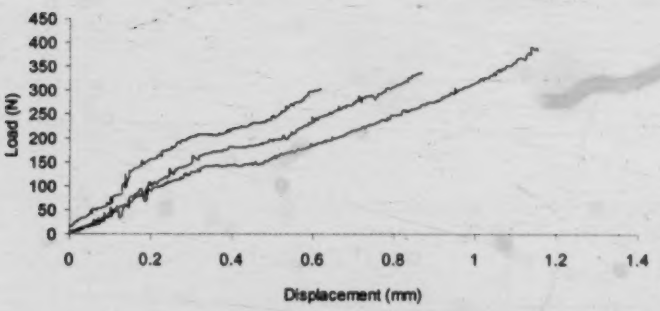

Figure D20 Load displacement curve for Tunnelguard on split granite substrate.

Table D20 Thicknesses, adhesion and failure type results of Tunnelguard on split granite substrate.

Adhesion (MPa)	Thickness (mm)	Failure Type
0.39	6	Cohesive
0.35	6	Cohesive
0.46	6	Cohesive

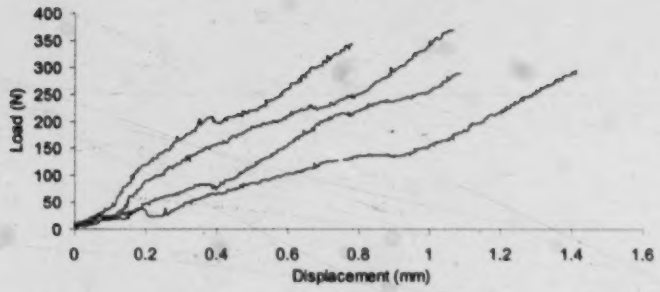

Figure D21 Load displacement curve for Tunnelguard on sawn granite substrate.

Table D21 Thicknesses, adhesion and failure type results of Tunnelguard on sawn granite substrate.

Adhesion (MPa)	Thickness (mm)	Failure Type
0.35	4	Cohesive
0.34	4	Cohesive
0.40	6	Cohesive
0.43	4	Cohesive

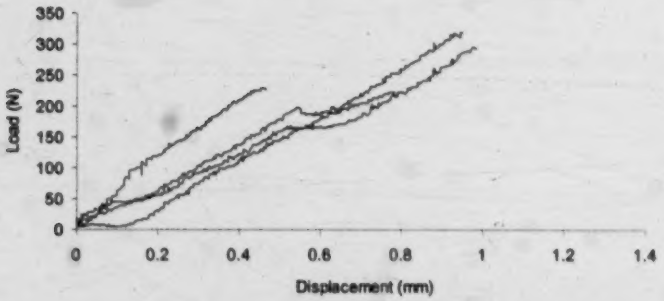

Figure D22 Load displacement curve for Tunnelguard on split limestone substrate.

Table D22 Thicknesses, adhesion and failure type results of Tunnelguard on limestone substrate.

Adhesion (MPa)	Thickness (mm)	Failure Type
0.35	6	Cohesive
0.37	6	Cohesive
0.27	4	Cohesive
0.26	3	Cohesive

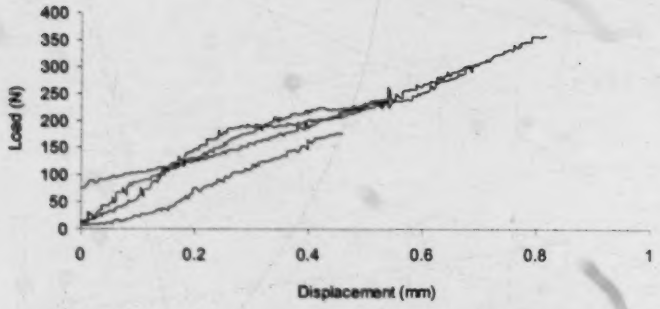

Figure D23 Load displacement curve for Tunnelguard on split sandstone substrate.

Table D23 Thicknesses, adhesion and failure type results of Tunnelguard on split sandstone substrate.

Adhesion (MPa)	Thickness (mm)	Failure Type
0.21	3.5	Interface
0.42	6	Interface
0.28	6	Interface
0.36	6	Interface

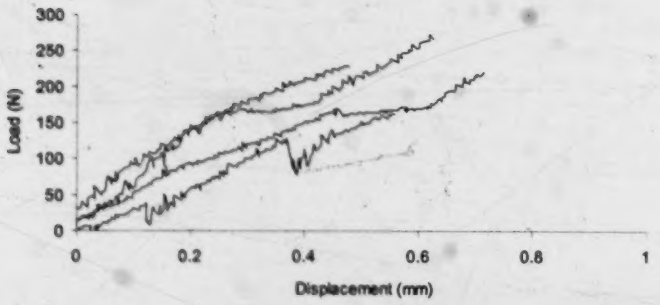

Figure D24 Load displacement curve for Tekflex on highly dusty paving stone substrate.

Table D24 Thicknesses, adhesion and failure type results of Tekflex on highly dusty paving stone substrate.

Adhesion (MPa)	Thickness (mm)	Failure Type
0.21	3.5	Interface
0.42	4	Interface
0.28	3	Interface
0.36	3	Interface

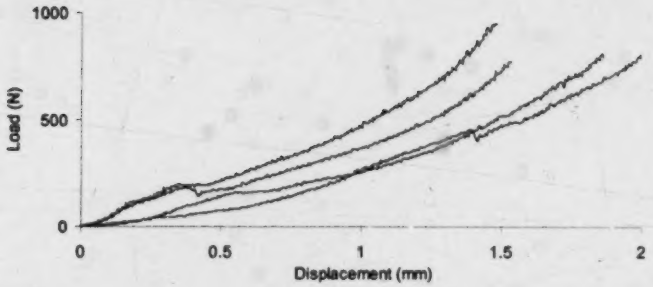

Figure D25 Load displacement curve for Tekflex on moderately dusty paving stone substrate.

Table D25 Thicknesses, adhesion and failure type results of Tekflex on moderately dusty paving stone substrate.

Adhesion (MPa)	Thickness (mm)	Failure Type
0.95	4	Interface
1.11	3.5	Interface
0.95	3	Interface
0.91	4	Interface

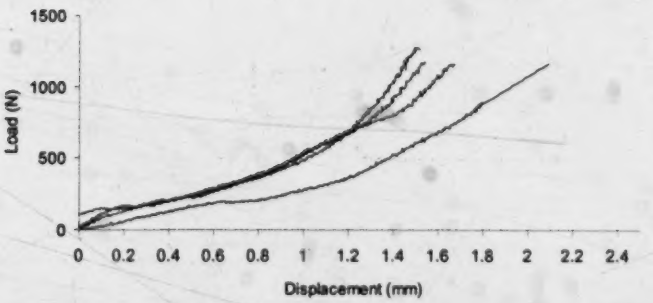

Figure D26 Load displacement curve for Tekflex on lightly dusty paving stone substrate.

Table D26 Thicknesses, adhesion and failure type results of Tekflex on lightly dusty paving stone substrate.

Adhesion (MPa)	Thickness (mm)	Failure Type
1.37	5	Interface
1.49	4	Interface
1.35	5	Interface
1.36	3.5	Interface

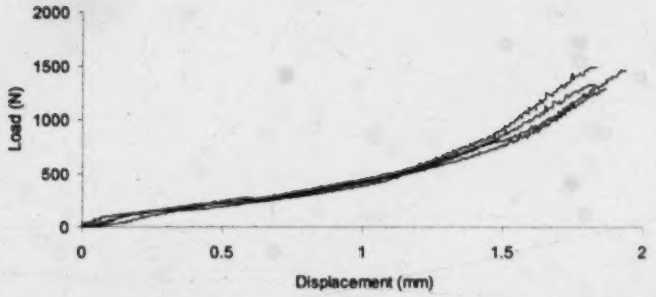

Figure D27 Load displacement curve for Tekflex on clean paving stone substrate.

Table D27 Thicknesses, adhesion and failure type results of Tekflex on clean paving stone substrate.

Adhesion (MPa)	Thickness (mm)	Failure Type
1.71	4	Interface
1.55	4	Interface
1.50	3	Interface
1.74	4	Interface

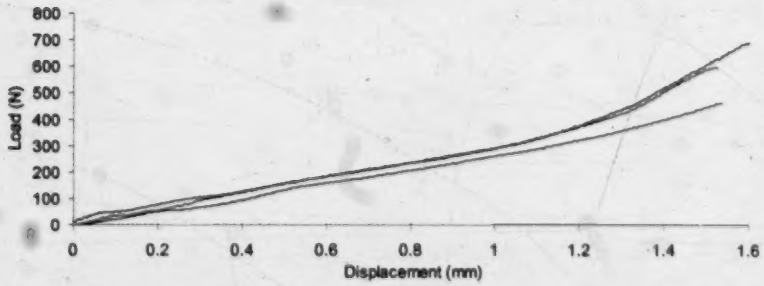

Figure D28 Load displacement curve for Tekflex on dusty cinder block substrate.

Table D28 Thicknesses, adhesion and failure type results of Tekflex on highly dusty cinder block substrate.

Adhesion (MPa)	Thickness (mm)	Failure Type
1.05	1.5	Interface
0.82	1.5	Interface
0.70	1.5	Interface
0.54	1.5	Interface

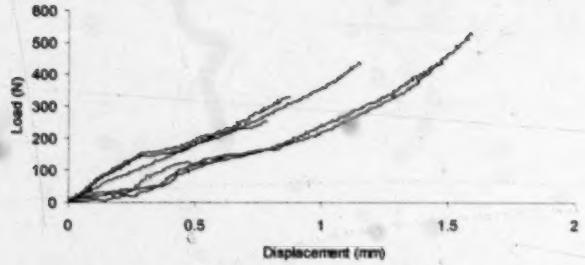

Figure D29 Load displacement curve for Tunnelguard on dusty paving stone substrate.

Table D29 Thicknesses, adhesion and failure type results of Tunnelguard on highly d5sty paving stone substrate.

Adhesion (MPa)	Thickness (mm)	Failure Type
0.30	4	Cohesive
0.51	6	Cohesive
0.62	6	Cohesive
0.19	6	Cohesive
0.38	6	Cohesive
0.51	6	Cohesive

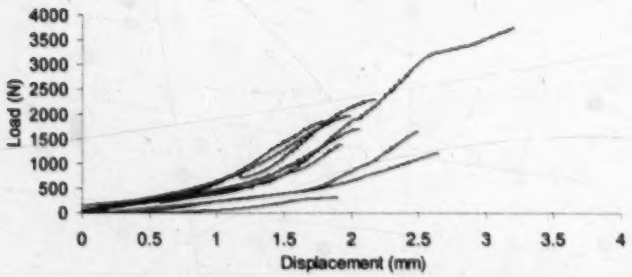

Figure D30 Clean norite substrate load displacement curve.

Table D30 Thicknesses, adhesion and failure type results of Rock Web on clean norite substrate.

Adhesion (MPa)	Thickness (mm)	Failure Type
1.42	3.5	Interface
0.37	2	Interface
4.46	2	Epoxy
2.68	2	Epoxy
1.61	2	Substrate
2.30	2	Epoxy
1.94	2	Epoxy
0.62	2	Interface
1.98	2.5	Interface
2.16	2	Interface

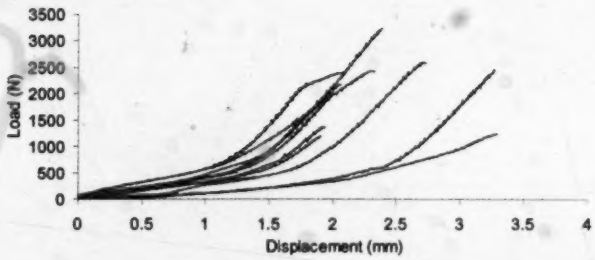

Figure D31 Dusty norite substrate load displacement curve.

Table D31 Thicknesses, adhesion and failure type results of Rock Web on dusty norite substrate.

Adhesion (MPa)	Thickness (mm)	Failure Type
1.46	2	Interface
2.80	2	Interface
3.03	2	Interface
2.85	2.5	Interface
0.13	2	Cohesive
2.33	2	Epoxy
3.10	2	Interface
3.78	2	Epoxy
2.55	2	Interface
0.50	2	Epoxy
1.40	2	Cohesive
0.60	3	Interface
1.60	2	Interface

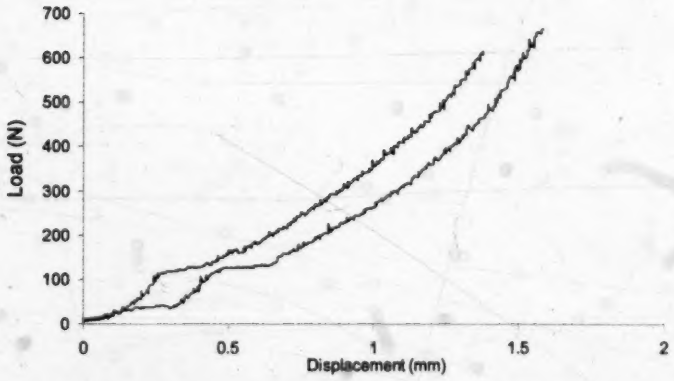

Figure D32 Lightly oily paving stone substrate load displacement curve.

Table D32 Thicknesses, adhesion and failure type results of Tekflex on lightly oily paving stone substrate.

Adhesion (MPa)	Thickness (mm)	Failure Type
0.72	2.5	Interface
0.78	4	Interface

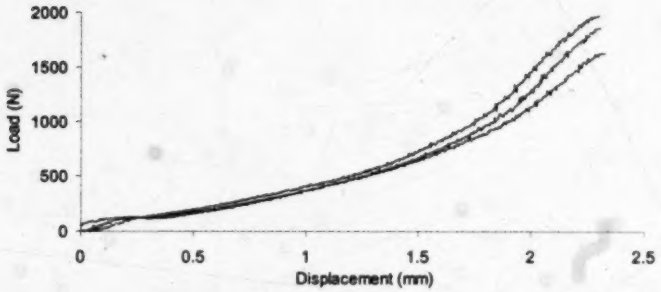

Figure D33 Load displacement curve for Tekflex on damp paving stone substrate.

Table D33 Thicknesses, adhesion and failure type results of Tekflex on damp paving stone substrate.

Adhesion (MPa)	Thickness (mm)	Failure Type
2.17	4	Interface
1.90	3.5	Interface
2.30	4	Interface

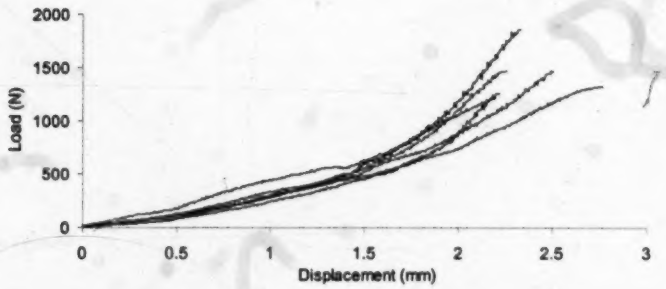

Figure D34 Load displacement curve for Castonite on damp paving stone substrate.

Table D34 Thicknesses, adhesion and failure type results of Castonite on damp paving stone substrate.

Adhesion (MPa)	Thickness (mm)	Failure Type
1.41	3	Epoxy
1.47	3	Epoxy
1.72	3	Epoxy
2.18	3	Cohesive
1.54	3	Cohesive
1.72	3	Cohesive

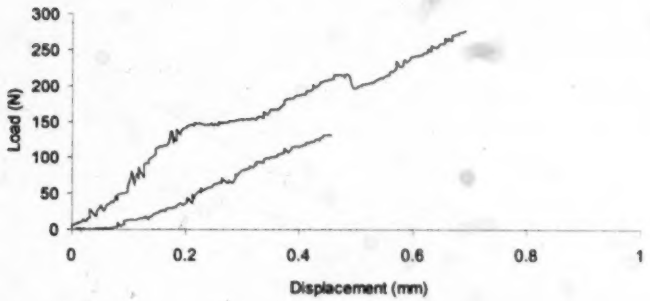

Figure D35 Load displacement curve for Tekflex PM on damp paving stone substrate.

Table D35 Thicknesses, adhesion and failure type results of Tekflex PM on damp paving stone substrate.

Adhesion (MPa)	Thickness (mm)	Failure Type
0.15	4	Interface
0.32	6	Interface

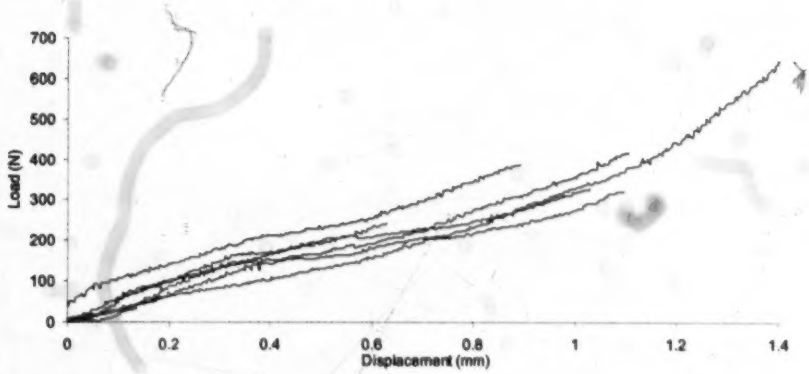

Figure D36 Load displacement curve of Tekflex PM on damp paving stone substrate.

Table D36 Thicknesses, adhesion and failure type results of Tunnelguard on damp paving stone substrate.

Adhesion (MPa)	Thickness (mm)	Failure Type
0.49	4	Cohesive
0.28	3	Cohesive
0.75	3.5	Cohesive
0.38	6	Cohesive
0.45	4	Cohesive
0.38	4	Cohesive

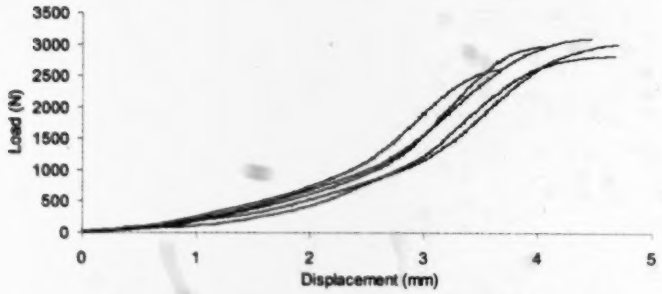

Figure D37 Load displacement curve of 1 month cured Tekflex on paving stone substrate.

Table D37 Thicknesses, adhesion and failure type results of Tekflex on 1 month cured clean paving stone substrate.

Adhesion (MPa)	Thickness (mm)	Failure Type
3.48	6	Interface
3.04	6	Interface
3.62	6	Interface
3.30	6	Interface
3.52	6	Interface

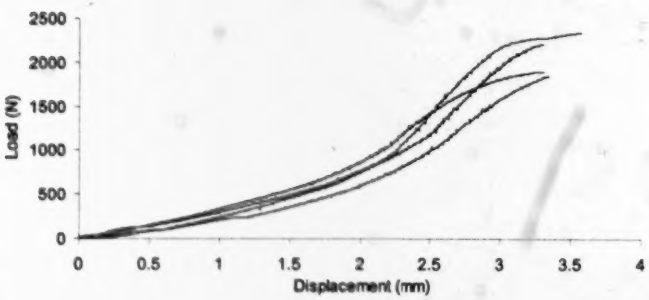

Figure D38 Load displacement curve of 1 month cured Tekflex on sawn granite substrate.

Table D38 Thicknesses, adhesion and failure type results of Tekflex on 1 month cured saw cut granite substrate.

Adhesion (MPa)	Thickness (mm)	Failure Type
2.74	3	Interface
2.61	3.5	Interface
2.22	6	Interface
2.23	5	Interface

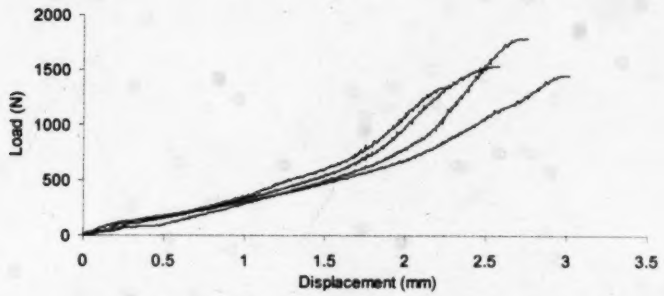

Figure D39 Load displacement curve of 1 month cured Tekflex on split granite substrate.

Table D39 Thicknesses, adhesion and failure type results of Tekflex on 1 month cured split granite substrate.

Adhesion (MPa)	Thickness (mm)	Failure Type
1.70	2	Interface
2.09	2	Interface
1.80	2	Interface
1.57	2	Interface

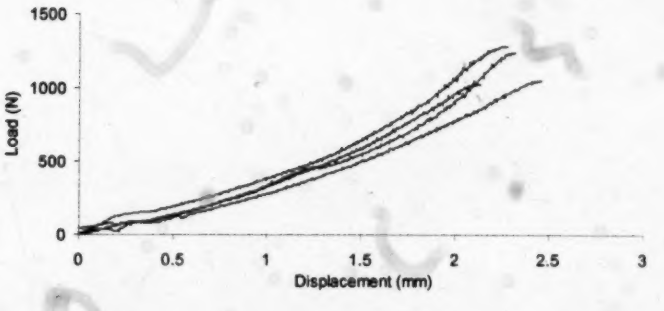

Figure D40 Load displacement curve of 1 month cured Tekflex on dusty paving ston% substrate.

Table D40 Thicknesses, adhesion and failure type results of Tekflex on 1 month cured dusty paving stone substrate.

Adhesion (MPa)	Thickness (mm)	Failure Type
1.45	4	Interface
1.50	4	Interface
1.23	4	Interface
1.20	4	Interface

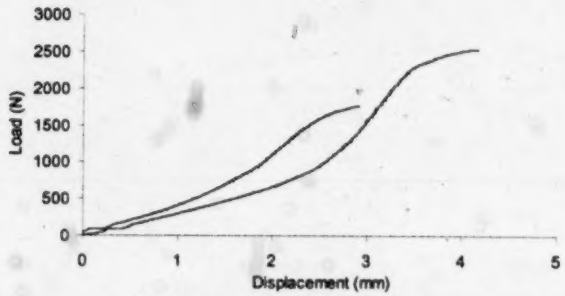

Figure D41 Load displacement curve of 1 month cured Tekflex on damp paving stone substrate.

Table D41 Thicknesses, adhesion and failure type results of Tekflex on 1 month cured damp paving stone substrate.

Adhesion (MPa)	Thickness (mm)	Failure Type
2.96	6	Interface
2.06	4	Interface

APPENDIX E: TEST OF SIGNIFICANCE

The significance of different test results can be found out for a given confidence interval, using the number of tests, mean and standard deviations of each test. The procedure explained below is the method used in this study to compare significance of adhesion tests of different products for different substrates and contamination conditions.

The variable T can be used to test the hypothesis: H: $\mu_1=\mu_2$, where μ_1 and μ_2 are the expected values for two independent and normally distributed observations.

(a) If the variances σ^1 and σ^2 can be assumed to be equal, T is defined as (Blank 1980)

$$T = \frac{m_1 - m_2}{s}\sqrt{\frac{n_1 n_2}{n_1 + n_2}} \tag{E1}$$

where m_1 and m_2 are the means, n_1 and n_2 are the number of samples for the two measurements and

$$s^2 = \frac{(n_1 - 1)s_1^2 + (n_2 - 1)s_2^2}{n_1 + n_2 - 2} \tag{E2}$$

is the pooled variance.

According to Blank (1980), T has a Student distribution $t_{\alpha/2}(\mathrm{df})$, where $\mathrm{df}=n_1+n_2-2$ is the degree of freedom. If

$$|T| > t_{\alpha/2}(df) \tag{E3}$$

the hypothesis H is rejected and there is a significant difference between μ_1 and μ_2.

(b) $\sigma^1 \neq \sigma^2$, the test can be done with a similar but approximate test, then T can be defined as (Blank 1980)

$$T = \left| \frac{m_1 - m_2}{\sqrt{s_1^2/n_1 + s_2^2/n_2}} \right| \tag{E4}$$

If

$$|T| > t_{\alpha/2}(df) \tag{E5}$$

the hypothesis H is rejected and there is a significant difference between μ_1 and μ_2. In this case

$$df = \frac{\left(s_1^2/n_1 + s_2^2/n_2\right)^2}{\frac{\left(s_1^2/n_1\right)^2}{n_1 + 1} + \frac{\left(s_2^2/n_2\right)^2}{n_2 + 1}} - 2 \tag{E6}$$

(c) To make the significance test according to paragraph (a) and (b), a test to find out if the variances σ^1 and σ^2 are equal or not must be done. The test can be done according to Blank (1980). If

$$s_1^2/s_2^2 > F_{\alpha/2}(n_1-1, n_2-1)$$
$$or \qquad \text{(E7)}$$
$$s_2^2/s_1^2 > F_{\alpha/2}(n_2-1, n_1-1)$$

σ^1 and σ^2 cannot be assumed to be equal, $F_{\alpha/2}(n_1-1, n_2-1)$ and $F_{\alpha/2}(n_2-1, n_1-1)$ are the F-distribution (Blank 1980), and n_1 and n_2 are the number of tests.